Rain-wind-induced vibrations of cables

Master thesis of Dhiretjh Sewdoelaré

Delft University of Technology

Delft University of Technology
Faculty of Electrical Engineering, Mathematics and Computer Science
Delft Institute of Applied Mathematics

Rain-wind-induced vibrations of cables

A thesis submitted to the
Delft Institute of Applied Mathematics
in partial fulfillment of the requirements

for the degree

MASTER OF SCIENCE
in
APPLIED MATHEMATICS

by

Dhiretjh Sewdoelaré

Delft, the Netherlands
Juli 2010

Delft University of Technology

MSc THESIS APPLIED MATHEMATICS

"Rain-wind-induced vibrations of cables"

Dhiretjh Sewdoelaré

Delft University of Technology

Daily supervisor	**Responsible professor**
Dr. ir. W.T. van Horssen	Prof. dr. ir. A. W. Heemink

Other thesis committee members

Prof. dr. A.V. Metrikine
Dr. Ir. M. B. van Gijzen

Juli 2010 Delft, the Netherlands

Definitions

A	cross-sectional area
dx	infinitely small element
ρ	density
E	Youngs modulus or modulus of elasticity
I	moment of inertia about the x-axis
EI	stiffness
f	external force
λ	separation constant
M	bending moment
R	radius of the cylinder
t	time
θ	angle between neutral axis and x-axis
V	internal transverse force

Table of contents

Introduction

On a raining day rain water can track down along the lower surface of cables of bridges. In combination with wind, rivulets can be formed. In the past years it has become clear that the combination of rain and wind can produce unwanted vibrations like in the Yapanese Meikonishi bridge, and the Erasmus bridge in Rotterdam, see figure I.1. This phenomenon is called rain-wind-induced vibrations (RWIV).

In this report a model will be given of the cable with a rivulet and wind and drag forces. The results of several researchers is taken into account. Since the rivulet can be viewed as a small disturbance, asymptotic approximations will be used for analysis. Analytic methods are used in the analysis of the models described in this report.

The analytic methods will comprise of solving partial differential equations (PDEs) via separation of variables, perturbation calculus and solving Diophantine-like equations . Moreover, the analysis will be centered around internal resonance and stability.

In the first chapter the model will be described, the assumptions will be discussed and the general PDE will be derived. In the second chapter perturbation calculus will be applied and the corresponding differential equations will be derived. Moreover, a model will be given which includes wind and drag forces.

In the third and fourth chapter the O(1)-problem and respectively the $O(\varepsilon)$-problem will be discussed and the results of internal resonance and stability will be analyzed. Chapter 5 focuses on the rivulet modeled as a block signal. In chapter 6 and 7 the presence of a quadratic and cubic term in the velocity of the cable will be discussed. Finally in chapter 8 recommendations and directions are given towards a continuation of this research.

Figure I.1: Attachment of dampers at the Erasmus bridge to suppress rain-wind-induced-vibrations.

Literature research

There are a lot of papers written over RWIV. Some of them treat observations in the field while others use analytical model to explain the phenomenon. In this literature research 9 papers about RWIV scattered over the years are treated. For more information regarding this subject the reader is referred to these 9 papers and their references within.

In [1] Hikami and Shirashi were the first to note the RWIV and claim that the vibrations at the Meikonishi bridge weren't due to vortex-induced oscillation nor wake galloping. They performed full scale measurements which confirmed that the frequency of the observed vibration was well below the critical frequency of the vortex-induced oscillation. For the observed vibration to be a wake galloping, the distance between the cables was too large to cause any interference with each other.

The authors in [1] reported a very important observation: the upper rivulet formed through the combination of rain and wind plays an important role in the occurrence of the vibrations. They also mention that the vibrations only occur within a limited range of the wind velocity, and under certain angles of the cable. The measurements show that not all the cables of the bridge exhibited vibrations.

The modes excited by rain and wind fell in the range of 1-3 Hz and were mostly of a single mode, there were a few occasions when two or three modes were involved. They mention that two possible mechanisms of instability could be the Den Hartog instability and instability due to coupled aerodynamic forces. In the paper none of the causes are further investigated.

In [2] Yamaguchi attempted to create an analytical model using 2 degrees of freedom to investigate the causes of the instability. He used a circular cylinder with diameter D and attached to that a small cylinder, with diameter d, acting as a rivulet. He investigated several diameter ratios: $\frac{d}{D} = 0.1, 0.2, 0.4$ with varying angle of attacks he measured the coefficients C_D, C_L and C_M, see figure L.1.

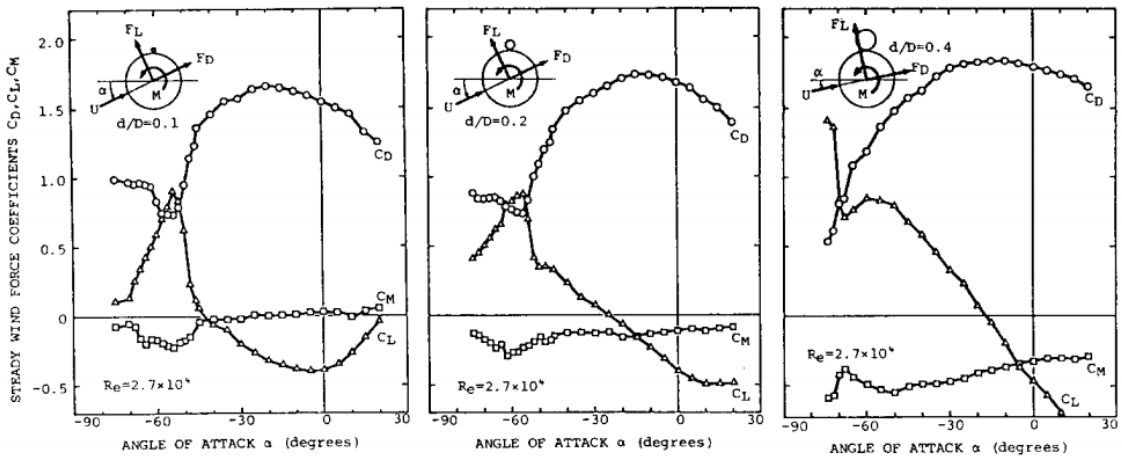

Figure L.1: Measured values of C_D, C_L and C_M for different diameter ratios, taken from [2].

He attempted to test the two causes of the instability mentioned in [1]. He found that the Den Hartog mechanism can't be the cause of the instability (of course under certain model assumptions) due to the failing of the criterion $C_D + \frac{dC_L}{d\alpha} < 0$.

Analysis of the second cause gives no conclusion but gives two important results. First of all the fundamental frequency of the circumferential oscillation of the upper rivulet is proportional to the wind speed and could coincide with the natural frequency of the cable at wind speeds around 10 m/s. Second of all the upper rivulet is able to oscillate in circumferential direction because of the aerodynamic stiffness.

For this thesis report the shape and the dimensions of the rivulet are required. The authors in [3] investigated a rivulet on a tube to find out what the characteristics are for the flow of the rivulet for heat exchangers, condensers and so on. In their setup they used a nozzle to feed ethanol on a glass tube inclined under an angle. Their results show two important shapes of the rivulet and confirm that the rivulet can be seen as a small disturbance.

Moreover, in [3] the wave profiles of the rivulet become apparent; figure L.2 shows that the rivulet can take two shapes. The first shape is sinusoidal and the second shape is approximately a block function. In this report both the sinus-function as the block function will be used to model the rivulet. From figure L.2 it's also clear that the amplitude is small and can thus be regarded as a disturbance. The function which describes the sinus function is $f(x,t) = c + \varepsilon \sin\left(\beta(x - \Omega t)\right)$ and for the block function this becomes $m(x,t) = c + \sum_{k=-\infty}^{\infty} Q[x - \omega(t - c_k)] - Q[x - \omega(t - d_k)]$, this will be clarified in the next chapters.

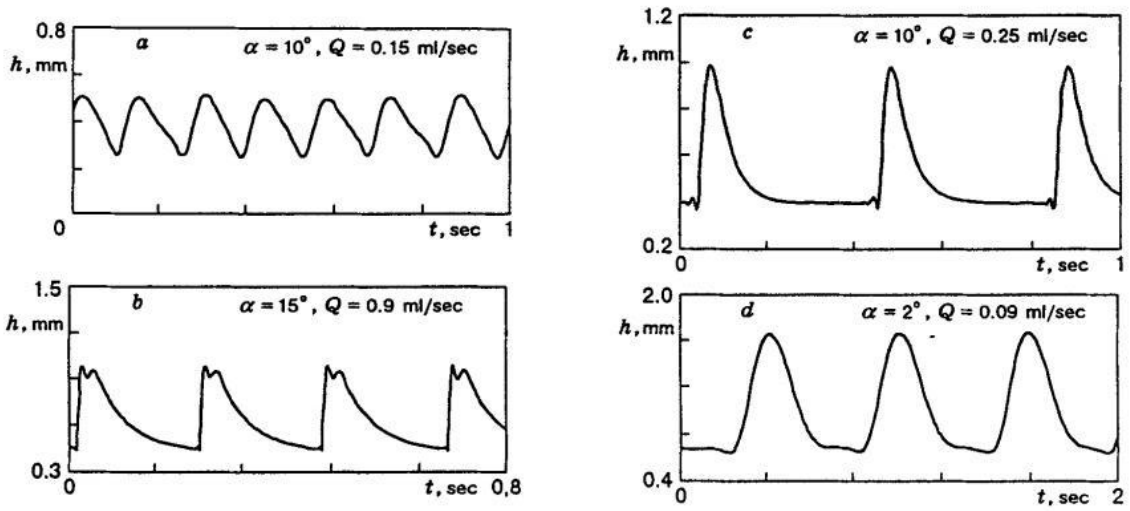

Figure L.2: The height h of the rivulet measured for different inclination angles α and different flows Q, taken from [3].

In [4] a stochastic approach is implemented. The rivulet is modeled by a small added mass undergoing stochastic motion on the circumference. The motion is described by the response of a band pass filter. Such a filter can be thought of as an ideal system that, when excited by white noise input gives a response whose power spectral density (PSD) induces the PSD of the moving rivulet.

The authors chose a 1 DOF model and incorporate measurements of C_L and C_D from [1]. They found stochastic vibrations and for appropriate parameters the system can rapidly evolve around a stochastic state. The most important result is that the vibrations occurred with positive damping while the Den Hartog mechanism requires anti-damping.

In [5] an attempt is made to create an analytical model based on a single DOF. This model incorporates the lift and drag forces via a power series approximation of the data of C_L and C_D found in [1]. The analytical model captures the main vibrations features such as the velocity and amplitude restriction. Although the model could be improved by adding axial flow and turbulence it captures the trend lines of the observations found in [1].

In [6] an overview is given of the result of previous investigation in the first part of the paper. They mention that large-amplitude cable stay vibrations have been observed on a number of bridges in the United states and abroad during relatively low wind speeds with and without the presence of rain. The proposed cause of the vibrations is the change in the cross sectional shape of the cable stay that occurs when rain forms one or more rivulets along the cable surface. This modified cross section affects the aerodynamics of the cable stay. As a result large vibrations occurs at wind speeds above the known Karman-vortex shedding winds speeds for cylindrical bodies.

Excessive cable-stay vibrations can distress the cable stays themselves and subject to them to stress states for which they were not designed. Long term fatigue damage to the cable stays is another concern. Thus safety perception to the public is an important issue.

The second and main part of paper [6] focuses on preventing the vibrations while this report doesn't deals with these forms of prevention it's important to note that these vibrations can be suppressed effectively.

Currently, cable-stay oscillations caused by rain–wind induced aerodynamic forces are controlled by one or a combination of the following methods: (1) single-point mechanical dampers, typically at the base of each cable, see figure L.3, (2) restraining cable devices, known as cross-ties, that connect adjacent cables at various locations along the length of the cable resulting in a reduced effective length for each cable; and (3) distributed passive approaches such as surface treatment of cables using grooves, protuberances, or dimples. This paper [6] presents data on the effectiveness of one such approach using a distributed passive device.

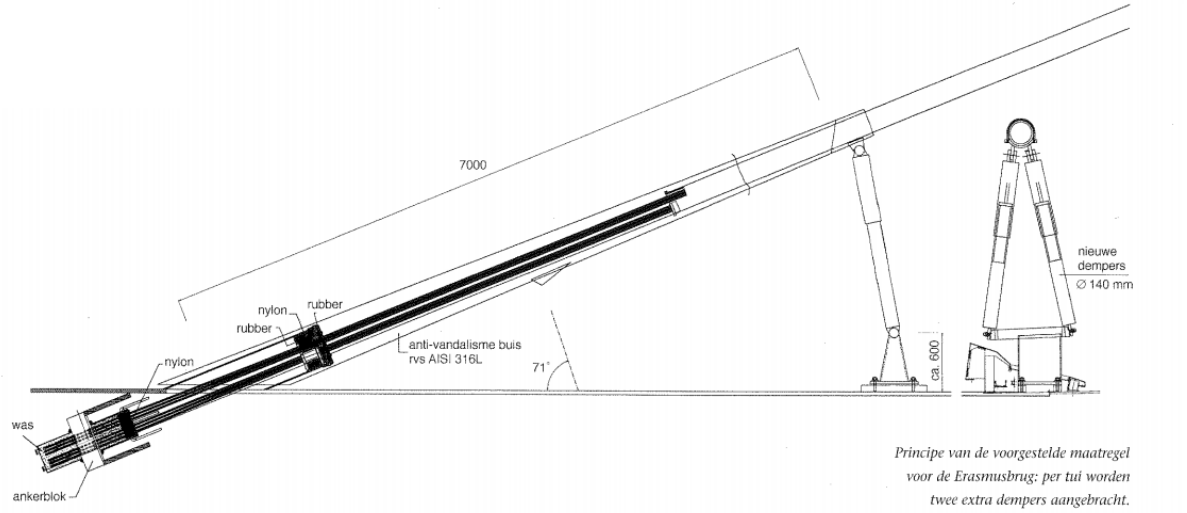

Figure L.3: The first method of preventing RWIV, additional dampers implemented at the Erasmus bridge in Rotterdam in the Netherlands, taken from [6].

The Veterans Memorial bridge was instrumented to monitor its cable stay vibrations. They found several results. First of all RWIV occurred when the wind speed was between 6.3 and 14 m/s. Secondly velocity restricted response was often triggered when there was no rain and wind speeds were between 7 and 11 m/s. And finally the rings attached to the cable stays added aerodynamic damping and reduced the amplitudes of the vibrations.

In [7] the rivulet itself was investigated. They investigate the condition for appearance of rivulets and the relation between their position and physical parameters such as wind velocity, surface tension, viscosity of water, thickness of the water film, cable diameter and tension, see figure L.4. Also the equation governing the dynamics of a thin film of liquid on a cylinder subjected to wind is derived in the paper. Finally they propose a simple criterion to estimate the position of the rivulet.

To test their model they used a self made experimental set up. They explain the appearance of rivulets via a balance between gravity and wind load. The overall position of the rivulet seems to be depend more on the variation of the external load than on local nonlinear effects.

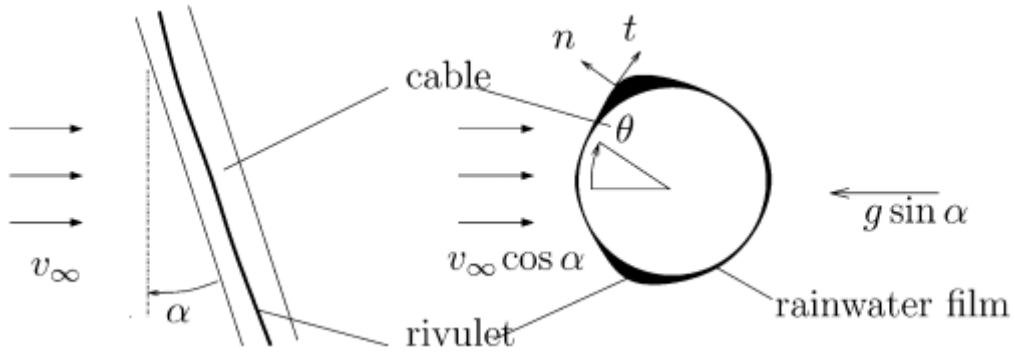

Figure L.4: A picture of the model used in [7].

Peil et al. give an elaborate model for rain-wind-induced vibrations (RWIV) in [8]. They derive the equation of motion in 3D taking into account sagging of the cable, the elasticity of the cable, longitudinal elongation and they coupled the equation of motion for the rivulet where the two dimensional Navier Stokes equations are taken as a basis.

Although the model looks extensive at first sight a detailed look towards the rivulets equation of motion reveals neglection of small terms which considerably simplify the equations, it's not argumented that those terms can be neglected other than the simplification. The result of the model shows agreement with the observation in situ. They conclude that self-induced vibrations lead to the instability.

In the introduction of [9] they explain that the width of the rivulet was about 1-2 cm. and that the cables in cables-stayed bridges have diameter of 10-18 cm. This means that, if a simulation was exerted with the same measurements for the rivulet and cables, the measurements of pressure and wind acting along the rivulet would be almost impossible. To cope with this fact while staying in the same Reynolds regime the test wind speed, the diameter of the cable and the model length are adjusted.

In the wind test performed by the authors they took both the rivulets into account as opposed to other simulations where the lower rivulet was left out, see figure L.5. Also by rearranging 176 pressure taps the aerodynamic forces could be measured with accuracy. Moreover, the C_D and C_L of both the rivulet at the cable are measured while varying the initial position of the rivulet. An analytical model was set up (as discussed in appendix section C) and measured values of C_D and C_L were inserted.

Figure L.5: Photo of the test set-up of Gu et al.

The mechanism behind the instability which they suggest is galloping for if the rivulets initial position is in a so-called 'danger zone' the position could eventually end up in the unstable zone (according to the Den Hartog criterion). The analytical model set up to run numerical simulations differs from others in the sense that the friction force is in this paper composed of a linear damping force and a Coulomb damping force. Unfortunately the authors Gu et al. had difficulty in determining its correct value.

1 Setting up a model

§1.1 Model setup

All of the models from the papers regarding rain-wind-induced vibrations (RWIV) see the rivulet as a lumped mass moving circumferentially around the cable. Some researchers even took the elasticity and strain of the cable into account. In this report a model will be created by modeling the rivulet as an perturbation. In this chapter firstly a simplification will be carried out after that the PDE can be derived. Finally the restrictions of the model will be analyzed.

§1.2 Simplification

The cable under consideration is a cable-stay from a bridge and consists of several polystyrene cables along with a reinforced ring. A schematic display is given in figure 1.1 as well as the coordinate axis.

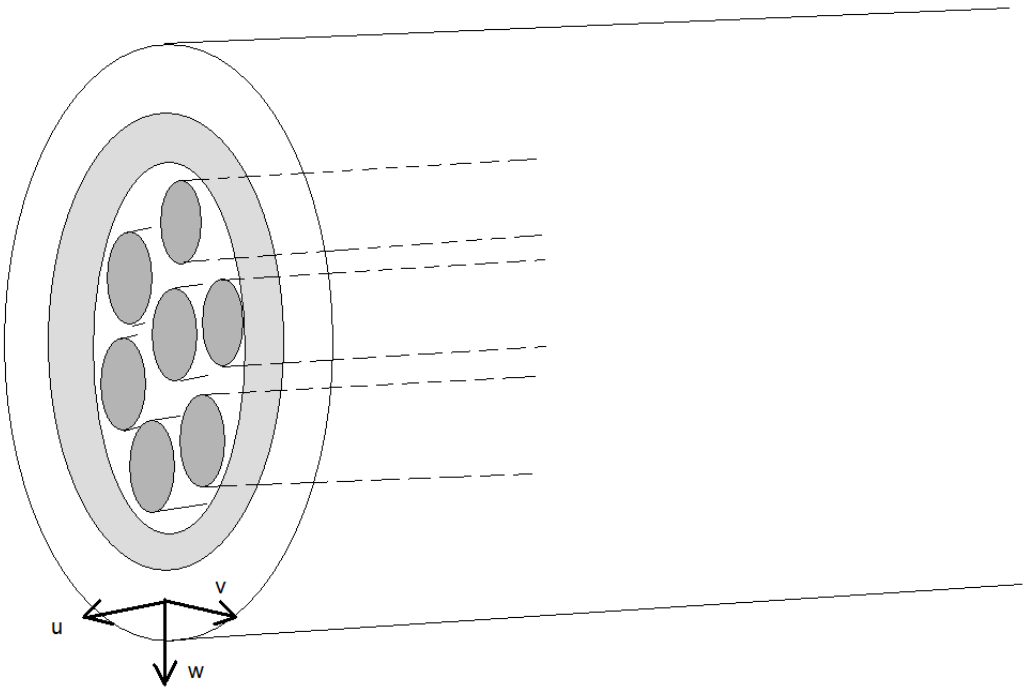

Figure 1.1: Cable stay from a bridge with chosen coordinate axis.

In this report only the vertical displacements will be analyzed. Moreover, the cable will be modeled via a cylinder shell in 1D. The rest of the cylinder will be modeled as an sequence of springs with spring constant γ, see the dark grey area in figure 1.2a and the model in figure 1.2b.

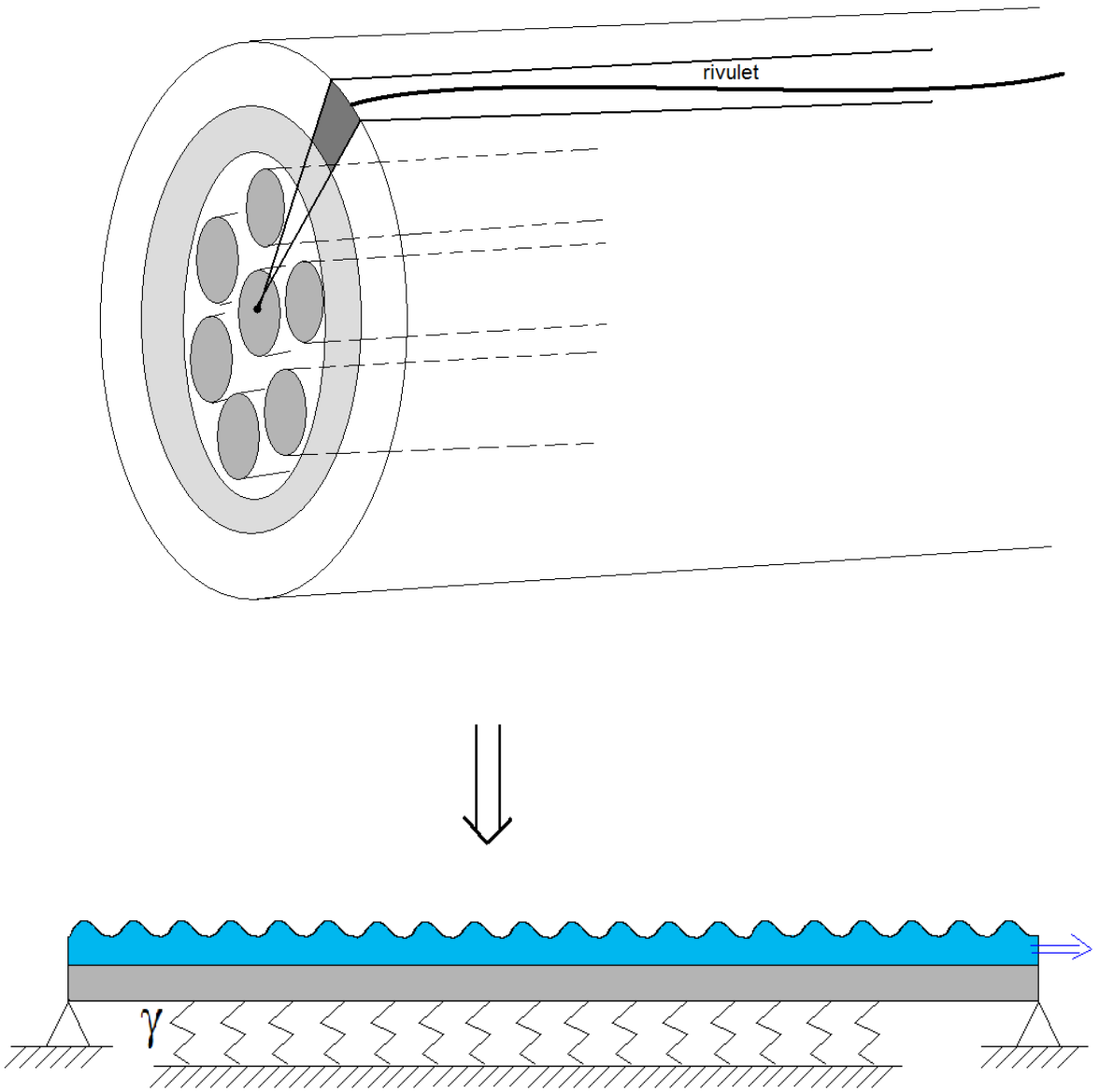

Figure 1.2a: (on top) A slice of the cylinder will be analyzed. Figure 1.2b: The shell is modeled via a beam and the rest as a sequence of springs.

Two models will be analyzed with in each a different form of the rivulet. In the first model the rivulet will be a "wave" moving to the right: $m(x,t) = m_0 + A_{wave} \sin\left(\beta(x - \Omega t)\right)$. Note that according to [3] A_{wave} is small. Furthermore both ends will be simply supported. Now we are ready to derive the equations of motion. The rivulet is assumed to be small compared to the beam and is highly exaggerated displayed in figure 1.2a.

§1.3 Equations of motion

We look at an infinitely small element dx of the beam with length L. The beam has an modulus of elasticity E, a moment of inertia I and a cross sectional area A. The beam is placed on a sequence of springs with spring constant γ, subjected to an external force f(x,t) and an axial tension T, see figure 1.3.

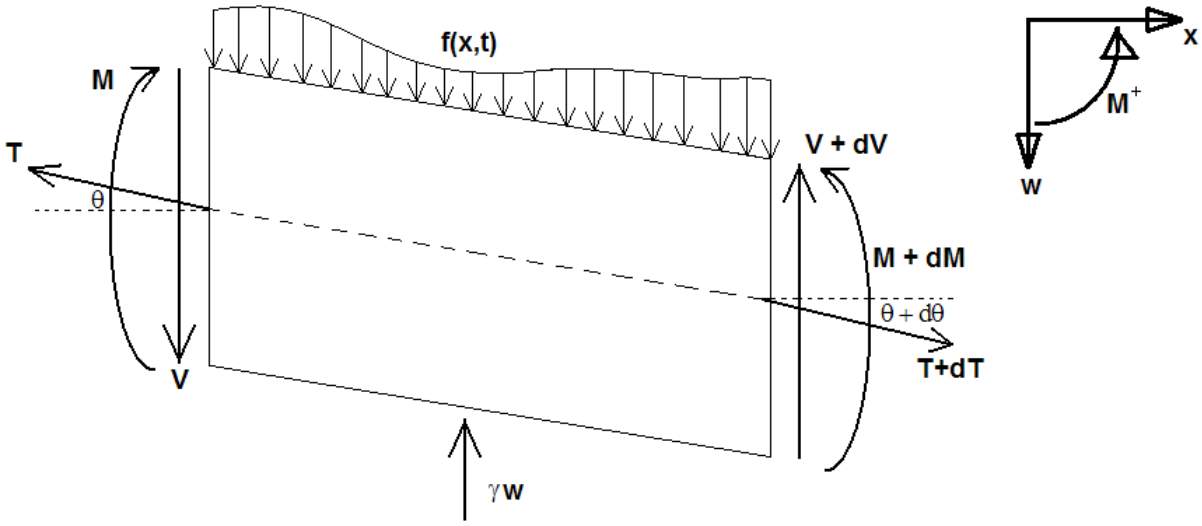

Figure 1.3: An infinitely small element from the beam subjected to an external load f and a tensile force T.

Summing forces in vertical direction gives (subscript denotes partial derative):

$$\rho A dx \cdot w_{tt} = V - (V + dV) + \int_{x}^{x+dx} f(\xi, t)\, d\xi + (T + dT)\sin(\theta + d\theta) - T\sin(\theta) - \gamma w dx$$

$$= -dV + f(\tilde{x}, t)dx - T\frac{\partial w}{\partial x} + (T + dT)\left[\frac{\partial w}{\partial x} + \frac{\partial}{\partial x}\left(\frac{\partial w}{\partial x}\right)dx\right] - \gamma w dx,$$

with a specific $\tilde{x}$ for $x \le \tilde{x} \le x + dx$ according to the mean value theorem and the assumption

$$\sin(\theta) \approx \tan(\theta) = \frac{\partial w}{\partial x} \ll 1 \text{ and } \sin(\theta + d\theta) \approx \theta + d\theta = \frac{\partial w}{\partial x} + \frac{\partial}{\partial x}\left(\frac{\partial w}{\partial x}\right)dx.$$

Now with neglection of dx^2-terms:

$$\rho A dx \cdot w_{tt} = -\frac{\partial V}{\partial x}dx + f(\tilde{x}, t)dx + T\frac{\partial^2 w}{\partial x^2}dx + \frac{\partial T}{\partial x}\frac{\partial w}{\partial x}dx - \gamma w dx.$$

Dividing by dx and since dx is infinitely small $\tilde{x} \approx x$ this results in:

$$\rho A w_{tt} = -\frac{\partial V}{\partial x} + f(x, t) + \left(T w_x\right)_x - \gamma w.$$

From mechanics of materials we know $M = EI\frac{d^2w}{dx^2}$ and $\frac{dM}{dx} = V$ (with the chosen sign convention forces downward are positive and CCW-moments are positive as displayed in figure 3).

$$\rho A w_{tt} = -\frac{d^2M}{dx^2} + f(x,t) + \left(Tw_x\right)_x - \gamma w$$

$$= \left(-EIw_{xx}\right)_{xx} + f(x,t) + \left(Tw_x\right)_x - \gamma w,$$

with the assumption that ρ, A, EI, T are constants we get:

$$\rho A w_{tt} = -EIw_{xxxx} + f(x,t) + Tw_{xx} - \gamma w.$$

Thus we finally found the resulting partial differential equation:

$$\rho A w_{tt} + EIw_{xxxx} - Tw_{xx} + \gamma w = f(x,t). \tag{1.1}$$

Now introducing nondimensional parameters:

$$\bar{x} = \frac{\pi}{L}x,\ \bar{t} = \frac{\pi}{L}ct,\quad \bar{w} = \frac{\pi}{L}cw,\ \ c = \frac{\pi}{L}\sqrt{\frac{EI}{\rho A}},\ \ q^2 = \frac{T}{\rho A c^2},\ \ p^2 = \frac{\gamma}{\rho A}\left(\frac{L}{\pi c}\right)^2.$$

This gives as a final result (with the bars immediately dropped):

$$w_{tt} + w_{xxxx} - q^2 w_{xx} + p^2 w = \frac{L}{c\pi\rho A} f(x,t). \tag{1.2}$$

A different form for the equation of motion can be found in [13], using Donnels shell theory applied to a circular cylindrical shell one can find a set of three coupled PDE's describing the displacement:

$$R^2\frac{\partial^2 u}{\partial x^2}+\frac{1-\nu}{2}\frac{\partial^2 u}{\partial \theta^2}+R\frac{1+\nu}{2}\frac{\partial^2 v}{\partial x\,\partial\theta}-\nu R\frac{\partial w}{\partial x}=\rho\frac{1-\nu^2}{E}R^2\frac{\partial^2 u}{\partial t^2},$$

$$\frac{\partial^2 v}{\partial \theta^2}+R^2\frac{1-\nu}{2}\frac{\partial^2 v}{\partial x^2}+R\frac{1+\nu}{2}\frac{\partial^2 u}{\partial x\,\partial\theta}-\frac{\partial w}{\partial \theta}=\rho\frac{1-\nu^2}{E}R^2\frac{\partial^2 v}{\partial t^2},$$

$$\nu R\frac{\partial u}{\partial x}+\frac{\partial v}{\partial \theta}-w-k\left(R^4\frac{\partial^4 w}{\partial x^4}+2R^2\frac{\partial^4 w}{\partial x^2\,\partial\theta^2}+\frac{\partial^4 w}{\partial \theta^4}\right)=\rho\frac{1-\nu^2}{E}R^2\frac{\partial^2 w}{\partial t^2},$$

with u, v and w defined in figure 1.1 and θ the angle of rotation.

From the last equation (1.2) it can be seen that under certain assumptions the partial differential equation (PDE) derived above can be found with additional terms due to the rotation . See [14] for a more difficult model taking ovally shaped circular cylindrical shells and the other modes into account.

§1.4 Choice for an analytical model

The PDE (1.1) derived in §1.4 will, with f(x,t) specified later on, become an nonautonomous nonlinear differential equation. Since exact analytical solutions of nonlinear systems often aren't available qualitative analysis is used. Moreover, it's used to predict general features of the motion including stability and long term behavior. The most useful tool for qualitative analysis of a nonlinear system is the state plane: a graphical history of the relationship between two variables, although this isn't often used in this thesis.

Analytical solutions are preferable to numerical solutions because they can be used to predict trends, analyze the effect of parameters and investigate the stability. Approximate analytical methods are often used to approximate the solution of nonlinear problems. If the magnitude of the nonlinear term is small, say in the order of ε, with $\varepsilon \ll 1$, then a perturbation method can be used to develop an approximate solution.

For a one-degree-of-freedom system, the generalized coordinate is expanded in a series of power of ε, $x(t)=x_0(t)+\varepsilon x_1(t)+\varepsilon^2 x_2(t)+\ldots$. This equation can be substituted in the governing differential equations thereafter coefficients of like powers of ε are collected and set to zero independently. The result is a set of differential equations that are successively solved for $x_i(t),\ i=1,2,3\ldots$

The series can be convergent and if terms of the homogenous solutions appear in the right-hand-side then *secular* terms may occur. These terms are unbounded for all t and ε and must be removed. A variety of perturbation methods are developed to remove secular terms.

These include the method of strained parameters, the method of renormalization, the method of averaging and the method of multiple time scales. Some methods only remove periodic terms that's why in this report the method of multiple time scales is used, since implementing this method results in finding all solutions, for more information see [16].

§1.5 Restrictions of the model

In this paragraph the most important assumptions are listed below.
In this model

- Only one rivulet is modeled, the effect of the other rivulet is not taken into account;
- The upper rivulet doesn't moves circumferentially on the cable;
- The rivulet is modeled as a perfect sine/ block signal;
- Only 1D effect are taken into account;
- Torsional effects are left out;
- The mass of the rivulet is assumed to be small in comparison with mass of the cable;
- The rivulet moves frictionless on the cable;
- The moment of inertia of the rivulet is neglected;
- Material properties are constant throughout the cable;
- The cable is modeled as a beam;
- Gravity is omitted.

§1.6 Conclusion

In this chapter a PDE has been derived for the cable in conditions where RWIV might occur. The cable is modeled as an Euler-Bernoulli beam subject to a tensile force, placed on a spring bed and the beam is in line with the x-axis. Also, the reasons for an analytic model are given, the most important being: analytic models can predict stability for parameter ranges and can outline long term behavior.

Perturbation expansions can be used if certain terms are small compared to others. Care must be taken when secular terms occur. Finally it's noted that only under certain important assumptions the results can be called plausible.

2 Perturbation calculus

In this chapter the model of the rivulet will be added to the PDE derived in chapter 1. Perturbation calculus will then be applied to find an approximation of the analytical solution. To simplify the model several assumptions are made.

§2.1 Adding the model of the rivulet to the PDE

The rivulet on the beam can be considered to be a mass varying with time and space: m(x,t). To include this in the model the first term in the PDE (1.1) from chapter 1 must be changed. In this chapter the rivulet is modeled as a circular cylinder. The amplitude of the wave-shape of the rivulet is small compared to the mass of the cable and can thus be considered as a disturbance.

Locally the total mass is:

$$\left[mw_t\right]_t = m_{cable} w_{tt} + \left[m(x,t)w_t\right]_t,$$

with

$$m(x,t) = \rho_w A_w(x,t)dx = \rho_w dx \frac{\pi}{4}\left(c + \varepsilon \sin\left(\beta(x - \bar{\Omega}t)\right)\right)^2,$$

$$m_{cable} = \rho_{cable} A_{cable} dx.$$

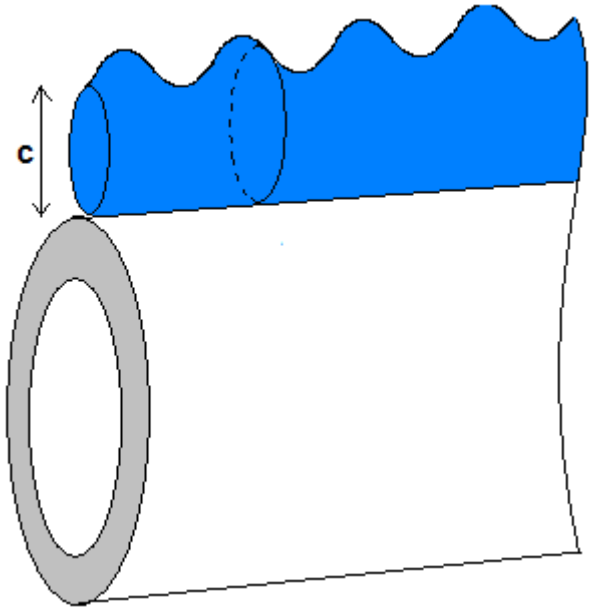

Figure 2.1: A schematic representation of the rivulet with a circular cylinder shape and with its height prescribed by a sine function on a cable-stay of a bridge.

$\rho_{cable}, A_{cable}, \rho_w, A_w$ are the density and cross sectional area of the cable and respectively the rivulet, c is the height at which the sine is present and the presence of $\frac{\pi}{4}$ and the square is just the total area of a circular disc of the rivulet, see figure 2.1. β and $\bar{\Omega}$ are two parameters to give the sine a general form.

Now with neglection of ε^2 – terms:

$$m(x,t) \approx \rho_w dx \frac{\pi}{4} c^2 + \varepsilon \sin\left(\beta(x - \bar{\Omega} t)\right) dx.$$

So mass term becomes:

$$\left[m_{tot} w_t\right]_t = m_0 w_{tt} + \left[m(x,t) w_t\right]_t,$$

with $m_0 = m_{cable} + \frac{\pi}{4} c^2 \rho_w dx = \rho_{cable} A_{cable} dx + \frac{\pi}{4} c^2 \rho_w dx = \rho A dx, \quad \rho A = \rho_{cable} A_{cable} + \frac{\pi}{4} c^2 \rho_w.$

The dx is divided in the final step of the derivation of the PDE in chapter 1. Now the PDE can be reformulated. The PDE with the rivulet and without an external load is:

$$\rho A w_{tt} + EI w_{xxxx} - T w_{xx} + \gamma w = \varepsilon\left[-\tilde{m}(x,t) w_t\right]_t.$$

Introducing nondimensional parameters:

$$\bar{x} = \frac{\pi}{L} x, \ \bar{t} = \frac{\pi}{L} ct, \quad \bar{w} = \frac{\pi}{L} cw, \ \ c = \frac{\pi}{L}\sqrt{\frac{EI}{\rho A}}, \ q^2 = \frac{T}{\rho A c^2}, \ p^2 = \frac{\gamma}{\rho A}\left(\frac{L}{\pi c}\right)^2, \ \bar{\varepsilon} = \varepsilon \frac{L}{c\pi\rho A},$$

which leads to the PDE:

$$\bar{w}_{\bar{t}\bar{t}} + \bar{w}_{\bar{x}\bar{x}\bar{x}\bar{x}} - q^2 \bar{w}_{\bar{x}\bar{x}} + p^2 \bar{w} = \varepsilon\left[-\tilde{m}(\bar{x},\bar{t}) \bar{w}_{\bar{t}}\right]_{\bar{t}} = \varepsilon\left[\tilde{m}_{\bar{t}}(\bar{x},\bar{t}) \bar{w}_{\bar{t}} + \frac{\pi}{L} c \cdot \tilde{m}(\bar{x},\bar{t}) \bar{w}_{\bar{t}\bar{t}}\right],$$

with

$$\tilde{m}(\bar{x},\bar{t}) = \sin\left(\beta \frac{L}{\pi} \bar{x} - \bar{\Omega}\beta \frac{L}{\pi c} \bar{t}\right) = \sin(s\bar{x} - \Omega\bar{t}), \quad s = \beta \frac{L}{\pi}, \ \Omega = \bar{\Omega}\beta \frac{L}{\pi c}.$$

§2.2 The two time scales perturbation method

The PDE has a component of $O(\varepsilon)$ and perturbation analysis is best suited to find an approximation of the solution. The convergence of the approximation is discussed in the appendix section E. To prevent secular terms the two time scales perturbation method will be invoked and applied to this PDE:

$$w_{tt} + w_{xxxx} - q^2 w_{xx} + p^2 w = \varepsilon\left[-\tilde{m}(x,t) w_t\right]_t,$$

Note that the bars are dropped. Now with $w = \tilde{w}(x,t,\tau) = \tilde{w}(x,t,\varepsilon t)$ we get:

$$\left(\tilde{w}_{tt} + 2\varepsilon \tilde{w}_{t\tau} + \varepsilon^2 \tilde{w}_{\tau\tau}\right) + \tilde{w}_{xxxx} - q^2 \tilde{w}_{xx} + p^2 \tilde{w} = \varepsilon\left[-\tilde{m}(x,t)\left(\tilde{w}_t + \varepsilon \tilde{w}_\tau\right)\right]_t.$$

Now expand $\tilde{w}$ as follows: $\tilde{w}(x,t,\tau) = w_0(x,t,\tau) + \varepsilon w_1(x,t,\tau) + \varepsilon^2(..)$. After substitution we get:

$$\left(w_{0_{tt}} + \varepsilon w_{1_{tt}} + ...\right) + 2\varepsilon\left(w_{0_{t\tau}} + \varepsilon w_{1_{t\tau}} + ...\right) + \varepsilon^2\left(w_{0_{\tau\tau}} + \varepsilon w_{1_{\tau\tau}} + ...\right) + \left(w_{0_{xxxx}} + \varepsilon w_{1_{xxxx}} + ...\right)$$
$$-q^2\left(w_{0_{xx}} + \varepsilon w_{1_{xx}} + ...\right) + p^2\left(w_0 + \varepsilon w_1 + ...\right) = \varepsilon\left[-\tilde{m}(x,t)\left(w_{0_t} + \varepsilon\left(w_{0_t} + \varepsilon w_{1_t} + ...\right)\right)\right]_t,$$

where the dots represent higher order terms.

Collecting all order 1 terms gives:

$$O(\varepsilon^0): w_{0_{tt}} + w_{0_{xxxx}} - q^2 w_{0_{xx}} + p^2 w_0 = 0.$$

This PDE will be analyzed in chapter 3.

Collecting all order ε-terms:

$$O(\varepsilon^1): \quad w_{1_{tt}} + w_{1_{xxxx}} - q^2 w_{1_{xx}} + p^2 w_1 = -2w_{0_{t\tau}} + \left[-\tilde{m}(x,t) w_{0_t}\right]_t,$$

with $\tilde{m}(x,t) = \sin(sx - \Omega t).$

This PDE will be analyzed in chapter 4.

§2.3 Lift and drag forces

Equation (1.2) in chapter 1 can be made more realistically if lift and drag forces are inserted. To this end we place the cable under an inclination angle α, the yaw angle of the incident wind, with mean wind speed U_0, is designated as β just as in [5], see figure 2.2.

The radius of the cable is R and the angle of the static position of the rivulet with the vertical axis is θ_0. The angle between the static position of the rivulet θ_0 and the rivulet itself is θ, see figure 2.3. Since the cylinder is not perpendicular to the direction of the mean wind speed U_0 the component of U_0 perpendicular to the cable is needed:

$$U = U_0\sqrt{\cos^2(\alpha)\cos^2(\beta) + \sin^2(\alpha)} = U_0\sqrt{\sin^2(\alpha)\sin^2(\beta) + \cos^2(\beta)}.$$

For more information about the derivation of the equations, see appendix section C. Note that gravity is left out and that the angle β is a different β than the one used in the sine in chapter 1.

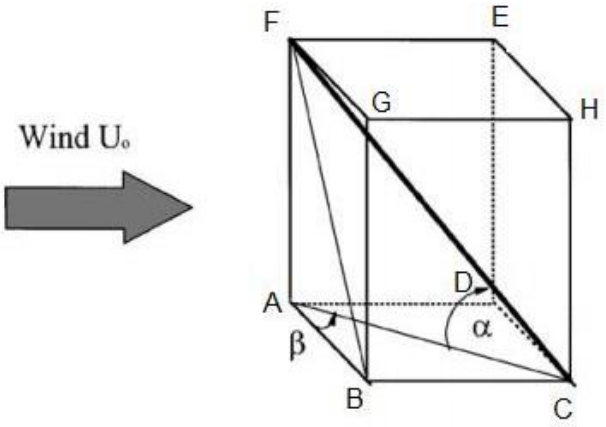

Figure 2.2: A representation of an inclined cable of a cable-stayed bridge under influence of wind.

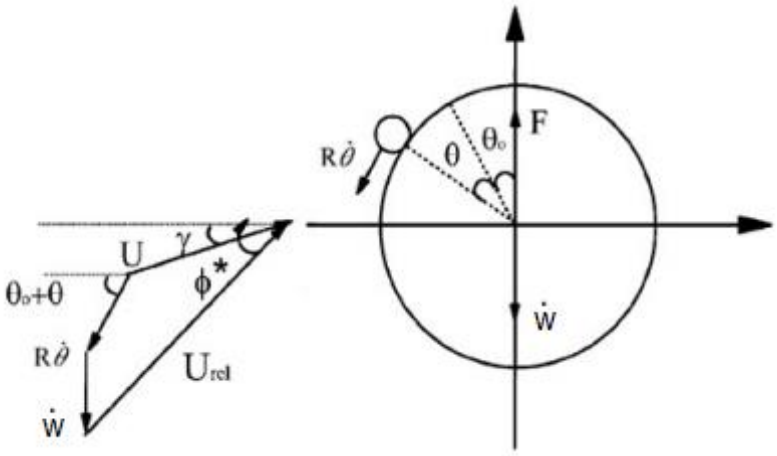

Figure 2.3: The velocity diagram of the rivulet and the cable.

The angle of attack is:

$$\sin(\gamma) = \frac{\sin(\alpha)\sin(\beta)}{\sqrt{\cos^2(\beta) + \sin^2(\alpha)\sin^2(\beta)}}.$$

The assumptions in this report are that: $\frac{\dot{w}}{U} \ll 1,\ R\dot{\theta} = 0$, so the wind speed is large as compared to the velocity of the beam in vertical direction and circumferential motion is not taken into account. The angle between the relative velocity U_{rel} and the horizontal axis in figure 2.3, is defined as ϕ^* which is:

$$\phi^* = \frac{U\sin(\gamma) + \dot{w} + R\dot{\theta}\sin(\theta + \theta_0)}{U\cos(\gamma)} \approx \tan(\gamma) + \frac{\dot{w}}{U\cos(\gamma)}.$$

The relative velocity becomes, with the earlier named assumptions:

$$U_{rel} = \sqrt{\left(U\cos(\gamma) + R\dot{\theta}\cos(\theta+\theta_0)\right)^2 + \left(U\sin(\gamma) + \dot{w} + R\dot{\theta}\sin(\theta+\theta_0)\right)^2}$$

$$\approx U\cos(\gamma)\sqrt{1+\left(\tan(\gamma) + \frac{\dot{w}}{U\cos(\gamma)}\right)^2}.$$

The net vertical force in w-direction is:

$$F = \frac{1}{2}\rho D U_{rel}^2 \left(C_L(\phi)\cos(\phi^*) + C_D(\phi)\sin(\phi^*)\right).$$

The angle ϕ is defined as $\phi = \phi^* - \theta - \theta_0$. C_L and C_D are functions of the angle of attack as shown in figure 2.4 below.

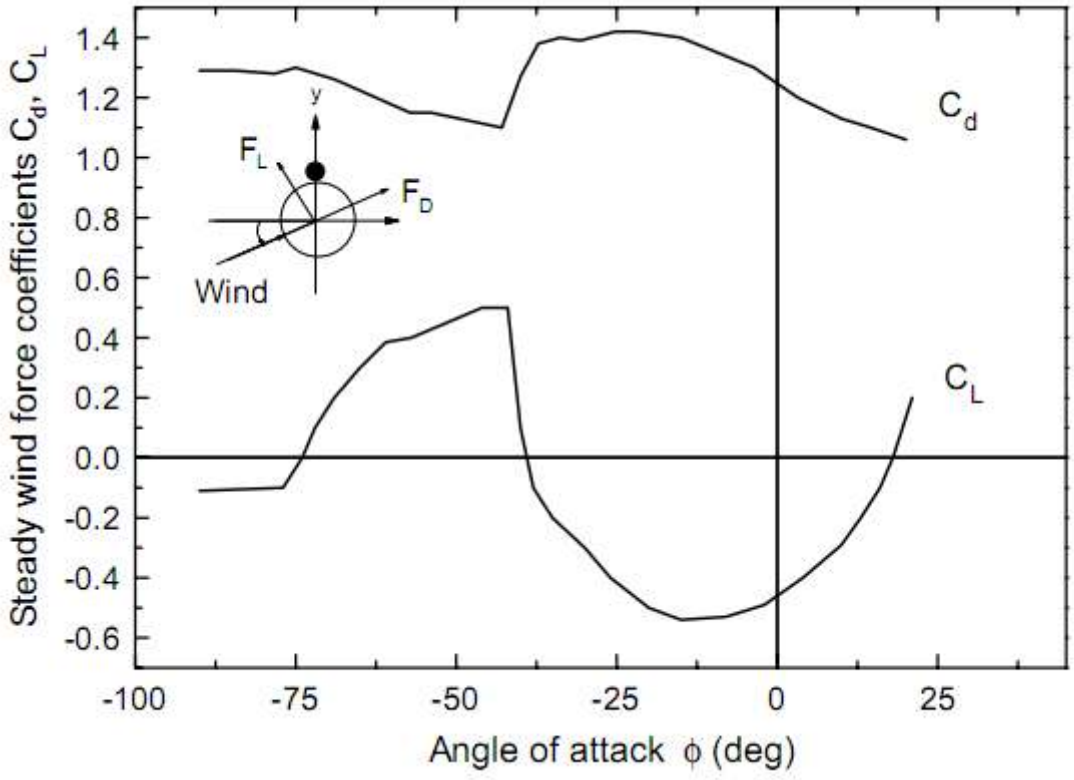

Figure 2.4: The 'coefficients' C_L and C_D which are a function of the angle of attack expressed in degrees, taken from [5].

Now using Taylor approximations around $\frac{\dot{w}}{U}$ leads to: $F = A_0 + A_1 \frac{w_t}{U} + A_2 \left(\frac{w_t}{U} \right)^2 + A_3 \left(\frac{w_t}{U} \right)^3$, with A_1, A_2 and A_3 constants. The quadratic and cubic term in w_t are investigated in respectively chapter 6 and 7.

§2.4 Conclusion

In this chapter the equations are derived outlining the analysis performed in this thesis. A term related to the rivulet was added to the PDE derived in chapter 1. Since this term is small a perturbation analysis is carried out, to give an approximation of the solution of the PDE: the equation for the order 1, O(1), and order ε, $O(\varepsilon)$, are derived.

Secular terms emerged after which the multiple time scales method was applied. Moreover, a model for the lift and drag acting on the cable was given. After linearization a quadratic and cubic term arose in the RHS which needed further attention.

3 The $O(\varepsilon^0)$-problem

The PDE in the $O(\varepsilon^0)$-problem is linear and homogeneous thus the superscript is dropped and separation of variables is performed. As stated in chapter 1 the beam is presumed to be simply supported at both ends.

§3.1 Separation of variables

The complete problem to be analyzed is:

$$\begin{cases} w_{tt} + w_{xxxx} - q^2 w_{xx} + p^2 w = 0, & 0 < x < \pi,\ t > 0, \\ w(0,t) = w(\pi,t) \equiv 0, & t \geq 0, \\ w_{xx}(0,t) = w_{xx}(\pi,t) \equiv 0, & t \geq 0, \\ w(x,0) = g(x),\ \ w_t(x,0) = h(x), & 0 < x < \pi. \end{cases}$$

We presume nontrivial solutions of the form: $w = w(x,t) = X(x)T(t)$

Substitution results in:

$$\frac{\ddot{T}}{T} = \frac{-X'''' + q^2 X'' - p^2 X}{X} = -\lambda,$$

where the dots represents time derivative and the prime represents derative with respect to x. The separation constant $-\lambda$ is negative and it can be proven that is real and that the corresponding eigenfunctions are orthogonal, see Appendix section A for details. So the assumption is $\lambda > 0$.

Solving for X(x):

$$\left.\begin{aligned} &-X'''' + q^2 X'' + (\lambda - p^2)X = 0, \\ &X(x) = e^{kx}, \end{aligned}\right\} \quad -k^4 + q^2 k^2 + (\lambda - p^2) = 0.$$

This is a quadratic equation in k^2. The discriminant of this equation in k^2 is: $q^4 + 4(\lambda - p^2)$. We have to distinguish three cases:

1) $q^4 + 4(\lambda - p^2) > 0;$
2) $q^4 + 4(\lambda - p^2) = 0;$
3) $q^4 + 4(\lambda - p^2) < 0.$

In case 1 we again have three cases:

$$1)\ q^2 > \sqrt{q^4 + 4(\lambda - p^2)};$$
$$2)\ q^2 = \sqrt{q^4 + 4(\lambda - p^2)};$$
$$3)\ q^2 < \sqrt{q^4 + 4(\lambda - p^2)}.$$

Define $E = q^4 + 4(\lambda - p^2),$ so we need to look at the following cases:

1) $E > 0$ and $q^2 > \sqrt{E};$
2) $E > 0$ and $q^2 = \sqrt{E};$
3) $E > 0$ and $q^2 < \sqrt{E};$
4) $E = 0;$
5) $E < 0.$

In each upcoming paragraph a case is worked out.

§3.1.1 Case 1 $E > 0$ and $q^2 > \sqrt{E}$

We now have four real roots, so we take as a solutions:

$$X(x) = C_1 \cosh(k_1 x) + C_2 \sinh(k_1 x) + C_3 \cosh(k_2 x) + C_4 \sinh(k_2 x),$$

with the constants C_1,..,C_4 determined via the boundary conditions (BCs).

After applying the BCs: $X(0) = X(\pi) = X''(0) = X''(\pi) = 0$ a set of 4 equations with 4 unknowns will result. This set only has a nontrivial solution iff the determinant is zero:

$$\det\left(\begin{bmatrix} 1 & 0 & 1 & 0 \\ \cosh(k_1\pi) & \sinh(k_1\pi) & \cosh(k_2\pi) & \sinh(k_2\pi) \\ k_1^2 & 0 & k_2^2 & 0 \\ k_1^2\cosh(k_1\pi) & k_1^2\sinh(k_1\pi) & k_2^2\cosh(k_2\pi) & k_2^2\sinh(k_2\pi) \end{bmatrix}\right) = 0 \rightarrow$$

$$\begin{vmatrix} 1 & 0 & 1 & 0 \\ \cosh(k_1\pi) & \sinh(k_1\pi) & \cosh(k_2\pi) & \sinh(k_2\pi) \\ k_1^2 & 0 & k_2^2 & 0 \\ k_1^2\cosh(k_1\pi) & k_1^2\sinh(k_1\pi) & k_2^2\cosh(k_2\pi) & k_2^2\sinh(k_2\pi) \end{vmatrix}$$

$$= \begin{vmatrix} \sinh(k_1\pi) & \cosh(k_2\pi)-\sinh(k_1\pi) & \sinh(k_2\pi) \\ 0 & k_2^2-k_1^2 & 0 \\ k_1^2\sinh(k_1\pi) & k_2^2\cosh(k_2\pi)-k_1^2\cosh(k_1\pi) & k_2^2\sinh(k_2\pi) \end{vmatrix}$$

$$= \left(k_2^2-k_1^2\right)^2 \sinh(k_1\pi)\sinh(k_2\pi) = 0 \quad \rightarrow \quad k_1 = ni \quad \vee \quad k_2 = ni \quad \vee \quad k_1 = \pm k_2, \quad n \in \mathbb{Z}.$$

The first two complex solutions are in contradiction with the assumption that the roots are real. The last solution $k_1 = \pm k_2$ will lead to the trivial solution because then $\sqrt{q^4 + 4(\lambda - p^2)} = 0$, which is in contradiction with the assumption that $q^4 + 4(\lambda - p^2) > 0$.

§3.1.2 Case 2 $E > 0$ and $q^2 = \sqrt{E}$

Now we have $k_{1,3} = \pm q$ and $k_{2,4} = 0$ we take as a solution:

$$X(x) = C_1 x + C_2 + C_3\cosh(k_1 x) + C_4\sinh(k_1 x).$$

Applying the BCs results in the matrix:

$$\left[\begin{array}{cccc|c} 0 & 1 & 0 & 0 & 0 \\ \pi & 1 & \cosh(k_1\pi) & \sinh(k_1\pi) & 0 \\ 0 & 0 & k_1^2 & 0 & 0 \\ 0 & 0 & k_1^2\cosh(k_1\pi) & k_1^2\sinh(k_1\pi) & 0 \end{array}\right],$$

setting the determinant to zero gives $k_1^4\sinh(k_1\pi) \neq 0,$

so only the trivial solution will result.

§3.1.3 Case 3 $E > 0$ and $q^2 < \sqrt{E}$

$k_{1,3}$ will give two real roots and $k_{2,4}$ two purely imaginary $\pm ai$, with $a = \sqrt{\frac{\sqrt{q^4 + 4(\lambda - p^2)} - q^2}{2}}$, so we take as a solution:

$$X(x) = C_1 \cosh(k_1 x) + C_2 \sinh(k_1 x) + C_3 \cos(ax) + C_4 \sin(ax),$$

Applying the BCs results in the matrix:

$$\left[\begin{array}{cccc|c} 1 & 0 & 1 & 0 & 0 \\ \cosh(k_1\pi) & \sinh(k_1\pi) & \cos(a\pi) & \sin(a\pi) & 0 \\ k_1^2 & 0 & -a^2 & 0 & 0 \\ k_1^2\cosh(k_1\pi) & k_1^2\sinh(k_1\pi) & -a^2\cos(a\pi) & -a^2\sin(a\pi) & 0 \end{array}\right],$$

with its determinant equal to zero leading to:

$$\sinh(k_1\pi)\sin(a\pi)\left(k_1^2 + a^2\right)^2 = 0 \;\rightarrow\; k_1 = ni \;\vee\; a = n \;\vee\; k_1^2 + a^2 = 0.$$

The first solution contradicts with the assumption that k_1 is a real root. The second solution leads to the matrix:

$$\left[\begin{array}{cccc|c} 1 & 0 & 1 & 0 & 0 \\ \cosh(k_1\pi) & \sinh(k_1\pi) & \cos(a\pi) & 0 & 0 \\ k_1^2 & 0 & -a^2 & 0 & 0 \\ k_1^2\cosh(k_1\pi) & k_1^2\sinh(k_1\pi) & -a^2\cos(a\pi) & 0 & 0 \end{array}\right],$$

which means that C_4 is free and $C_1 = C_2 = C_3 = 0$, thus this results in $X(x) = W_n \sin(nx)$ with coefficients W_n.

The third solution isn't possible because both a and k_1 are real.

§3.1.4 Case 4 $E = 0$

If $q^4 + 4(\lambda - p^2) = 0$, then $k_{1,3} = \frac{q}{\sqrt{2}}$, $k_{2,4} = -\frac{q}{\sqrt{2}}$, so we take as a solution:

$$X(x) = C_1 \cosh(kx) + C_2 x\cosh(kx) + C_3 \sinh(kx) + C_4 x\sinh(kx).$$

Applying the BCs results in the matrix:

$$\left[\begin{array}{cccc|c} 1 & 0 & 0 & 0 & 0 \\ \cosh(k\pi) & \pi\cosh(k\pi) & \sinh(k\pi) & \pi\sinh(k\pi) & 0 \\ k^2 & 0 & 0 & 2k & 0 \\ k^2\cosh(k\pi) & 2k\sinh(k\pi)+k^2\pi\cosh(k\pi) & k^2\sinh(k\pi) & 2k\cosh(k\pi)+k^2\pi\sinh(k\pi) & 0 \end{array}\right],$$

setting the determinant to zero gives:

$$-2k\sinh^2(k\pi)\neq 0,$$

so only the trivial solution will result.

§3.1.5 Case 5 $\mathbf{E < 0}$

In this case there are four complex valued roots where they appear in couples and have nonzero imaginary parts. Suppose the roots have the following form: $k_{1,2,3,4}=\pm\nu_1\pm i\nu_2$, with ν_1,ν_2 real-valued and $\nu_2\neq 0$, then we take as a solution:

$$X(x)=C_1\cosh(\nu_1 x)\cos(\nu_2 x)+C_2\sinh(\nu_1 x)\cos(\nu_2 x)+C_3\cosh(\nu_1 x)\sin(\nu_2 x)+C_4\sinh(\nu_1 x)\sin(\nu_2 x).$$

Applying the BCs results in the matrix:

$$\left[\begin{array}{cccc} 1 & 0 & 0 & 0 \\ \cosh(\nu_1\pi)\cos(\nu_2\pi) & \sinh(\nu_1\pi)\cos(\nu_2\pi) & \cosh(\nu_1\pi)\sin(\nu_2\pi) & \sinh(\nu_1\pi)\sin(\nu_2\pi) \\ \nu_1^2-\nu_2^2 & 0 & 0 & 2\nu_1\nu_2 \\ \left(\nu_1^2-\nu_2^2\right)\cosh(\nu_1\pi)\cos(\nu_2\pi)- & \left(\nu_1^2-\nu_2^2\right)\sinh(\nu_1\pi)\sin(\nu_2\pi)- & \left(\nu_1^2-\nu_2^2\right)\cosh(\nu_1\pi)\sin(\nu_2\pi)+ & \left(\nu_1^2-\nu_2^2\right)\sinh(\nu_1\pi)\sin(\nu_2\pi)+ \\ 2\nu_2\nu_1\sinh(\nu_1\pi)\sin(\nu_2\pi) & 2\nu_2\nu_1\cosh(\nu_1\pi)\sin(\nu_2\pi) & 2\nu_1\nu_2\sinh(\nu_1\pi)\cos(\nu_2\pi) & 2\nu_1\nu_2\cosh(\nu_1\pi)\cos(\nu_2\pi) \end{array}\right],$$

setting the determinant to zero leads to:

$$\left(\nu_1^2-\nu_2^2\right)\sinh(\nu_1\pi)\cosh(\nu_1\pi)\sin(\nu_2\pi)\left[\cos(\nu_2\pi)-\sin(\nu_2\pi)\right]+$$
$$2\nu_1\nu_2\left[\sinh^2(\nu_1\pi)\cos^2(\nu_2\pi)+\cosh^2(\nu_1\pi)\sin^2(\nu_2\pi)\right]\neq 0.$$

Thus only trivial solutions will result. Note that ν_1,ν_2 can be deduced by taking the principal part when calculating the root of the complex number (the result is omitted here).

§3.2 The final solution

We proceed with the infinite solutions found in case 1.3. Now the ODE for the time can be solved:

$$\frac{\ddot{T}}{T} = -\lambda \quad \rightarrow \quad \ddot{T} + \lambda_n T = 0 \quad \rightarrow \quad T_n(t) = C_5 \cos(\omega_n t) + C_6 \sin(\omega_n t),$$

with $\omega_n = \sqrt{\lambda_n} = \sqrt{n^4 + q^2 n^2 + p^2}$.

The final solution becomes:

$$w(x,t) = \sum_{n=1}^{\infty} \{G_n \cos(\omega_n t) + H_n \sin(\omega_n t)\} \sin(nx),$$

with initial conditions:

$$w(x,0) = g(x),$$
$$w_t(x,0) = h(x).$$

The coefficients can be determined at t = 0 by using orthogonality of sines and cosines and integrating from 0 to π for x this results in:

$$G_n = \frac{2}{\pi} \int_0^{\pi} g(x) \sin(nx)\, dx,$$
$$H_n = \frac{2}{\pi} \frac{1}{\omega_n} \int_0^{\pi} h(x) \sin(nx)\, dx.$$

Note that we can have (mathematical) problems if the stiffness of the beam goes to zero. We have to look at this problem separately.

§3.3 A string-like model

Suppose we look at a vibrating string-like model or equivalently we let the stiffness of the beam go to zero then the nondimensional PDE:

$$w_{tt} + w_{xxxx} - q^2 w_{xx} + p^2 w = \frac{L}{c\pi\rho A} f(x,t),$$

becomes with new nondimensional parameters (not explicitly shown here):

$$w_{tt} - w_{xx} + a^2 w = \frac{L}{c\pi\rho A} f(x,t).$$

We take f=0 and we use separation of variables: $w(x,t) = X(x)T(t)$,

$$w_{tt} - w_{xx} + a^2 w = 0 \quad \rightarrow \frac{\ddot{T}}{T} = \frac{X'' - a^2 X}{X} = -\lambda \quad \rightarrow$$

$$X'' + \left(\lambda - a^2\right) X = 0 \quad \rightarrow \quad X(x) = C_1 \cos\left(\sqrt{\lambda - a^2} \cdot x\right) + C_2 \sin\left(\sqrt{\lambda - a^2} \cdot x\right),$$
$$\ddot{T} + \lambda T = 0 \quad \rightarrow \quad T(t) = C_3 \cos\left(\sqrt{\lambda} t\right) + C_4 \sin\left(\sqrt{\lambda} t\right).$$

We use fixed ends, so $X(0) = X(\pi) \equiv 0$, which results in

$$0 = \sin\left(\left(\sqrt{\lambda - a^2}\right)\pi\right) \quad \rightarrow \quad \lambda - a^2 = n^2, \; n = 1, 2, 3, \ldots$$

With the assumption that $\lambda > 0.$

Thus the solution is: $w(x,t) = \sum_{n=1}^{\infty} \left\{ G_n \cos(\omega_n t) + H_n \sin(\omega_n t) \right\} \sin(nx)$ with $\omega_n = \sqrt{\lambda_n} = \sqrt{n^2 + a^2}$,

with initial conditions:

$$w(x,0) = g(x),$$
$$w_t(x,0) = h(x).$$

The coefficients can be determined at t = 0 by using orthogonality of sines and cosines and integrating from 0 to π with respect to x which results in:

$$G_n = \frac{2}{\pi} \int_0^{\pi} g(x) \sin(nx)\, dx,$$
$$H_n = \frac{2}{\pi} \frac{1}{\omega_n} \int_0^{\pi} h(x) \sin(nx)\, dx.$$

The model hardly changes: the number of parameters is reduced from two to one which makes upcoming frequency calculations easier to perform.

§3.4 Conclusion

In this chapter separation of variables is performed to solve the O(1)-problem. The beam under consideration is simply supported. The boundary equations leads to a set of equations for the coefficients which eventually lead to a matrix of 4x4.

If the determinant is zero then there are infinite solutions. Several cases for the roots of the equation for the spatial coordinate lead to trivial solutions except for one case. Finally the eigenfunctions and the eigenvalues are derived and a string-like model reduces the number of parameters to one.

4 The $O(\varepsilon^1)$-problem

In chapter 2 we've found that the $O(\varepsilon)$-problem is:

$$O(\varepsilon^1): \quad w_{1_{tt}} + w_{1_{xxxx}} - q^2 w_{1_{xx}} + p^2 w_1 = -2w_{0_{t\tau}} + \left[-\sin(sx - \Omega t) w_{0_t}\right]_t . \tag{4.1}$$

In the last chapter w_0 has been determined, using w_0 the order ε-part $w_1(x,t,\tau)$ can now be determined. The homogenous solution is the same as the solution for w_0. Attention must be paid to the particular solution for unbounded solutions are not wanted.

§4.1 Preventing secular terms

The boundary conditions suggest a solution of the form: $\sum_{n=1}^{\infty} B_n(t,\tau)\sin(nx)$, substituting this solution in the PDE (4.1) gives:

$$\sum_{n=1}^{\infty}\left\{\frac{\partial^2 B_n}{\partial t^2} + \left(n^4 + q^2 n^2 + p^2\right)B_n\right\}\cdot\sin(nx)(-1) =$$

$$\sum_{n=1}^{\infty}\left\{\frac{dG_n}{d\tau}\left(-\sin(\omega_n t)\right) + \frac{dH_n}{d\tau}\cos\left(\omega_n t\right)\right\}\cdot 2\omega_n \sin(nx) +$$

$$\sum_{n=1}^{\infty}\left\{G_n\left(-\sin(\omega_n t)\right) + H_n\cos\left(\omega_n t\right)\right\}\omega_n s\cos\left(sx - \Omega t\right)\sin(nx) +$$

$$\sum_{n=1}^{\infty}\left\{G_n\cos(\omega_n t) + H_n\sin\left(\omega_n t\right)\right\}(-\omega_n^2)\cdot\sin\left(sx - \Omega t\right)\cdot\sin(nx),$$

with $\omega_n = \sqrt{\lambda_n} = \sqrt{n^4 + q^2 n^2 + p^2}$.

Note that the minus signs of RHS are collected and put at the left hand side. Now to get rid of the summations the orthogonality of the sine will be used e.g. multiply with $\frac{2}{\pi}\sin(mx)$ and integrate x from 0 to π gives the result on the next page.

$$\frac{\partial^2 B_m}{\partial t^2} + \left(m^4 + q^2 m^2 + p^2\right) B_m(-1) =$$

$$2\omega_m \left\{ \frac{dG_m}{d\tau}\left(-\sin(\omega_m t)\right) + \frac{dH_m}{d\tau}\cos\left(\omega_m t\right) \right\} +$$

$$\frac{2}{\pi}\sum_{n=1}^{\infty}\left\{G_n \cdot \left(-\sin(\omega_n t)\right) + H_n \cos\left(\omega_n t\right)\right\} \cdot \omega_n s \cdot \int_0^{\pi} \cos\left(sx - \Omega t\right)\sin(nx)\sin(mx)dx +$$

$$\frac{2}{\pi}\sum_{n=1}^{\infty}\left\{G_n \cos(\omega_n t) + H_n \sin\left(\omega_n t\right)\right\} \cdot (-\omega_n^2) \cdot \int_0^{\pi} \sin\left(sx - \Omega t\right) \cdot \sin(nx)\sin(mx)dx.$$

The four cases where the denominator of the result of the integrals is zero will eventually lead to the same conclusions, to that end the analysis of those four cases is omitted. The result of the integrals and more information about the calculation can be found in Appendix section B.

In order to prevent unbounded terms the coefficients of the $\sin(\Omega t)$ and $\cos(\Omega t)$ must be set to zero. It's therefore clear that four distinct cases must considered:

1) $\Omega \neq \omega_N \pm \omega_M$;
2) $\Omega = \omega_N + \omega_M$;
3) $\Omega = \omega_M - \omega_N$;
4) $\Omega = \omega_N - \omega_M$.

Note that in conditions 2 and 3 the assumption remains that $\Omega > 0$ so M > N, the situation that $\Omega < 0$ (with N>M) gives the same result with the only difference that the rivulet moves to the left. So, only three cases have to be checked. Note that all three cases are forms of *internal resonance.*

1) $\Omega \neq \omega_N \pm \omega_M$;
2) $\Omega = \omega_N + \omega_M$;
3) $\Omega = \omega_M - \omega_N$, $M > N$.

§4.1.1 Case 1 $\Omega \neq \omega_N \pm \omega_M$

In this case there are no resonating terms which leads to:

$$\frac{dG_n}{d\tau} = 0 \quad \rightarrow G_n(\tau) = G_n(0) = \frac{2}{\pi}\int_0^{\pi} g(x)\sin(nx)\,dx, \quad \text{for } n = 1,2,3...$$

$$\frac{dH_n}{d\tau} = 0 \quad \rightarrow G_n(\tau) = H_n(0) = \frac{2}{\pi}\frac{1}{\omega_n}\int_0^{\pi} h(x)\sin(nx)\,dx, \quad \text{for } n = 1,2,3...$$

G_n and H_n are thus independent of τ. So, if we start with zero initial energy in the *n*th mode, there will be no energy present up to $O(\varepsilon)$ on a time scale of order $\frac{1}{\varepsilon}$. We say that coupling between the modes is of $O(\varepsilon)$. This allows truncation to those modes that have nonzero initial energy.

§4.1.2 Case 2 $\Omega = \omega_N + \omega_M$

Suppose $\Omega = \omega_N + \omega_M$ for a certain natural numbers N and M. In case 2 the equation to be solved for n and m is:

$$\omega_n + \omega_m = \Omega = \omega_N + \omega_M,$$

leading to n = N and m = M (or m =N and n=M). It's difficult to prove the presence of nontrivial solutions therefore the analysis towards nontrivial solutions is omitted.

$$\begin{cases} \frac{dG_M}{d\tau} = C_1(M,N)\cdot G_N + C_2(M,N)\cdot H_N, \\ \frac{dH_M}{d\tau} = C_2(M,N)\cdot G_N + C_3(M,N)\cdot H_N, \\ \frac{dG_N}{d\tau} = C_1(N,M)\cdot G_M + C_2(N,M)\cdot H_M, \\ \frac{dH_N}{d\tau} = C_2(N,M)\cdot G_M + C_3(N,M)\cdot H_M. \end{cases}$$

with

$$\begin{cases} C_1(i,j) = D(i,j)\cdot\frac{1}{4}\frac{\omega_j}{\omega_i}\left(1-\omega_j\frac{\pi}{L}c\right)\sin(\pi s)(-1)^{i+j+1}, \\ C_2(i,j) = D(i,j)\cdot\frac{1}{4}\frac{\omega_j}{\omega_i}\left(1+\omega_j\frac{\pi}{L}c\right)\left(1+\cos(\pi s)(-1)^{i+j+1}\right), \\ C_3(i,j) = D(i,j)\cdot\frac{1}{4}\frac{\omega_j}{\omega_i}\left(1+\omega_j\frac{\pi}{L}c\right)\sin(\pi s)(-1)^{i+j+1}, \\ D(i,j) = \left(\frac{2}{\pi}\right)\cdot\frac{-2ijs}{(i-j+s)(i-j-s)(i+j+s)(i+j-s)}. \end{cases}$$

Note that for $n \neq N, m \neq M$ or $m \neq N, n \neq M$ the results of §4.1.1 Case 1 apply. The D(i,j) is the result of the integrals multiplied by a constant. The solution of the set ODEs in the above example is instable. To explain this we need to look at the characteristic equation, which is:

$$\lambda^4 - \left(C_1^2 + 2C_2^2 + C_3^2\right)\lambda^2 + \left(C_1^2C_3^2 - 2C_1C_2^2C_3 + C_2^4\right) = 0.$$

This is a fourth order real monic polynomial. A real monic fourth order polynomial $x^4 + ax^3 + bx^2 + cx + d$ is only stable if the coefficients satisfy:

$$\begin{cases} a > 0; \\ b > 0; \\ 0 < c < ab; \\ 0 < d < \dfrac{abc - c^2}{a^2}. \end{cases}$$

Notice that there's no λ^3-term in the characteristic equation! Thus condition a > 0 is violated. Conclusion: the polynomial in not stable e.g. there is at least one eigenvalue with a positive real part.

The case: $\omega_n - \omega_m = \Omega = \omega_N + \omega_M$ is investigated in §4.2.

§4.1.3 Case 3 $\Omega = \omega_M - \omega_N$

Suppose $\Omega = \omega_M - \omega_N$ for a certain natural numbers N and M. In case 3 the equation to be solved for n and m is:

$$\omega_n - \omega_m = \Omega = \omega_M - \omega_N,$$

leading to n = N and m = M (or m =N and n=M).

$$\begin{cases} \dfrac{dG_M}{d\tau} = C_1(M,N)\cdot G_N + C_5(M,N)\cdot H_N, \\ \dfrac{dH_M}{d\tau} = -C_5(M,N)\cdot G_N + C_3(M,N)\cdot H_N, \\ \dfrac{dG_N}{d\tau} = C_1(N,M)\cdot G_M - C_2(N,M)\cdot H_M, \\ \dfrac{dH_N}{d\tau} = C_2(N,M)\cdot G_M + C_3(N,M)\cdot H_M. \end{cases}$$

with $C_5 = D_{ij}\cdot\dfrac{1}{4}\dfrac{\omega_j}{\omega_i}\left(1-\omega_j\dfrac{\pi}{L}c\right)\left(1+\cos(s\pi)(-1)^{i+j+1}\right).$

Here the same conclusion as in §4.1.2 applies e.g. the set of ODEs has an unstable solution.

§4.2 Combination resonances

When two different forms of resonance merge the resonance is called a *combination resonance*. The following form of combinations resonance can occur:

$$\omega_n - \omega_m = \Omega = \omega_N + \omega_M$$

To solve $\omega_n - \omega_m = \omega_N + \omega_M$ with $n > m \geq 1$ an upper bound can be found via an estimation (this approach is similar to that in [15]). This is illustrated via an example; take N = 1 and M = 2, thus the equation to be solved is (introduce $c=p^2$,$b=q^2$):

$$\sqrt{n^4 + bn^2 + c} = \sqrt{m^4 + bm^2 + c} + \sqrt{1 + b + c} + \sqrt{16 + 4b + c}$$

$$= m\sqrt{m^2 + b + \frac{c}{m^2}} + \sqrt{1 + b + c} + 2\sqrt{4 + b + \frac{c}{4}} \quad \Rightarrow$$

$$n\sqrt{n^2 + b + \frac{c}{n^2}} < m\sqrt{n^2 + b + \frac{c}{n^2}} + 1 \cdot \sqrt{n^2 + b + \frac{c}{n^2}} + 2 \cdot \sqrt{n^2 + b + \frac{c}{n^2}}.$$

The last line is valid if:

$$m^2 + \cancel{b} + \frac{c}{m^2} < n^2 + \cancel{b} + \frac{c}{n^2} \quad \Rightarrow \quad \frac{1}{c}\left(m^2 - n^2\right) < \frac{1}{n^2} - \frac{1}{m^2} \quad \Rightarrow \quad \frac{1}{c} < \frac{1}{m^2 n^2}.$$

The supremum lies at m=1, n=2 thus the upper bound found is valid if: $\frac{1}{c} < \frac{1}{4}$.

Now under this assumption the estimation becomes:

$$n\sqrt{n^2 + b + \frac{c}{n^2}} < (m+3)\sqrt{n^2 + b + \frac{c}{n^2}}, \text{ thus } \quad m < n < m+3 \quad \Rightarrow \quad n = m+1 \ \vee \ n = m+2.$$

With $d = \frac{1}{c}$, $f = \frac{b}{c}$ the equation to be analyzed is:

$$\sqrt{dn^4 + fn^2 + 1} = \sqrt{dm^4 + fm^2 + 1} + \sqrt{16d + 4f + 1} + \sqrt{d + f + 1}.$$

Tables 4.1, 4.2 and 4.3 give results for d = 0.24 computed with Matlab, see Appendix section D for the M-code. Note that a great deal of the results can be expressed symbolically (with increasing n these formulas become large), these symbolic formulas are omitted. Table 4.1 gives the result for n = m+1, table 4.2 for n = m+2 and finally table 4.3 $\omega_n - \omega_m = 2\omega_1$ with n = m+1.

n	m	f
2	1	-
3	2	-
4	3	0.0508
5	4	0.9385
6	5	2.0455
7	6	3.3728
8	7	4.9209
9	8	6.6899
10	9	8.6799
11	10	10.8909

n	m	f
3	1	0.1201
4	2	3.5600
5	3	8.0377
6	4	13.7290
7	5	20.6637
8	6	28.8499
9	7	38.2910
10	8	48.9882
11	9	60.9424
12	10	74.1540

n	m	f
2	1	-
3	2	0.1201
4	3	1.8246
5	4	4.0565
6	5	6.8348
7	6	10.1643
8	7	14.0466
9	8	18.4822
10	9	23.4717
11	10	29.0150

Tables 4.1, 4.2 and 4.3: the results are shown respectively for n = m + 1, n = m + 2 and in the last one n = m + 1 for $\omega_n-\omega_m=2\omega_1$.

Note that the values of d and f do **not** have influence on the stability of the system. The estimation shown here is to verify that in certain situations four modes are coupled. It's clear that the analysis performed with two degrees of freedom isn't easy, keeping this in mind the restoring force term is removed in the analysis in chapter 6 and 7.

§4.3 Moment of inertia of rivulet added

One of the assumptions is that the moment of inertia of the rivulet is negligible. In this paragraph the influence of the addition of the moment of inertia to the PDE is investigated. Remember that in this report the rivulet is modeled as a circular cylinder thus for the moment of inertia of the rivulet, we use the moment of inertia of a circular cylinder.

In this paragraph the effect of the moment of inertia is shown by isolating the terms connected to this term. The assumption in this paragraph is that the entire rivulet is a circular cylinder with variable height having a sine wave-like shape, see figure 2.1:

$$I_{\text{rivulet},x} = \frac{\pi R^4}{4} = \frac{\pi D^4}{64} = \frac{\pi}{64}\left(c + \varepsilon \sin\left(\beta(x - \bar{\Omega}t)\right)\right)^4$$

Now we neglect $O(\varepsilon^2)$-terms which results in: $I_{\text{rivulet},x} \approx \frac{\pi}{64} c^4 + \varepsilon \sin\left(\beta\left(x - \bar{\Omega}t\right)\right)$

The term with the flexural rigidity needs to be adjusted:

$$\left(EIw_{xx}\right)_{xx} = EI_{xx}w_{xx} + 2EI_x w_{xxx} + EIw_{xxxx}$$

Inserting the sine function leads to:

$$EI_0 w_{xxxx} + \varepsilon E\left[\sin\left(\beta\left(x - \bar{\Omega}t\right)\right)w_{xxxx} + 2\beta\cos\left(\beta\left(x - \bar{\Omega}t\right)\right)w_{xxx} - \beta^2\sin\left(\beta\left(x - \bar{\Omega}t\right)\right)w_{xx}\right]$$

The term I_0 refers to the moment of inertia of the beam I_{cable} and the constant part of $I_{rivulet}$. The last three terms need to be investigated further for the first term was already taken into account in the original PDE.

We now apply the same steps as in §4.1 for the three terms. After applying orthogonality, substitution of $\sum_{n=1}^{\infty} B_n(t,\tau)\sin(nx)$ and introduction of nondimensional parameters, we get the following product terms:

$$\sum_n \int_0^{\pi} \sin(sx-\Omega t)\sin(nx)\sin(mx)dx \cdot \left(G_n \cos(\omega_n t) + H_n \sin(\omega_n t)\right)$$

$$\sum_n \int_0^{\pi} \cos(sx-\Omega t)\cos(nx)\sin(mx)dx \cdot \left(G_n \cos(\omega_n t) + H_n \sin(\omega_n t)\right)$$

$$\sum_n \int_0^{\pi} \sin(sx-\Omega t)\sin(nx)\sin(mx)dx \cdot \left(G_n \cos(\omega_n t) + H_n \sin(\omega_n t)\right)$$

Note that constant terms have been left out to show the general idea. We see that similar terms like the ones found §4.1.1-§4.1.3! The conclusion of §4.1.2 regarding Routh-Hurwitz remains valid. Therefore the introduction of the moment of inertia of the rivulet doesn't change the outcome: instability.

§4.4 Conclusion

In this chapter the $O(\varepsilon)$-problem is solved under the assumption that the rivulet has a sine wave shape. After removing secular terms via the multiple time scales method a set of ODEs was derived in case the frequency with which the rivulet moves is a combination of eigenfrequencies. In all cases the solution of the set of ODEs proved to be instable.

There are still open problems in the calculation of the frequencies. In §4.1.2 it's already mentioned that we look at the trivial solutions. There can be more, this is also the case for the trivial solutions in §4.1.3 and §4.2.

In the case of combination resonances the situation became difficult . Only specific combinations of the material constants of the beam can lead to resonance. Due to the two parameters p and q, one had to be fixed, in order to show that there can be situation in which four modes are coupled. This situation also led to instability. In the end, the moment of inertia of the rivulet was taken into account to show that the instability isn't changed.

5 The block signal

In this chapter the shape of the rivulet changes to a block form. The analysis is similar to that of the sine -shape in chapter 4. First of all the mass function of the rivulet must be changed. The details for the calculation can be found in the appendix section F.

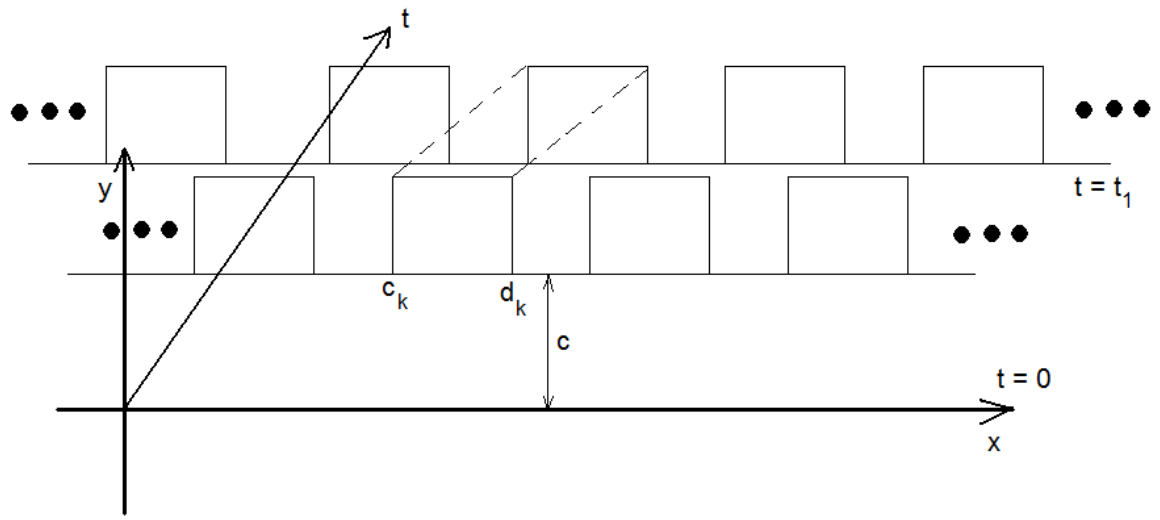

Figure 5.1: A schematic display of the rivulet shape.

§5.1 Model of the block function

The shape of the rivulet is a block signal of infinite length. The height of the block is 1, the width is d_k-c_k =constant. The block signal is elevated a distance c of the x-axis (please don't confuse this c with that of the interval c_k), see figure 5.1.

The corresponding mass function now becomes:

$$m(x,t) = c + \sum_{k=-\infty}^{\infty} Q[x - \Omega(t - c_k)] - Q[x - \Omega(t - d_k)],$$

with Q the step function: $Q(x) = \begin{cases} 1, & x \geq 0, \\ 0, & x < 0. \end{cases}$

The analysis is now fast forwarded to the prevention of secular terms in the $O(\varepsilon)$-part. Upon substitution of the block model function in the nondimensional PDE we get:

$$w_{1_{tt}} + w_{1_{xxxx}} - q^2 w_{1_{xx}} + p^2 w_1 = -2w_{0_{t\tau}} + \left[\left(-\sum_{k=-\infty}^{\infty} Q\left(\frac{L}{\pi} x - \Omega\left(\frac{L}{\pi c} t - c_k \right) \right) - Q\left(\frac{L}{\pi} x - \Omega\left(\frac{L}{\pi c} t - d_k \right) \right) \right) w_{0_t} \right]_t .$$

The boundary conditions suggest a solution of the form: $\sum_{n=1}^{\infty} B_n(t,\tau)\sin(nx)$, substituting this solution in the PDE above gives:

$$\sum_{n=1}^{\infty}\left\{\frac{\partial^2 B_n}{\partial t^2}+\left(n^4+q^2n^2+p^2\right)B_n\right\}\cdot\sin(nx)(-1)=$$

$$\sum_{n=1}^{\infty}\left\{\frac{dG_n}{d\tau}\left(-\sin(\omega_n t)\right)+\frac{dH_n}{d\tau}\cos\left(\omega_n t\right)\right\}\cdot 2\omega_n\sin(nx)+$$

$$\sum_{n=1}^{\infty}\left\{G_n\left(-\sin(\omega_n t)\right)+H_n\cos\left(\omega_n t\right)\right\}\cdot\omega_n\cdot\left(\sum_{k=-\infty}^{\infty}\delta\left(\frac{L}{\pi}x-\Omega\left(\frac{L}{\pi c}t-c_k\right)\right)-\delta\left(\frac{L}{\pi}x-\Omega\left(\frac{L}{\pi c}t-d_k\right)\right)\right)\cdot\sin(nx)+$$

$$\sum_{n=1}^{\infty}\left\{G_n\cos(\omega_n t)+H_n\sin\left(\omega_n t\right)\right\}\cdot(-\omega_n^2)\left(\sum_{k=-\infty}^{\infty}Q\left(\frac{L}{\pi}x-\Omega\left(\frac{L}{\pi c}t-c_k\right)\right)-Q\left(\frac{L}{\pi}x-\Omega\left(\frac{L}{\pi c}t-d_k\right)\right)\right)\cdot\sin(nx),$$

with $\omega_n=\sqrt{\lambda_n}=\sqrt{n^4+q^2n^2+p^2}$.

Now using orthogonality: multiplying both sides with $\frac{2}{\pi}\sin(mx)$ leads to:

$$\frac{\partial^2 B_m}{\partial t^2}+\left(m^4+q^2m^2+p^2\right)B_m(-1)=2\omega_m\left\{\frac{dG_m}{d\tau}\left(-\sin(\omega_m t)\right)+\frac{dH_m}{d\tau}\cos\left(\omega_m t\right)\right\}+$$

$$\sum_{n=1}^{\infty}\left\{G_n\cdot\left(-\sin(\omega_n t)\right)+H_n\cos\left(\omega_n t\right)\right\}\cdot\frac{2}{\pi}\frac{L}{\pi}\cdot I_1(n,t)+\sum_{n=1}^{\infty}\left\{G_n\cos(\omega_n t)+H_n\sin\left(\omega_n t\right)\right\}\cdot\frac{2}{\pi}\frac{L}{\pi}\cdot I_2(n,t).$$

with I_1 and I_2 specified in the appendix section F.

In principle the series with the step and Dirac delta functions are periodic in x and can be rewritten in a Fouries series. By using orthogonality the result of the integrals I_1 and I_2 shows that there can be four cases in which resonance might occur. These four cases are investigated in the next paragraph.

§5.2 Internal resonance

Resonance will occur in four cases:

$$1)\quad a=\omega_N-\omega_M,\quad N>M \quad\leftrightarrow\quad \Omega=c\cdot\frac{\omega_N-\omega_M}{N-M},\quad N>M,$$

$$2)\quad a=\omega_N+\omega_M,\quad N>M \quad\leftrightarrow\quad \Omega=c\cdot\frac{\omega_N+\omega_M}{N-M},\quad N>M,$$

$$3)\quad e=\omega_N-\omega_M,\quad N>M \quad\leftrightarrow\quad \Omega=c\cdot\frac{\omega_N-\omega_M}{N+M},\quad N>M,$$

$$4)\quad e=\omega_N+\omega_M \quad\leftrightarrow\quad \Omega=c\cdot\frac{\omega_N+\omega_M}{N+M},$$

with $a=(n-m)\Omega\frac{1}{c},\ \ e=(n+m)\Omega\frac{1}{c}.$

In case n = m two of the denominators above can become zero, the only resonance case is then $2\Omega m\frac{1}{c}$, the analysis of this case is similar to the ones performed for the four cases above and therefore omitted. Below the sets of ODEs corresponding to the cases above are given.

§5.2.1 Case 1 $a=\omega_N-\omega_M$ with N > M

$$\begin{cases}
2\omega_M\dfrac{dG_M}{d\tau}=\displaystyle\sum_k\left(\frac{\omega_N^2}{4(N-M)}-\frac{\omega_N}{4}\right)(\cos(bc_k)-\cos(bd_k))G_N-\left(\frac{\omega_N^2}{4(N-M)}+\frac{\omega_N}{4}\right)(\sin(bc_k)-\sin(bd_k))H_N,\\
2\omega_M\dfrac{dH_M}{d\tau}=\displaystyle\sum_k-\left(\frac{\omega_N}{4}+\frac{\omega_N^2}{4(N-M)}\right)(\cos(bc_k)-\cos(bd_k))H_N+\left(\frac{\omega_N}{4}+\frac{\omega_N^2}{4(N-M)}\right)(\sin(bc_k)-\sin(bd_k))G_N,\\
2\omega_N\dfrac{dG_N}{d\tau}=\displaystyle\sum_k\left(\frac{\omega_M^2}{4(M-N)}+-\frac{\omega_M}{4}\right)(\cos(bc_k)-\cos(bd_k))G_M+\left(\frac{\omega_M}{4}-\frac{\omega_M^2}{4(M-N)}\right)(\sin(bc_k)-\sin(bd_k))H_M,\\
2\omega_N\dfrac{dH_N}{d\tau}=\displaystyle\sum_k\left(-\frac{\omega_M}{4}+\frac{\omega_M^2}{4(M-N)}\right)(\cos(bc_k)-\cos(bd_k))H_M+\left(-\frac{\omega_M}{4}+\frac{\omega_M^2}{4(M-N)}\right)(\sin(bc_k)-\sin(bd_k))G_M.
\end{cases}$$

Note that the coefficients of G_M, H_M, G_N and H_N are all constants.

§5.2.2 Case 2 $a = \omega_N + \omega_M$ with N > M

$$\begin{cases} 2\omega_M \dfrac{dG_M}{d\tau} = \displaystyle\sum_k \left(\frac{\omega_N}{4} + \frac{\omega_N^2}{4(N-M)} \right) \big(\cos(bc_k) - \cos(bd_k)\big) G_N + \left(\frac{\omega_N}{4} + \frac{\omega_N^2}{4(N-M)} \right) \big(\sin(bc_k) - \sin(bd_k)\big) H_N, \\ 2\omega_M \dfrac{dH_M}{d\tau} = \displaystyle\sum_k \left(-\frac{\omega_N^2}{4(N-M)} + \frac{\omega_N}{4} \right) \big(\cos(bc_k) - \cos(bd_k)\big) H_N + \left(\frac{\omega_N}{4} + \frac{\omega_N^2}{4(N-M)} \right) \big(\sin(bc_k) - \sin(bd_k)\big) G_N, \\ 2\omega_N \dfrac{dG_N}{d\tau} = \displaystyle\sum_k \left(\frac{\omega_M}{4} + \frac{\omega_M^2}{4(M-N)} \right) \big(\cos(bc_k) - \cos(bd_k)\big) G_M + \left(\frac{\omega_M}{4} + \frac{\omega_M^2}{4(M-N)} \right) \big(\sin(bc_k) - \sin(bd_k)\big) H_M, \\ 2\omega_N \dfrac{dH_N}{d\tau} = \displaystyle\sum_k \left(-\frac{\omega_M^2}{4(M-N)} + \frac{\omega_M}{4} \right) \big(\cos(bc_k) - \cos(bd_k)\big) H_M + \left(\frac{\omega_M}{4} + \frac{\omega_M^2}{4(M-N)} \right) \big(\sin(bc_k) - \sin(bd_k)\big) G_M. \end{cases}$$

If Ω isn't equal to any of the four cases mentioned above then the results of §4.2 apply. Case 3 and 4 are in the appendix section F, moreover the sum over k is a finite sum for a given t.

The two sets of differential equations displayed above are instable. Just as in chapter 4 the diagonal of the matrix A of the equation $\dot{\mathbf{x}} = A\mathbf{x}$ contains a zero diagonal and therefore all of the eigenvalues of A are positive, the same conclusion applies to case 3 and case 4 found in the appendix and the case n =m.

§5.3 Conclusion

If the rivulet shape attains a block signal then four cases of resonance can occur. In all of those four cases instability is the result. Apparently this is something that the sine wave and the block shape have in common.

6 A quadratic term

§6.1 Formulating the problem

The PDE described in chapter 1 can be more realistic if the lift and drag forces are added. The magnitude of the angles involved are small and can be thus linearized for small angles. As is explained in §2.3 linearization brought about two terms in the RHS which need further attention.

The quadratic and cubic term in the RHS involve each a different approach, that's why the analysis is separated in two chapters: in this chapter the PDE (1), displayed below, with an quadratic term will be studied, in the next chapter the cubic term will be analyzed. Moreover, as noted in §4.2 the restoring force term is omitted.

In this paragraph the model of the rivulet will be omitted to be added later. The analysis resembles chapter 3 of [11] but differs greatly at some points. The problem under consideration in this chapter is:

$$(1)\begin{cases} \rho A w_{tt} + EI w_{xxxx} - P w_{xx} = \varepsilon w_t^2, & 0 < x < L, t > 0, \\ w(0,t) = w(L,t) \equiv 0, & t \geq 0, \\ w_{xx}(0,t) = w_{xx}(L,t) \equiv 0, & t \geq 0, \\ w(x,0) = g(x), \quad w_t(x,0) = h(x), & 0 < x < L. \end{cases}$$

Using dimensionless variables $\bar{x} = \frac{\pi}{L}x,\ \bar{t} = \frac{\pi}{L}ct,\quad \bar{w} = \frac{\pi}{L}cw,\ \ c = \frac{\pi}{L}\sqrt{\frac{EI}{\rho A}},$ and introducing $\bar{\varepsilon} = \varepsilon\frac{L}{c\pi\rho A},\quad \mu^2 = \frac{P}{\rho A c^2},$ the problem becomes:

$$(2)\begin{cases} \bar{w}_{\bar{t}\bar{t}} + \bar{w}_{\bar{x}\bar{x}\bar{x}\bar{x}} - \mu^2 \bar{w}_{\bar{x}\bar{x}} = \bar{\varepsilon}\bar{w}_{\bar{t}}^2, & 0 < \bar{x} < \pi, \bar{t} > 0, \\ \bar{w}(0,\bar{t}) = \bar{w}(\pi,\bar{t}) \equiv 0, & \bar{t} \geq 0, \\ \bar{w}_{\bar{x}\bar{x}}(0,\bar{t}) = \bar{w}_{\bar{x}\bar{x}}(\pi,\bar{t}) \equiv 0, & \bar{t} \geq 0, \\ \bar{w}(\bar{x},0) = g(\bar{x}), \quad \bar{w}_{\bar{t}}(\bar{x},0) = h(\bar{x}), & 0 < \bar{x} < \pi. \end{cases}$$

If the right hand side is identically equal to zero e.g. $\varepsilon \equiv 0$ then the solution can be determined via separation of variables with the following result:

$$\begin{cases} \bar{w}(\bar{x},\bar{t}) = \sum_{n=1}^{\infty}\left\{G_n \cos(\omega_n \bar{t}) + H_n \sin(\omega_n \bar{t})\right\}\sin(n\bar{x}), \\ G_n = \frac{2}{\pi}\int_0^{\pi} g(\bar{x})\sin\left(n\bar{x}\right)d\bar{x}, \\ H_n = \frac{2}{\pi\omega_n}\int_0^{\pi} h(\bar{x})\sin\left(n\bar{x}\right)d\bar{x}, \\ \lambda_n = n^4 + \mu^2 n^2, \quad \omega_n = \sqrt{\lambda_n}. \end{cases}$$

From this point on the bars will be dropped. Note that w_t^2 is not an 2π-periodic odd function whereas w_{tt}, w_{xxxx} and w_{xx} are. To see this w(x,t) must be analyzed, the boundary conditions imply that w can be written in the form of a sine series:

$$w(x,t) = \sum_{n=1}^{\infty} w_n(t)\sin(nx).$$

Now look at the deratives:

$$w_{tt}(x,t) = \sum_{n=1}^{\infty} w_n''(t)\sin(nx) \to 2\pi\text{-periodic odd function.}$$

$$w_{xxxx}(x,t) = \sum_{n=1}^{\infty} w_n(t)n^4\sin(nx) \to 2\pi\text{-periodic odd function.}$$

$$w_{xx}(x,t) = \sum_{n=1}^{\infty} w_n(t)n^2\sin(nx) \to 2\pi\text{-periodic odd function.}$$

$$w_t^2(x,t) = \sum_{k=1}^{\infty}\sum_{l=1}^{\infty} w_k'(t)w_l' k^2 l^2 \sin(kx)\sin(lx)$$

$$\sin(kx)\sin(lx) = \frac{1}{2}\left\{\cos\left((k-l)x\right) - \cos\left((k+l)x\right)\right\}.$$

Thus this term is even. The addition of a function j(x) makes this part of the RHS odd and a 2π-periodic function: $j(x) = 1$ for $x \in (0,\pi)$ and $j(0) = j(\pi) = 0$. The derivation of the Fourier series is as follows:

$$1 = \sum_{n=1}^{\infty} a_n \sin(nx) \to \quad \int_0^{\pi} \sin(mx)dx = a_m \frac{\pi}{2} \to \quad a_m = \frac{2}{\pi}\int_0^{\pi} \sin(mx)dx = \frac{4}{\pi}\frac{1}{2m+1}, m = 0,1,2,\ldots \to$$

$$j(x) = \frac{4}{\pi}\sum_{n=1}^{\infty}\frac{1}{2m+1}\sin\left((2m+1)x\right), \quad m = 0,1,2,\ldots$$

§6.2 A formal expansion

If a regular asymptotic expansion for w(x,t) is performed, terms of the homogeneous solution will appear in the RHS, to prevent these secular terms the two-time-scales-method is utilized.

$$w(x,t) = \tilde{w}(x,t,\tau) \text{ with } \tau = \varepsilon t.$$

Upon substituting in problem (2) and using the formal expansion
$\tilde{w}(x,t,\tau) = w_0(x,t,\tau) + \varepsilon w_1(x,t,\tau) + \ldots$

we get:

$$\left[w_0 + \varepsilon w_1\right]_{tt} + 2\varepsilon\left[w_0 + \varepsilon w_1\right]_{t\tau} + \varepsilon^2\left[w_0 + \varepsilon w_1\right]_{\tau\tau} + \left[w_0 + \varepsilon w_1\right]_{xxxx} - \mu^2\left[w_0 + \varepsilon w_1\right]_{xx} = \varepsilon\left[\left(w_0 + \varepsilon w_1\right)^2\right]_t.$$

The order 1 and order ε-problem are:

$$O(1): w_{0_{tt}} + w_{0_{xxxx}} - \mu^2 w_{0_{xx}} = 0,$$
$$O(\varepsilon): w_{1_{tt}} + w_{1_{xxxx}} - \mu^2 w_{1_{xx}} = -2w_{0_{t\tau}} + j(x)w_{0_t}^2.$$

The solution for the O(1)-problem is:

$$\begin{cases} w_0(x,t,\tau) = \sum_{n=1}^{\infty}\left\{G_n(\tau)\cos(\omega_n t) + H_n(\tau)\sin(\omega_n t)\right\}\sin(nx), \\ G_n(0) = \frac{2}{\pi}\int_0^{\pi} g(x)\sin\left(nx\right)dx, \\ H_n(0) = \frac{2}{\pi\omega_n}\int_0^{\pi} h(x)\sin\left(nx\right)dx, \\ \lambda_n = n^4 + \mu^2 n^2, \quad \omega_n = \sqrt{\lambda_n}. \end{cases}$$

The boundary conditions imply a solution of the form: $\sum_{n=1}^{\infty} q_n(t,\tau)\sin(nx)$, substitution leads to:

$$\sum_{n=1}^{\infty}\left(\ddot{q}_n + n^4 + \mu^2 n^2 q_n\right)\sin(nx) = \sum_{n=1}^{\infty} -2\omega_n\left(\frac{dG_n}{d\tau}(-\sin(\omega_n t) + \frac{dH_n}{d\tau}\cos(\omega_n t)\right) +$$

$$\sum_{k=1}^{\infty}\sum_{l=1}^{\infty}\sum_{j=0}^{\infty}\frac{1}{2j+1}\dot{q}_m\dot{q}_k\sin(kx)\sin(lx)\sin\left((2j+1)x\right).$$

Note that:

$$\sin(lx)\sin(kx)\sin(dx) = \frac{1}{4}\sin\left((l+k-d)x\right) - \sin\left((l-k-d)x\right) - \sin\left((l+k+d)x\right) + \sin\left((l-k+d)x\right)$$

with d=2j+1, j=0,1,2,...

Now using orthogonality: multiplying both sides with $\frac{2}{\pi}\sin(mx)$ and using the symmetry in l and k we get:

$$\ddot{q}_m + \left(m^4 + \mu^2 m^2\right)q_m = -2\omega_m\left(\frac{dG_m}{d\tau}(-\sin(\omega_m t) + \frac{dH_m}{d\tau}\cos(\omega_m t)\right) +$$
$$\frac{1}{\pi}\left(2\sum_{m=l-k+d} - 2\sum_{m=l-k-d} + \sum_{m=l+k-d} - \sum_{m-l+k+d} - \sum_{m=-l-k+d}\right)\frac{1}{2j+1}\Phi,$$

with $\Phi = \omega_l\omega_k\left\{G_k(-\sin(\omega_k t)) + H_k\cos(\omega_k t)\right\}\left\{G_l(-\sin(\omega_l t)) + H_l\cos(\omega_l t)\right\}$.

The last term can be rewritten using goniometric relations:

$$\Phi = \frac{\omega_l \omega_k}{2}\left\{\left(G_k G_l + H_k H_l\right)\cos\left(\left(\omega_k - \omega_l\right)t\right) + \left(-G_k G_l + H_k H\right)_l \cos\left((\omega_k + \omega_l)t\right)\right\} +$$
$$\frac{\omega_l \omega_k}{2}\left\{-\left(G_k H_l + H_k G_l\right)\sin\left((\omega_k + \omega_l)t\right) + \left(G_k H_l - H_k G_l\right)\sin\left((\omega_l - \omega_k)t\right)\right\}.$$

In the appendix section G it's shown for what cases resonance might occur, for $\mu^2 \leq 45$, by solving Diophantine-like equations:

$$\begin{cases} m = k + l \pm d \ \vee \ m = k - l \pm d \ \vee \ m = -k - l + d, \\ \pm\sqrt{m^4 + m^2\mu^2} = \pm\sqrt{k^4 + k^2\mu^2} \pm \sqrt{l^4 + l^2\mu^2}, \end{cases}$$

with $j, k, l, m \in \mathbb{N},\ d = 2j + 1.$ From the appendix it becomes clear that only specific values of d, k, l, m and μ^2 give rise to internal resonance (mode interactions). In the table below several mode interactions are given.

m,l,k,d	μ^2
3,2,2,1	17/7
4,2,3,1	9,27
5,2,4,1	18,48
6,3,3,1	27,36
6,2,5,1	30,01
7,2,6	43,86
19,6,18	2,028
...	...

Table 6.1: Only for special cases of μ^2 resonance can occur.

§6.3 Addition of the rivulet

In [11] some mode interactions are investigated without the model of the rivulet so we omit these analyses, instead we add the model of the rivulet and review these cases. In a *worst case scenario* resonance will appear for a specific value of μ^2 *and* for the frequency with which the rivulet moves. The scenario with $\mu^2 = \frac{17}{7}$ and $\Omega = \omega_3 + \omega_N$ gives the set of ODE's on the next page.

$$\begin{cases} \dfrac{dG_2}{d\tau} = -\dfrac{16}{21\pi}\dfrac{\omega_2^2}{\omega_3}\left(G_2H_3 - H_2G_3\right), \\ \dfrac{dH_2}{d\tau} = \dfrac{16}{21\pi}\dfrac{\omega_2^2}{\omega_3}\left(G_2G_3 + H_2H_3\right), \\ \dfrac{dG_3}{d\tau} = \dfrac{16}{21\pi}\dfrac{1}{\omega_3}\left(2G_2H_2\right) + C_1G_N + C_2H_N, \\ \dfrac{dH_3}{d\tau} = \dfrac{16}{21\pi}\dfrac{1}{\omega_3}\left(-G_2^2 + H_2^2\right) + C_2G_N + C_3H_N, \\ \dfrac{dG_N}{d\tau} = C_1G_3 + C_2H_3, \\ \dfrac{dH_N}{d\tau} = C_2G_3 + C_3H_3. \end{cases}$$

If $n \neq 2,3,N$ then

$$\frac{\partial G_n}{\partial \tau} = 0 \rightarrow G_n = \frac{2}{\pi}\int_0^{\pi} g(x)\sin\left(nx\right)dx,$$
$$\frac{\partial H_n}{\partial \tau} = 0 \rightarrow H_n = \frac{2}{\pi\omega_n}\int_0^{\pi} h(x)\sin\left(nx\right)dx.$$

The coefficients C_i can be found in the appendix, note that they're dependent on N and M. It's clear that if one specific critical value of μ^2 is analyzed then the presence of the rivulet can bring about the addition of an extra mode, in this case a mode N. Note that Ω has a fixed value and because N is still a parameter there are infinitely many extra modes that can appear for a specific Ω in the case of resonance for a critical value of μ^2.

If Ω is a combination of two frequencies which already are involved in the case for a critical μ^2 no extra modes are added but the set of ODE's will be more complicated. To illustrate we choose $\Omega = \omega_3 + \omega_2$ and the same μ^2 as above:

$$\begin{cases} \dfrac{dG_2}{d\tau} = -\dfrac{16}{21\pi}\dfrac{\omega_2^2}{\omega_3}\left(G_2H_3 - H_2G_3\right) + C_1G_3 + C_2H_3, \\ \dfrac{dH_2}{d\tau} = \dfrac{16}{21\pi}\dfrac{\omega_2^2}{\omega_3}\left(G_2G_3 + H_2H_3\right) + C_2G_3 + C_3H_3, \\ \dfrac{dG_3}{d\tau} = \dfrac{16}{21\pi}\dfrac{1}{\omega_3}\left(2G_2H_2\right) + C_1G_2 + C_2H_2, \\ \dfrac{dH_3}{d\tau} = \dfrac{16}{21\pi}\dfrac{1}{\omega_3}\left(-G_2^2 + H_2^2\right) + C_2G_2 + C_3H_2. \end{cases}$$

The equation solver of Matlab reveals that the only equibrilium point is (0,0,0,0) which is unstable found after linearization.

The next case is m = 4,3,2 with $\mu^2 = 9,27$ the corresponding ODE system with the a rivulet model is:

$$\begin{cases} \dfrac{dG_2}{d\tau} = \dfrac{32}{45\pi}\dfrac{\omega_4\omega_3}{\omega_2}\left(H_3G_4 - G_3H_4\right) + C_1G_3 + C_2H_3, \\ \dfrac{dH_2}{d\tau} = \dfrac{32}{45\pi}\dfrac{\omega_4\omega_3}{\omega_2}\left(G_3G_4 + H_3H_4\right) + C_2G_3 + C_3H_3, \\ \dfrac{dG_3}{d\tau} = \dfrac{32}{45\pi}\dfrac{\omega_2\omega_4}{\omega_3}\left(H_2G_4 - G_2H_4\right) + C_1G_2 + C_2H_2, \\ \dfrac{dH_3}{d\tau} = \dfrac{32}{45\pi}\dfrac{\omega_2\omega_4}{\omega_3}\left(G_2G_4 + H_2H_4\right) + C_2G_2 + C_3H_2, \\ \dfrac{dG_4}{d\tau} = \dfrac{32}{45\pi}\dfrac{\omega_2\omega_3}{\omega_4}\left(G_2H_3 + H_2G_3\right), \\ \dfrac{dH_4}{d\tau} = \dfrac{32}{45\pi}\dfrac{\omega_2\omega_3}{\omega_4}\left(-G_2G_3 + H_2H_3\right). \end{cases}$$

All of the cases above have unstable solutions: the eigenvalues of the linearized system around an equibrilium point has a zero diagonal resulting in an characteristic equation which has violated the Routh-Hurwitz criterium for a polynomial of degree four. This is not the case if $\Omega = 2\omega_M$, if case m=3,2,2 is reviewed with $\Omega = 2\omega_2$ then we get:

$$\begin{cases} \dfrac{dG_2}{d\tau} = -\dfrac{16}{21\pi}\dfrac{\omega_2^2}{\omega_3}\left(G_2H_3 - H_2G_3\right) + C_1G_2 + C_2H_2, \\ \dfrac{dH_2}{d\tau} = \dfrac{16}{21\pi}\dfrac{\omega_2^2}{\omega_3}\left(G_2G_3 + H_2H_3\right) + C_2G_2 + C_3H_2, \\ \dfrac{dG_3}{d\tau} = \dfrac{16}{21\pi}\dfrac{1}{\omega_3}\left(2G_2H_2\right), \\ \dfrac{dH_3}{d\tau} = \dfrac{16}{21\pi}\dfrac{1}{\omega_3}\left(-G_2^2 + H_2^2\right). \end{cases}$$

The Matlab solver reveals that the only "equibrilium point" is $(G_2, H_2, G_3, H_3) = (0, 0, a, b)$ with a and b arbitrary. So an entire plane in 4D is a solution. Figure 6.1 reveals that the solution becomes instable for an initial condition of (0.1, 0.1, 0.1, 0.1) = (G_2,H_2,G_3,H_3).

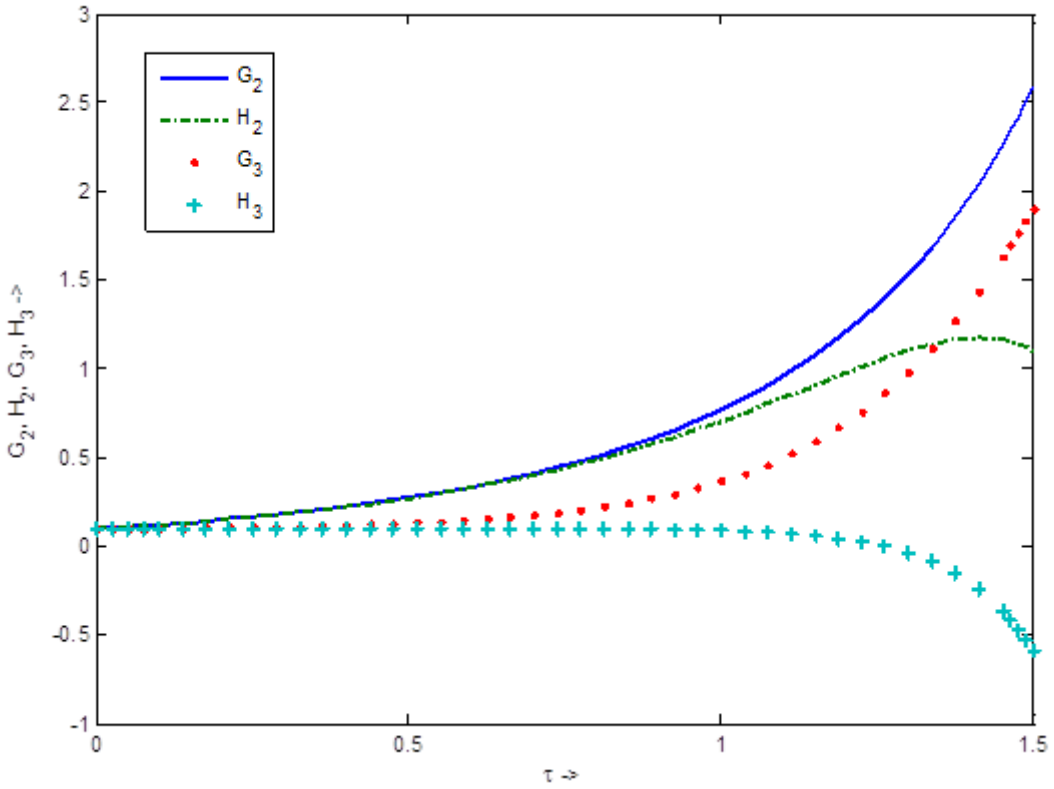

Figure 6.1: With an initial condition (0.1, 0.1, 0.1, 0.1) G_2, H_2, G_3 and H_3 all move away from the origin.

In the case that $\Omega = 2\omega_3$ we get:

$$\begin{cases} \dfrac{dG_2}{d\tau} = -\dfrac{16}{21\pi}\dfrac{\omega_2^2}{\omega_3}\left(G_2H_3 - H_2G_3\right), \\ \dfrac{dH_2}{d\tau} = \dfrac{16}{21\pi}\dfrac{\omega_2^2}{\omega_3}\left(G_2G_3 + H_2H_3\right), \\ \dfrac{dG_3}{d\tau} = \dfrac{16}{21\pi}\dfrac{1}{\omega_3}\left(2G_2H_2\right) + C_1G_3 + C_2H_3, \\ \dfrac{dH_3}{d\tau} = \dfrac{16}{21\pi}\dfrac{1}{\omega_3}\left(-G_2^2 + H_2^2\right) + C_2G_3 + C_3H_3. \end{cases}$$

There's only one equibrilium position (0,0,0,0) found via Matlab, analysis via transformation to polar coordinates, linearization nor finding a first integral gave plausible results. Although the blow-up method is an option a numerical integration was performed which shows instability, see figure 6.2.

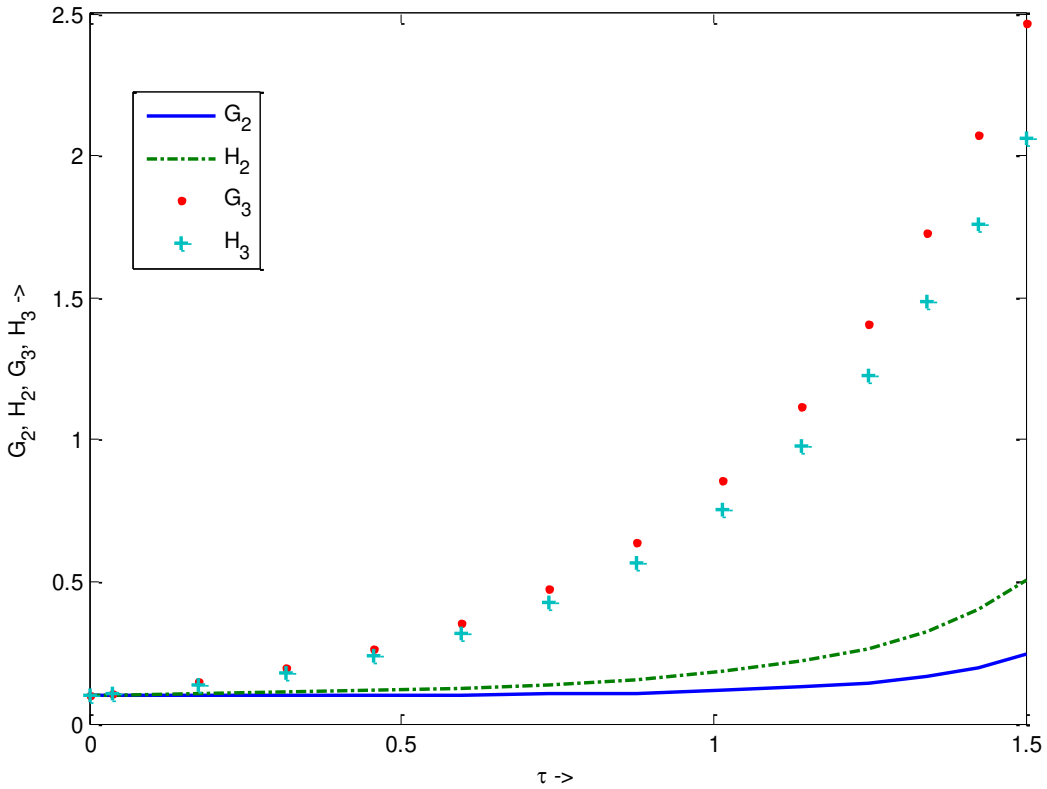

Figure 6.2: With an initial condition (0.1, 0.1, 0.1, 0.1) G_2, H_2, G_3 and H_3 all move away from the origin.

§6.4 Conclusion

Internal resonance will most likely not occur with the addition of the quadratic term: only for special values of μ^2 certain modes will cause resonance. In a worst case scenario the rivulet will cause additional resonance and can even add an extra mode where resonance occurs.

The addition of the model of the rivulet can thus result in internal resonance between four modes. If energy initially is present in one of the modes there will be continuously energy transition between the mode where internal resonance occurs. Truncation to those modes is then valid. In those cases instability will be the result.

7 A cubic term

§7.1 Formulating the problem

As is explained in §2.3 the addition of the lift and drag forces introduces a cubic term on the RHS. In this chapter the PDE (1) below with the cubic term will be analyzed. The analysis resembles chapter 2 of [11] but differs greatly at some points.

For now the model of the rivulet will be omitted. The problem under consideration is the beam satisfying the PDE from chapter 1, simply supported, with an cubic term in the RHS and as noted in §4.5 the restoring force term is omitted:

$$(1)\begin{cases} \rho A w_{tt} + EI w_{xxxx} - P w_{xx} = \varepsilon w_t^3, & 0 < x < L, t > 0, \\ w(0,t) = w(L,t) \equiv 0, & t \geq 0, \\ w_{xx}(0,t) = w_{xx}(L,t) \equiv 0, & t \geq 0, \\ w(x,0) = g(x), \quad w_t(x,0) = h(x), & 0 < x < L. \end{cases}$$

Using dimensionless variables $\bar{x} = \frac{\pi}{L}x,\ \bar{t} = \frac{\pi}{L}ct, \quad \bar{w} = \frac{\pi}{L}cw, \quad c = \frac{\pi}{L}\sqrt{\frac{EI}{\rho A}}$ and introducing $\bar{\varepsilon} = \varepsilon \frac{L}{c\pi\rho A}, \quad \mu^2 = \frac{P}{\rho A c^2}$, the PDE becomes:

$$(2)\begin{cases} \bar{w}_{\bar{t}\bar{t}} + \bar{w}_{\bar{x}\bar{x}\bar{x}\bar{x}} - \mu^2 \bar{w}_{\bar{x}\bar{x}} = \bar{\varepsilon}\bar{w}_{\bar{t}}^3, & 0 < \bar{x} < \pi, \bar{t} > 0, \\ \bar{w}(0,\bar{t}) = \bar{w}(\pi,\bar{t}) \equiv 0, & \bar{t} \geq 0, \\ \bar{w}_{\bar{x}\bar{x}}(0,\bar{t}) = \bar{w}_{\bar{x}\bar{x}}(\pi,\bar{t}) \equiv 0, & \bar{t} \geq 0, \\ \bar{w}(\bar{x},0) = g(\bar{x}), \quad \bar{w}_{\bar{t}}(\bar{x},0) = h(\bar{x}), & 0 < \bar{x} < \pi. \end{cases}$$

If the right hand side is identically equal to zero then the solution can be determined via separation of variables with the following result:

$$\begin{cases} \bar{w}(\bar{x},\bar{t}) = \sum_{n=1}^{\infty} \left\{ G_n \cos(\omega_n \bar{t}) + H_n \sin(\omega_n \bar{t}) \right\} \sin(n\bar{x}), \\ G_n = \frac{2}{\pi}\int_0^{\pi} g(\bar{x}) \sin(n\bar{x})\, d\bar{x}, \\ H_n = \frac{2}{\pi\omega_n}\int_0^{\pi} h(\bar{x}) \sin(n\bar{x})\, d\bar{x}, \\ \lambda_n = n^4 + \mu^2 n^2, \quad \omega_n = \sqrt{\lambda_n}. \end{cases}$$

§7.2 A formal expansion

From this point on the bars will be dropped. If a regular asymptotic expansion for w(x,t) is performed, terms of the homogeneous solution will appear on the RHS, to prevent these secular terms the two-time-scales-method is utilized.

$w(x,t) = \tilde{w}(x,t,\tau)$ with $\tau = \varepsilon t$.

Upon substituting in the PDE (2) and using the formal expansion:

$$\tilde{w}(x,t,\tau) = w_0(x,t,\tau) + \varepsilon w_1(x,t,\tau) + \ldots$$

we get:

$$\left[w_0 + \varepsilon w_1\right]_{tt} + 2\varepsilon\left[w_0 + \varepsilon w_1\right]_{t\tau} + \varepsilon^2\left[w_0 + \varepsilon w_1\right]_{\tau\tau} + \left[w_0 + \varepsilon w_1\right]_{xxxx} - \mu^2\left[w_0 + \varepsilon w_1\right]_{xx} = \varepsilon\left[\left(w_0 + \varepsilon w_1\right)^3\right]_t.$$

The order 1 and order ε-problem are:

$$O(1): w_{0_{tt}} + w_{0_{xxxx}} - \mu^2 w_{0_{xx}} = 0,$$
$$O(\varepsilon): w_{1_{tt}} + w_{1_{xxxx}} - \mu^2 w_{1_{xx}} = -2w_{0_{t\tau}} + w_{0_t}^3.$$

The solution for the O(1)-problem is:

$$\begin{cases} w_0(x,t,\tau) = \sum_{n=1}^{\infty}\left\{G_n(\tau)\cos(\omega_n t) + H_n(\tau)\sin(\omega_n t)\right\}\sin(nx), \\ G_n(0) = \frac{2}{\pi}\int_0^{\pi} g(x)\sin\left(nx\right)dx, \\ H_n(0) = \frac{2}{\pi\omega_n}\int_0^{\pi} h(x)\sin\left(nx\right)dx, \\ \lambda_n = n^4 + \mu^2 n^2, \quad \omega_n = \sqrt{\lambda_n}. \end{cases}$$

The boundary conditions imply a solution of the form: $\sum_{m=1}^{\infty} q_m(t,\tau)\sin(mx)$, substitution of this solution in the $O(\varepsilon)$-problem leads to:

$$\sum_{m=1}^{\infty}\left(\ddot{q}_m + \left(m^4 + \mu^2 m^2\right)q_m\right)\sin(mx) = \sum_{m=1}^{\infty} -2\omega_m\left(\frac{dG_m}{d\tau}(-\sin(\omega_m t) + \frac{dH_m}{d\tau}\cos(\omega_m t)\right) +$$

$$\sum_{j,k,m=1}^{\infty} \dot{q}_j\dot{q}_k\dot{q}_m \sin(mx)\sin(kx)\sin(jx).$$

Note that:

$$\sin(mx)\sin(kx)\sin(jx) = \frac{1}{4}\sin\left(\left(m+k-j\right)x\right) - \sin\left(\left(m-k-j\right)x\right) - \sin\left(\left(m+j+k\right)x\right) + \sin\left(\left(m-k+j\right)x\right).$$

Now using orthogonality: multiplying both sides with $\frac{2}{\pi}\sin(nx)$ and using the symmetry in m,k and j we get the result on the next page.

$$\ddot{q}_n + \omega_n^2 q_n = -2\omega_n \left(\frac{dG_n}{d\tau}(-\sin(\omega_n t) + \frac{dH_n}{d\tau}\cos(\omega_n t) \right) +$$

$$\frac{1}{4}\left(3 \sum_{n=m+k-j} -3 \sum_{n=-m-k+j} - \sum_{n=m+k+j} \right)\Phi,$$

with

$$\Phi = \omega_m \omega_k \omega_j \left(-G_m \sin(\omega_m) + H_m \cos(\omega_m)\right)\left(-G_k \sin(\omega_k) + H_k \cos(\omega_k)\right)\left(-G_j \sin(\omega_j) + H_j \cos(\omega_j)\right).$$

In the appendix it's shown that in order to find the secular terms the following Diophantine-like equations have to be solved.

$$\begin{cases} n = m + k - j \ \vee \ \ n = -m - k + j \ \ \vee \ \ n = m + k + j, \\ \pm\sqrt{n^4 + n^2\mu^2} = \pm\sqrt{m^4 + m^2\mu^2} \pm \sqrt{k^4 + k^2\mu^2} \pm \sqrt{j^4 + j^2\mu^2}. \end{cases}$$

Aside from the trivial solutions only specific combinations of j, k, m, n and will result in solutions of the equations above. In the next paragraph trivial solutions and the additional resonance occurring at $\mu^2 = 2.60$ is investigated and the case when $\mu^2 \neq 2.60$.

§7.3 Modal interaction

The removal of secular terms via the multiple time scale method leads to the following set of ODEs if $\mu^2 \neq 2.60$:

$$\begin{cases} \dfrac{dG_n}{d\tau} = -\dfrac{3}{2} G_n \left(\dfrac{1}{16}\omega_n^2 \left(G_n^2 + H_n^2\right) - \dfrac{1}{4}\displaystyle\sum_{k=1}^{\infty} \dfrac{\omega_k^2}{\omega_n} \left(G_k^2 + H_k^2\right) \right), \\ \dfrac{dH_n}{d\tau} = -\dfrac{3}{2} H_n \left(\dfrac{1}{16}\omega_n^2 \left(G_n^2 + H_n^2\right) - \dfrac{1}{4}\displaystyle\sum_{k=1}^{\infty} \dfrac{\omega_k^2}{\omega_n} \left(G_k^2 + H_k^2\right) \right). \end{cases}$$

Note that 1/16-term is present because the mode interaction (n,n,n) can only be counted once, the factor 3 originates from the summations in §7.2 where the case with one minus sign is counted 3 times. For n = 1,2,3.... We see that if $G_n(0) = H_n(0) = 0$ then $G_n(\tau) = H_n(\tau) = 0, \forall \tau > 0$. So if we start with zero initial energy in the nth mode then there will be no energy present up to $O(\varepsilon)$. This allows truncation to those modes that have nonzero initial energy.

We consider the case n = 1 and n = 3 and we rewrite the above ODEs with the transformation:

$$\bar{G}_n = \omega_n G_n, \ \ \bar{G}_n = \omega_n H_n .$$

With the introduction of polar coordinates:

$$\bar{G}_n = r_n \cos(\phi_n), \quad \bar{H}_n = r_n \sin(\phi_n),$$

with $r_n = r_n(\tau), \quad \phi_n = \phi_n(\tau),$ we get the result on the next page.

$$\begin{cases} \dot{r}_1 = \frac{3}{2} r_1 \left(\frac{3}{16} r_1^2 + \frac{1}{4} r_3^2 \right), \\ \dot{r}_3 = \frac{3}{2} r_3 \left(\frac{1}{4} r_1^2 + \frac{3}{16} r_3^2 \right), \\ r_1^2 \dot{\phi}_1 = 0, \\ r_3^2 \dot{\phi}_3 = 0. \end{cases}$$

In this case there's an O(1)-coupling between the modes 1 and 3, if there's initial energy present in the first mode then in general energy will be transferred to the third mode, thus in that case truncation to one mode is not valid. The two modes have to be taken into account.

The equations may suggest the presence of a limit cycle but a closer inspection of the coupled ODEs shows the presence of only one equibrilium point namely the origin. The only equibrilium point, the origin, is after linearization a degenerate case (eigenvalues are zero). The first integral can be derived by solving the homogeneous differential equation:

$\frac{dr_3}{dr_1} = \frac{r_3}{r_1} \frac{4 + 3\left(\frac{r_3}{r_1}\right)^2}{3 + 4\left(\frac{r_3}{r_1}\right)^2} = F\left(\frac{r_3}{r_1}\right)$ using the transformation $u = \frac{r_3}{r_1}$ a separable differential equation must be solved for: $\frac{dr_1}{r_1} = \frac{du}{F(u) - u}$. An implicit equation for the state plane can then be derived revealing that the origin is a source. Moreover, the phase plot (blue line are trajectories) shows that the origin is a source, see figure 7.1 on the next page for the phase plane generated with Matlab.

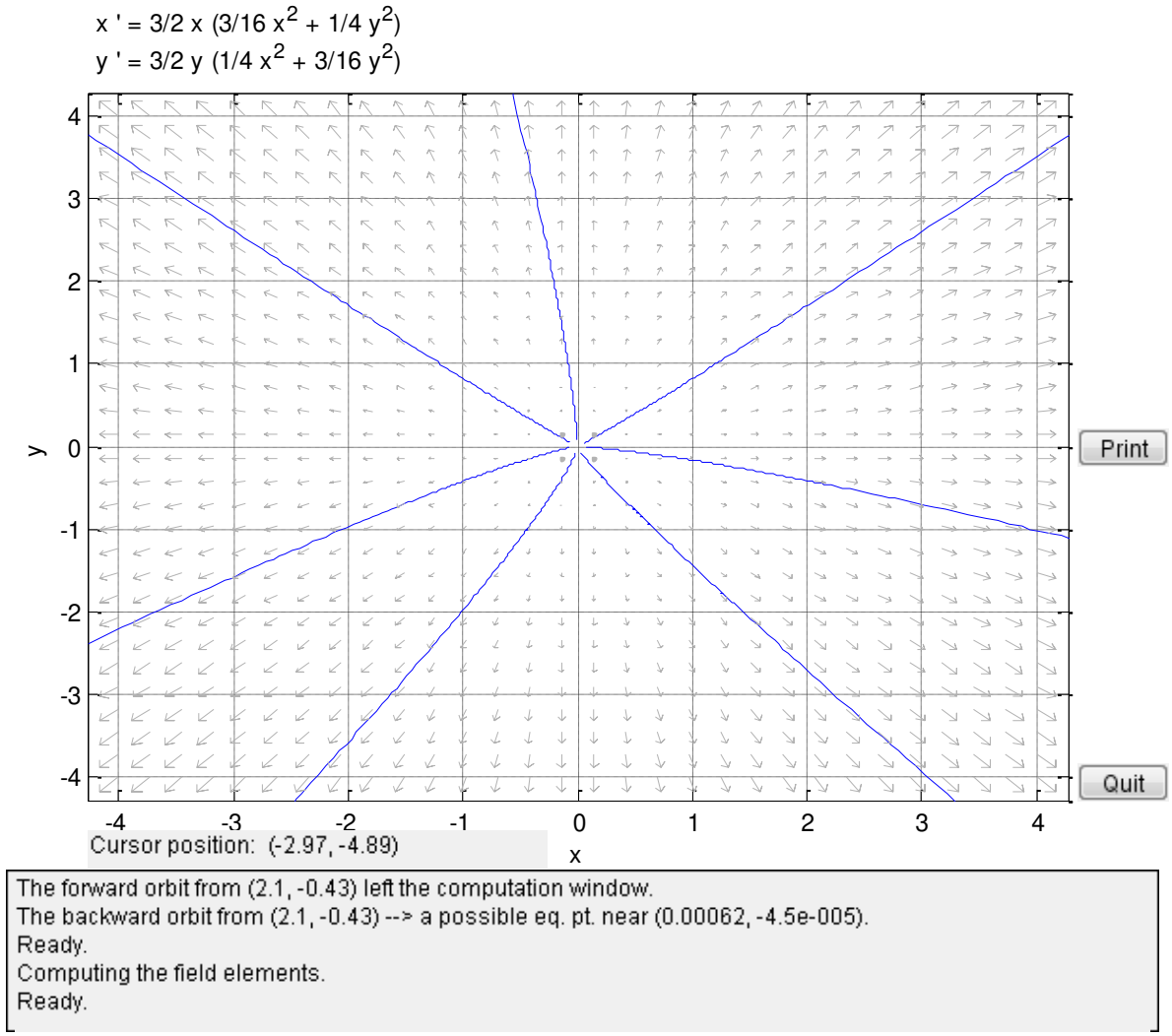

Figure 7.1: The phase plot created with Matlab reveals that the origin is a source.

Things get really hard for the case with m = 3, j = 1, k = 2 and $\mu^2 = 2.60$. The set of differential equations involved when removing secular terms is:

$$\begin{cases} \dfrac{d\bar{G}_n}{d\tau} = -\dfrac{3}{2}\bar{G}_n\left(\dfrac{1}{16}\left(\bar{G}_n^2+\bar{H}_n^2\right)-\dfrac{1}{4}\sum_{k=1}^{\infty}\left(\bar{G}_k^2+\bar{H}_k^2\right)\right)+\dfrac{1}{32}X_n, \\ \dfrac{d\bar{H}_n}{d\tau} = -\dfrac{3}{2}\bar{H}_n\left(\dfrac{1}{16}\left(\bar{G}_n^2+\bar{H}_n^2\right)-\dfrac{1}{4}\sum_{k=1}^{\infty}\left(\bar{G}_k^2+\bar{H}_k^2\right)\right)-\dfrac{1}{32}Y_n. \end{cases}$$

The set of ODEs above is valid for $n \le 4$ with the X and Y-terms. If $n > 5$ the X and Y-terms have to be removed. The X and Y-terms are displayed on the next page.

$$
\begin{aligned}
X_1 &= 2(-\bar{G}_2\bar{G}_3 + \bar{H}_2\bar{H}_3)\bar{G}_4 - 2(\bar{G}_2\bar{G}_3 + \bar{H}_2\bar{H}_3)\bar{H}_4,\\
X_2 &= -2(\bar{G}_1\bar{G}_4 + \bar{H}_1\bar{H}_4)\bar{G}_3 + 2(-\bar{G}_1\bar{H}_4 + \bar{H}_1\bar{H}_4)\bar{H}_3,\\
X_3 &= -2(\bar{G}_1\bar{G}_4 + \bar{H}_1\bar{H}_4)\bar{G}_2 + 2(-\bar{G}_1\bar{H}_4 + \bar{H}_1\bar{G}_4)\bar{H}_2,\\
X_4 &= 2(-\bar{G}_2\bar{G}_3 + \bar{H}_2\bar{H}_3)\bar{G}_1 + 2(\bar{G}_2\bar{H}_3 + \bar{H}_2\bar{G}_3)\bar{H}_1,\\
Y_1 &= 2(\bar{G}_2\bar{H}_3 + \bar{H}_2\bar{G}_3)\bar{G}_4 + 2(-\bar{G}_2\bar{G}_3 + \bar{H}_2\bar{H}_3)\bar{H}_4,\\
Y_2 &= 2(\bar{G}_1\bar{H}_4 - \bar{H}_1\bar{G}_4)\bar{G}_3 - 2(\bar{G}_1\bar{G}_4 + \bar{H}_1\bar{H}_4)\bar{H}_3,\\
Y_3 &= 2(\bar{G}_1\bar{H}_4 - \bar{H}_1\bar{G}_4)\bar{G}_2 - 2(\bar{G}_1\bar{G}_4 + \bar{H}_1\bar{H}_4)\bar{H}_2,\\
Y_4 &= 2(\bar{G}_2\bar{H}_3 + \bar{H}_2\bar{G}_3)\bar{G}_1 - 2(-\bar{G}_2\bar{G}_3 + \bar{H}_2\bar{H}_3)\bar{H}_1.
\end{aligned}
$$

In this case there's an O(1)-coupling between the modes 1, 2, 3 and 4, if there's initial energy present in the first three modes then in general energy will be transferred to the fourth mode thus in that case truncation to three modes is not valid. All four modes have to be taken into account.

The only equibrilium point is the origin which is degenerate, a stability analysis hasn't been performed. Most likely a numerical approach can decide whether the origin is unstable or not.

§7.4 Addition of the rivulet model

We now add the model of the rivulet. It's clear from §7.2 that the number of modes that can cause resonance depends on the amount of modes which have nonzero initial energy. In other words the set of ODEs can become as large as we theoretically can analyze. We start by looking at two modes with nonzero initial energy.

We review the case analyzed earlier but now with the rivulet model:

$$
\begin{cases}
\dfrac{d\bar{G}_1}{d\tau} = \dfrac{1}{2}\bar{G}_1\left(\dfrac{3}{16}\left(\bar{G}_1^2 + \bar{H}_1^2\right) + \dfrac{1}{4}\left(\bar{G}_3^2 + \bar{H}_3^2\right)\right) + C_1G_3 + C_2H_3,\\
\dfrac{d\bar{H}_1}{d\tau} = \dfrac{1}{2}\bar{H}_1\left(\dfrac{3}{16}\left(\bar{G}_3^2 + \bar{H}_3^2\right) + \dfrac{1}{4}\left(\bar{G}_1^2 + \bar{H}_1^2\right)\right) + C_2G_3 + C_3H_3,\\
\dfrac{d\bar{G}_3}{d\tau} = \dfrac{1}{2}\bar{G}_3\left(\dfrac{3}{16}\left(\bar{G}_3^2 + \bar{H}_3^2\right) + \dfrac{1}{4}\left(\bar{G}_1^2 + \bar{H}_1^2\right)\right) + C_1G_1 + C_2H_1,\\
\dfrac{d\bar{H}_3}{d\tau} = \dfrac{1}{2}\bar{H}_3\left(\dfrac{3}{16}\bar{G}_1^2 + \dfrac{1}{4}\left(\bar{G}_3^2 + \bar{H}_3^2\right)\right) + C_2G_1 + C_3H_1.
\end{cases}
$$

It's clear that transforming to polar coordinates won't give better results. There's only one equibrilium point, the origin found with Matlab. This equibrilium point remains unstable as seen from the eigenvalues of the linear approximation which all have positive real parts.

In contrast to the quadratic term in the previous chapter the equation of the set of ODEs can become infinitely large while in agreement with the previous chapter the model of the rivulet can add of mode of resonance. Unfortunately also in this case nothing is changed: the origin remains unstable.

$$
\begin{cases}
\dfrac{d\bar{G}_1}{d\tau} = \dfrac{1}{2}\bar{G}_1\left(\dfrac{3}{16}\left(\bar{G}_1^2+\bar{H}_1^2\right)+\dfrac{1}{4}\left(\bar{G}_3^2+\bar{H}_3^2\right)\right)+C_1G_3+C_2H_3, \\
\dfrac{d\bar{H}_1}{d\tau} = \dfrac{1}{2}\bar{H}_1\left(\dfrac{3}{16}\left(\bar{G}_3^2+\bar{H}_3^2\right)+\dfrac{1}{4}\left(\bar{G}_1^2+\bar{H}_1^2\right)\right)+C_2G_3+C_3H_3, \\
\dfrac{d\bar{G}_3}{d\tau} = \dfrac{1}{2}\bar{G}_3\left(\dfrac{3}{16}\left(\bar{G}_3^2+\bar{H}_3^2\right)+\dfrac{1}{4}\left(\bar{G}_1^2+\bar{H}_1^2\right)\right), \\
\dfrac{d\bar{H}_3}{d\tau} = \dfrac{1}{2}\bar{H}_3\left(\dfrac{3}{16}\bar{G}_1^2+\dfrac{1}{4}\left(\bar{G}_3^2+\bar{H}_3^2\right)\right), \\
\dfrac{dG_N}{d\tau} = C_1G_1+C_2H_1, \\
\dfrac{dH_N}{d\tau} = C_2G_1+C_3H_1.
\end{cases}
$$

The rivulet model added to the 'complicated case' doesn't changes things: the X and Y-terms can don't differ much from the rivulet model and it's likely that the same results for stability will emerge.

§7.5 Conclusion

In contrast to the quadratic term resonance will occur when the cubic term is present in the RHS, irrespective of the material constants. In this case there's an infinite number of modes coupled, though only the modes that have nonzero initial energy are eventually coupled.

For specific values of the material constants extra mode interactions can occur; the analysis can becomes tedious due to a large number of additional terms. If the analysis is directed towards truncation to a few modes, instability is the result. Lastly it is noted that the addition of the rivulet model makes no difference towards the instability, just as in the quadratic case.

8 Conclusions

In this thesis perturbation methods are applied to investigate rain-wind-induced vibrations. The analysis is focused on internal resonances and stability. Hereto a PDE was setup with a small time and space-varying term representing the rivulet. In addition a model was setup including lift and drag forces because small angles are involved linearization proved to be applicable.

Two shapes of the rivulet namely, a sine wave and a block signal, are investigated. The rivulet moves in both shapes to the right. When the mass of the rivulet is added to the PDE the resulting differential equation is a nonautonomous nonlinear differential equation. The mass of the rivulet is small as compared to the mass of the cable and thus can be represented as a disturbance.

The O(1)-problem can be solved with the method of separation of variables. In the $O(\varepsilon)$ -problem secular terms occurred where the need of the method of multiple time scales proved to be essential. When the sine wave was taken as the shape of the rivulet two different values of the excitation frequency of the rivulet result in resonance: $\Omega = \omega_N + \omega_M$ and $\Omega = \omega_M - \omega_N$.

Both of the excitation frequencies lead to an instable solution of the set of ODEs. There can be situations where four modes are coupled but it's difficult to find a general formula which describes the modes involved. In the situation of coupling of four modes the instability remained. The block signal also has four situations where resonance can occur. All four situations lead to instable solutions.

In linearizing the equation where lift and drag forces are present, a quadratic term and a cubic term emerge in the RHS. In chapters 6 and 7 these terms were separately investigated. To simplify the analysis the restoring force term was omitted. The presence of the quadratic term can only lead to resonance for specific values of the material constants. When resonance occurred the solution of the ODEs was instable.

The cubic term also leads to resonance where an infinite number of modes can be involved: the number of modes involved depends on the presence of initial energy. For special cases of the material constants additional modes can be involved just like in the analysis of the quadratic term. In contrast to the quadratic term case, the analysis of stability can become tedious.

9 Future directions

In this chapter recommendations are given so as to continue this research focused on RWIV using perturbation calculus. In §9.1 the absence of the restoring force term in chapters 6 and 7 is discussed. In §9.2 gravity is added to them so that the tensile force becomes a linear function and in §9.3 spring supported boundary conditions are analyzed. In §9.4 damping is discussed and in §9.5 rotations are taken into account. Finally in §9.6 the string-like model is improved.

§9.1 Addition of restoring force term

The analyses in chapters 6 and 7 was simplified by leaving out the restoring force thereby reducing the degrees of freedom to one. With this simplification it was shown how additional cases of resonance can be found. The analysis with two degrees of freedom can be carried out but most likely no general conclusions can be drawn.

The main difficulty lies in solving the Diophantine-like equations with two degrees of freedom p and q and the modes n, m, k and in the cubic case n, m, k, j. An approach can be made by fixing one of the parameters, like in §4.5. A second method is to confine the analysis to certain types of beams/cables where the material constants are related to each other. Then one of the parameters can be expressed in the other thereby reducing the degrees of freedom to one.

§9.2 Addition of gravity

In this section the effect of gravity on the beam is analyzed. The beam, with length L, is now inclined under an angle α, simply supported with a rivulet on top moving to the right, see figure 9.1 below.

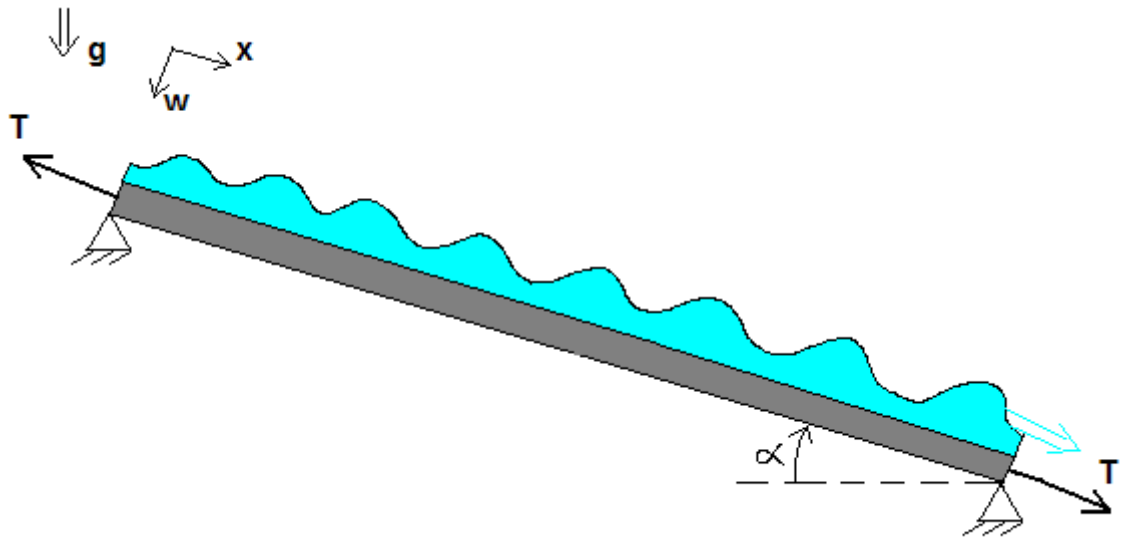

Figure 9.1: The beam earlier analyzed is now inclined and subject to gravity.

The PDE earlier under consideration in chapter 1 is:

$$\rho A w_{tt} = \left(-EI w_{xx}\right)_{xx} + f(x,t) - \left(T w_x\right)_x - \gamma w$$

We remove the restoring force term and the external load f(x,t) and redefine the tension T. The tension T is now adjusted to take the gravity force into account: $T = T_0 - \frac{x}{L} mg \sin(\alpha)$ with m the mass of the beam. The term $\left(Tw_x\right)_x$ needs to be recalculated:

$$\left(Tw_x\right)_x = \left(-\frac{1}{L} mg \sin(\alpha)\right) w_x + \left(T_0 - \frac{x}{L} mg \sin(\alpha)\right) w_{xx}$$

After applying separation of variables we end up with the differential equation:

$X'''' + \left(C_1 x + C_2\right) X'' + X' = 0$, with C_1 and C_2 constants.

This differential equation has a variable coefficient. None of the analytic methods available can be applied to the ODE. We conclude that there's no solution which can be expressed in elementary functions.

There are two ways to progress from this point on. First of all, use can be made of special function. Secondly, the term can be regarded as an disturbance and neglected versus another term, in this case perturbation calculus can be applied to calculate an approximation like done in [17]. For example the $x \sin(\alpha)$ can be small as compared to T_0.

Both method have disadvantages: working with non elementary functions can create difficulties. In addition, the small terms are probably both of a different size, ε_1 and ε_2, if they're almost equal or small enough then perturbation calculus can be applied with $\varepsilon_1 \approx \varepsilon_2 \ll 1$.

§9.3 Spring supported boundary conditions

In paper [5] the authors refer to an analytic description of a cable of a bridge subjected to lift and drag forces. They use spring supported boundary conditions. Moreover in [19] they mention that simulations often use such models, see figure 9.2 and 9.3.

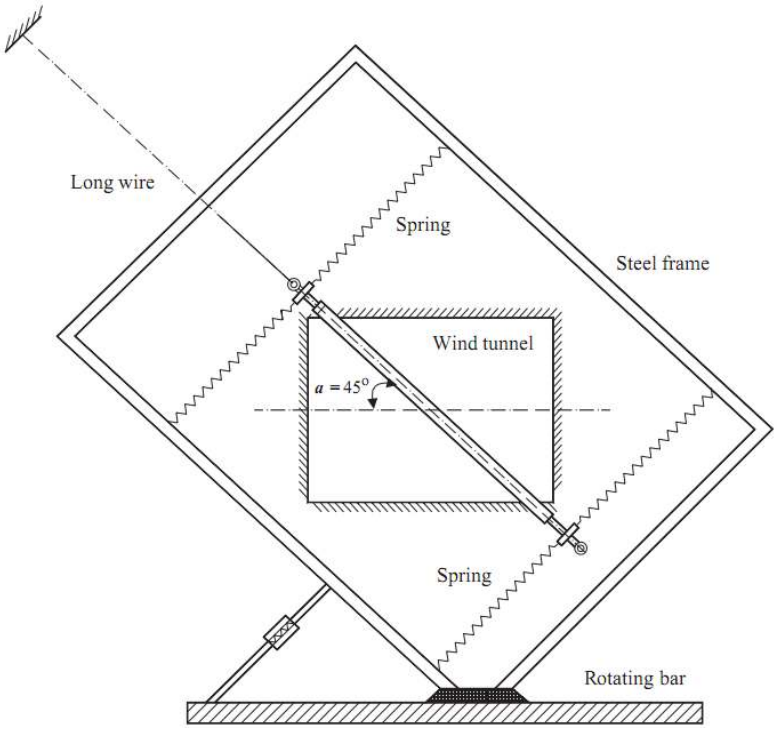

Figure 9.2: Commonly uses test setup for wind-rain-induced cable vibration.

Figure 9.3: New setup for wind-rain-induced cable vibration of [19].

To investigate this situation the set of boundary conditions of the earlier proposed disturbance model must be changed.

The boundary conditions now become:

$$\begin{cases} X''(0) = X''(\pi) \equiv 0, \\ X'''(0) + \gamma X(0) \equiv 0, \\ X'''(\pi) - \gamma X(\pi) \equiv 0. \end{cases}$$

If we look at case 1 of §3.1.1 then the proposed solution for the spatial coordinate becomes:

$$X(x) = C_1 \cosh(k_1 x) + C_2 \sinh(k_1 x) + C_3 \cosh(k_2 x) + C_4 \sinh(k_2 x).$$

Applying the boundary conditions leads to the following result:

$$\left[\begin{array}{cccc|c} k_1^2 & 0 & k_2^2 & 0 & 0 \\ k_1^2 \cosh(k_1\pi) & k_1^2 \sinh(k_1\pi) & k_2^2 \cosh(k_2\pi) & k_2^2 \sinh(k_2\pi) & 0 \\ \gamma & k_1^3 & \gamma & k_2^3 & 0 \\ k_1^3 \sinh(k_1\pi) - \gamma \cosh(k_1\pi) & k_1^3 \cosh(k_1\pi) - \gamma \sinh(k_1\pi) & k_2^3 \sinh(k_2\pi) - \gamma \cosh(k_2\pi) & k_2^3 \cosh(k_2\pi) - \gamma \sinh(k_2\pi) & 0 \end{array}\right]$$

This set of equations only has a nontrivial solutions if the determinant is zero:

$$\begin{aligned} &\sinh(k_1\pi)\sinh(k_2\pi)\left(-\gamma^2 k_1^4 - \gamma^2 k_2^4 - k_1^4 k_2^6 - k_1^6 k_2^4 + 2\gamma^2 k_1^2 k_2^2\right) + \\ &2k_1^5 k_2^5 \left(\cosh(\pi k_1)\cosh(\pi k_2) - 1\right) + \sinh(k_1\pi)\cosh(k_2\pi)(2\gamma k_1^2 k_2^5 + 2\gamma k_1^4 k_2^3) \\ &+ \sinh(k_2\pi)\cosh(k_1\pi)(2\gamma k_1^3 k_2^4 - 2\gamma k_1^5 k_2^2) \end{aligned}$$

Now k_1 and k_2 have to be found satisfying the above equation and it doesn't appear to have a solution other then the trivial solution. The other cases must be checked.

Although the analysis looks straightforward from this point on it doesn't look like this is going to lead to an analytic description. If we look at the free vibrations of a beam satisfying the nondimensional PDE:

$$\frac{\partial^2 w}{\partial t^2} = -\frac{\partial^4 w}{\partial x^4},$$

with one end fixed and the other spring supported then the characteristic equation doesn't lead to an explicit description for the separation constant. On the next pages a calculation performed by Kelly in [16] verifies the assertions.

9.5 Determine the first four natural frequencies for the beam of Fig. 9.14.

Solution:

From Table 9.3, the appropriate boundary conditions are

$$w(0,t) = 0 \qquad \frac{\partial w(0,t)}{\partial x} = 0$$

and

$$\frac{\partial^2 w(1,t)}{\partial^2 x} = 0 \qquad \frac{\partial^3 w(1,t)}{\partial x^3} = \beta w(1,t)$$

where

$$\beta = \frac{kL^3}{EI} = \frac{(2 \times 10^6 \text{ N/m})(1 \text{ m})^3}{(210 \times 10^9 \text{ N/m}^2)(5 \times 10^{-5} \text{ m}^4)} = 0.190$$

Application of the boundary conditions to Eq. (9.76) gives

$$0 = C_1 + C_3$$

$$0 = C_2 + C_4$$

$$0 = -C_1 \cos \lambda^{1/4} - C_2 \sin \lambda^{1/4} + C_3 \cosh \lambda^{1/4} + C_4 \sinh \lambda^{1/4}$$

$$(\lambda^{3/4} \sin \lambda^{1/4} - \beta \cos \lambda^{1/4})C_1 + (-\lambda^{3/4} \cos \lambda^{1/4} - \beta \sin \lambda^{1/4})C_2$$

$$0 = + (\lambda^{3/4} \sinh \lambda^{1/4} - \beta \cosh \lambda^{1/4})C_3 + (\lambda^{3/4} \cosh \lambda^{1/4} - \beta \sinh \lambda^{1/4})C_4$$

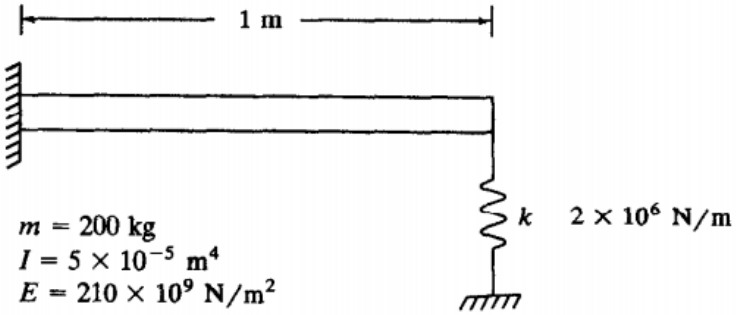

Figure 9.14 Beam of Example 9.5.

Figure 9.4a: A calculation performed by Kelly in [16] shows that there's no analytical solution with these BCs.

which leads to the solvability condition

$$\lambda^{3/4}(1 + \cos\lambda^{1/4}\cosh\lambda^{1/4}) = -\beta(\cosh\lambda^{1/4}\sin\lambda^{1/4} - \cos\lambda^{1/4}\sinh\lambda^{1/4})$$

For $\beta = 0.190$ the first four roots of this equation are

$$\lambda = 13.10, 486.2, 3807.0, 14161.6, \ldots$$

The nondimensional natural frequencies are the square roots of the values of λ that solve the characteristic equation. The dimensional natural frequencies are obtained by noting the relationship between the dimensional time and the nondimensional time and its application to Eq. (9.69),

$$\omega = \sqrt{\lambda\frac{EI}{\rho AL^4}} = 229.1\sqrt{\lambda}$$

The first four natural frequencies for this beam are

$$\omega_1 = 829.2 \text{ rad/s} \qquad \omega_2 = 5051 \text{ rad/s}$$
$$\omega_3 = 14140 \text{ rad/s} \qquad \omega_4 = 27260 \text{ rad/s}$$

Figure 9.4b: A calculation performed by Kelly in [16] shows that there's no analytical solution with these BCs.

Even in this simple situation no explicit solution is available for the eigenfrequencies let alone the more complicated PDE and more complicated boundary conditions: this is something that the future researcher should probably deal with.

§9.4 Addition of damping

In the introduction of this thesis figure I.1 shows the installment of dampers to suppress RWIV. Since the additional dampers have been applied at the Erasmus bridge in Rotterdam, in the Netherlands, no RWIV have been reported. The addition of damping could be investigated so as to find out if this model is stabilized. Perhaps it's best to start without the spring bed and without the tensile force but with the presence of a rivulet moving to the right, see figure 9.5.

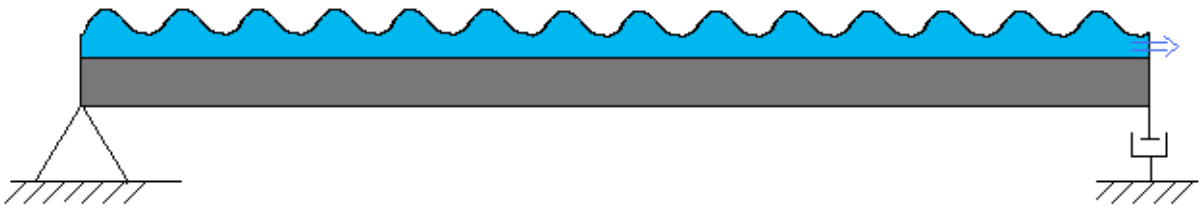

Figure 9.5: The proposed model of the beam without a tensile force and without the spring bed but with a damper.

Hereto the boundary conditions must be changed:

$$\begin{cases} w(0,t) = w_{xx}(0,t) \equiv 0, \\ w_{xx}(\pi,t) = 0, \\ w_{xxx}(\pi,t) = \beta w_t. \end{cases}$$

The damper is modeled as a viscous damper. The boundary condition with the damping is most likely going to prevent an explicit solution of the eigenfrequencies. See [22] for a numerical approach using a taut cable like model.

§9.5 Rotation included

In this thesis the rotations involved when RWIV occurs is completely left out. An idea is to somehow incorporate rotations with the PDE derived in this thesis. Hartono has created a model that included rotations when he investigated RWIV in [21], see figure 9.6.

It could be possible to couple the PDE derived in this thesis to the model with rotations, be it with Hartono's model or an another model. A set of 2 PDE's will result so analysis will become hard yet, with the right simplifications it could lead to new developments.

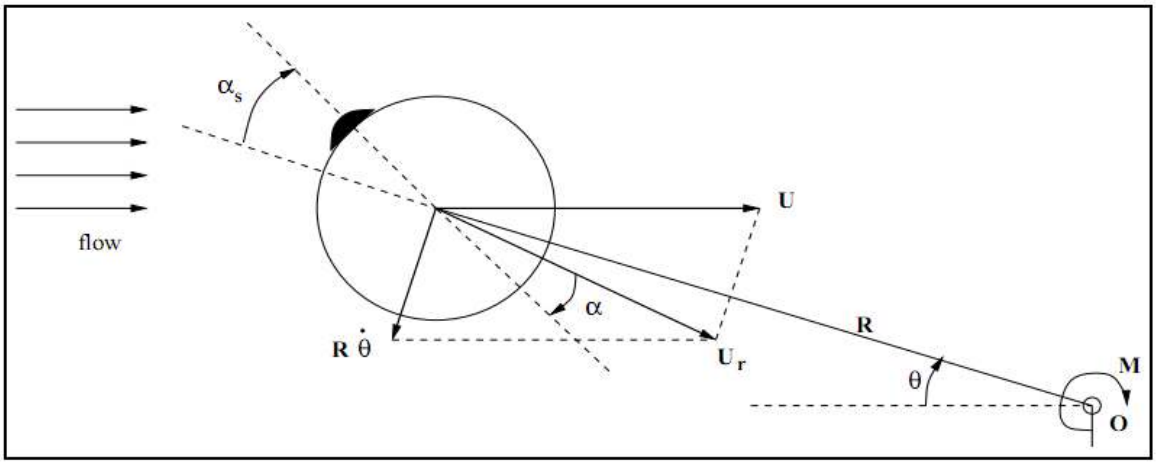

Figure 9.6: A model that describes the rotations involved when RWIV occurs made by Hartono.

§9.6 An improved string-like model

In the string-like model when assuming that the stiffness goes to zero the parameter a^2 is then actually also small and if neglected the PDE:

$$w_{tt} - w_{xx} + a^2 w = \frac{L}{c\pi\rho A} f(x,t), \text{ becomes } w_{tt} - w_{xx} = \frac{L}{c\pi\rho A} f(x,t).$$

What is interesting is that when Diophantine-like equations are analyzed they are surprisingly simple:

$$\omega_n \pm \omega_m = \Omega = \omega_N + \omega_M \rightarrow n \pm m = N \pm M,$$

where the plus or minus signs is appropriate depending on the focus on sum frequencies or a subtraction of two frequencies. Here we see something special: all modes are coupled! The upcoming analysis is thus difficult for the future researcher.

Appendix

Section A: Analysis of the eigenfunctions

Orthogonality eigenfunctions
Define operator H:

$$H(.) = -\frac{d^4}{dx^4}(.) + q^2 \frac{d^2}{dx^2}(.) - p^2(.).$$

From the PDE (1.1) follows that eigenfunctions ϕ_n and ϕ_m both satisfy the BCs:

$$\phi_i(0) = \phi_i(\pi) = \phi_i''(0) = \phi_i''(\pi) = 0, \quad \text{with } i = n, m,$$

and

$$H(\phi_m) + \lambda_m \phi_m = 0,$$
$$H(\phi_n) + \lambda_n \phi_n = 0,$$

with the eigenvalue λ_n belonging to eigenfunction ϕ_n and λ_m belonging to ϕ_m.

Now look at the following integral:

$$\int_0^\pi \phi_m H(\phi_n) - \phi_n H(\phi_m)\, dx = (\lambda_n - \lambda_m) \int_0^\pi \phi_m \phi_n \, dx$$

$$= \int_0^\pi \phi_m \left(-\phi_n'''' + q^2 \phi_n'' - p^2 \phi_n\right) dx - \int_0^\pi \phi_n \left(-\phi_m'''' + q^2 \phi_m'' - p^2 \phi_m\right) dx.$$

Note that with use of the BCs that terms in the brackets continously drop out:

$$\int_0^\pi \phi_m \phi_n'' - \phi_n \phi_m'' \, dx = \cancel{\left[\phi_m \phi_n' - \phi_n \phi_m'\right]_0^\pi} - \int_0^\pi \phi_m' \phi_n' - \phi_n' \phi_m' \, dx = 0.$$

$$\int_0^\pi \phi_m \phi_n'''' - \phi_n \phi_m'''' \, dx = \cancel{\left[\phi_m \phi_n''' - \phi_n \phi_m'''\right]_0^\pi} - \int_0^\pi \phi_m' \phi_n''' - \phi_n' \phi_m''' \, dx = -\cancel{\left[\phi_m' \phi_n'' - \phi_n' \phi_m''\right]_0^\pi} + \int_0^\pi \phi_m'' \phi_n'' - \phi_n'' \phi_m'' \, dx = 0.$$

So we conclude:

$$\left(\lambda_n - \lambda_m\right)\int_0^{\pi} \phi_n \phi_m \, dx = 0 \text{ with } \lambda_n \neq \lambda_m \text{ we get: } \boxed{\int_0^{\pi} \phi_n \phi_m \, dx = 0}$$

Real eigenvalue

Look at λ, ϕ and their complex conjugates $\bar{\lambda}, \bar{\phi}$:

$$H(\phi) + \lambda\phi = 0,$$
$$\overline{H(\phi) + \lambda\phi = 0} \quad \rightarrow \quad H(\bar{\phi}) + \bar{\lambda}\bar{\phi} = 0.$$

where the last step is justified because p^2 and q^2 are real constants.

With the result from above we get:

$$\left(\lambda - \bar{\lambda}\right)\int_0^{L} \phi\bar{\phi} \, dx = \left(\lambda - \bar{\lambda}\right)\int_0^{L} |\phi|^2 \, dx = 0 \quad \rightarrow \quad \boxed{\lambda = \bar{\lambda}}$$

Negative eigenvalue

Multiply the $H(\phi)$ with ϕ and integrate x from 0 to π to get:

$$\int_0^{\pi} \phi H(\phi) \, dx = \int_0^{\pi} \phi\left(-\lambda\phi\right) \, dx = -\lambda\int_0^{\pi} \phi^2 \, dx = \int_0^{\pi} -\phi\phi'''' + q^2\phi\phi'' - p^2\phi^2 \, dx.$$

Note that:

$$\int_0^{\pi} \phi\phi'''' dx = \cancel{\left[\phi\phi'''\right]_0^{\pi}} - \int_0^{\pi} \phi'\phi''' dx = -\cancel{\left[\phi'\phi''\right]_0^{\pi}} + \int_0^{\pi} \left(\phi''\right)^2 \, dx.$$

$$\int_0^{\pi} \phi\phi'' dx = \cancel{\left[\phi\phi'\right]_0^{\pi}} - \int_0^{\pi} \left(\phi'\right)^2 dx.$$

So that we get:

$$\int_0^{L} \phi H(\phi) \, dx = \left\{\int_0^{L} \left(\phi''\right)^2 + q^2\left(\phi'\right)^2 + p^2\phi^2 dx\right\} = \lambda\left\{\int_0^{L} \phi^2 \, dx\right\} > 0 \quad \rightarrow \quad \boxed{\lambda > 0}$$

Section B: Resonance analysis

The integrals are evaluated (for example via writing the sin/cosine in complex e-powers):

$$\int_0^{\pi} \cos\left(sx-\Omega t\right)\sin(nx)\sin(mx)dx = D(m,n)\left(\sin(\Omega t)+(-1)^{n+m}\sin(\pi s-\Omega t)\right)=$$
$$= D(m,n)(-1)^{n+m+1}\sin(\pi s)\cos(\Omega t)+D(m,n)\left(1+(-1)^{n+m+1}\cos(\pi s)\right)\sin(\Omega t),$$

$$\int_0^{\pi} \sin\left(sx-\Omega t\right)\sin(nx)\sin(mx)dx = D(m,n)\left(\cos(\Omega t)-(-1)^{n+m}\cos(\pi s-\Omega t)\right)=$$
$$= D(m,n)\sin(\Omega t)\left(\sin(\pi s)(-1)^{n+m+1}\right)+D(m,n)\cos(\Omega t)\left(1+\cos(\pi s)(-1)^{n+m+1}\right),$$

with

$$D(m,n)=\frac{-2mns}{(m-n+s)(m-n-s)(m+n+s)(m+n-s)}.$$

Now the following relations have to be used:

$$\cos(A)\cos(B)=\frac{1}{2}\left[\cos(A+B)+\cos(A-B)\right],$$

$$\sin(A)\sin(B)=\frac{1}{2}\left[\cos(A-B)-\cos(A+B)\right],$$

$$\sin(A)\cos(B)=\frac{1}{2}\left[\sin(A+B)+\sin(A-B)\right].$$

The result on the next page is found when calculating the product of the result of the integrals with w_t and w_{tt}.

$$\sum_{n=1}^{\infty} -\frac{1}{2} G_n \omega_n \tilde{C}_1 \left\{ \cos\left((\omega_n - \Omega)t\right) - \cos\left((\omega_n + \Omega)t\right) \right\} +$$
$$\frac{1}{2} G_n \omega_n \tilde{C}_2 \left\{ \sin\left((\omega_n + \Omega)t\right) - \sin\left((\omega_n - \Omega)t\right) \right\} +$$
$$\frac{1}{2} H_n \omega_n \tilde{C}_1 \left\{ \sin\left((\omega_n + \Omega)t\right) + \sin\left((\Omega - \omega_n)t\right) \right\} +$$
$$-\frac{1}{2} H_n \omega_n \tilde{C}_2 \left\{ \cos\left((\omega_n + \Omega)t\right) + \cos\left((\omega_n - \Omega)t\right) \right\} +$$

$$\frac{\pi}{L} c(-\omega_n^2) \cdot \frac{1}{2} G_n \tilde{C}_1 \left\{ \cos\left((\omega_n + \Omega)t\right) + \cos\left((\omega_n - \Omega)t\right) \right\} +$$
$$\frac{\pi}{L} c(-\omega_n^2) \cdot \frac{1}{2} G_n \tilde{C}_2 \left\{ \sin\left((\omega_n + \Omega)t\right) + \sin\left((\Omega - \omega_n)t\right) \right\} +$$
$$\frac{\pi}{L} c(-\omega_n^2) \cdot \frac{1}{2} H_n \tilde{C}_1 \left\{ \sin\left((\omega_n + \Omega)t\right) + \sin\left((\omega_n - \Omega)t\right) \right\} +$$
$$\frac{\pi}{L} c(-\omega_n^2) \cdot \frac{1}{2} H_n \tilde{C}_2 \left\{ \cos\left((\omega_n - \Omega)t\right) + \cos\left((\Omega + \omega_n)t\right) \right\},$$

with $\begin{cases} \tilde{C}_1 = D_{nm}\left(1 + \cos(\beta L)(-1)^{n+m+1}\right), \\ \tilde{C}_2 = D_{nm}\left(\sin(\beta L)(-1)^{n+m+1}\right). \end{cases}$

Now if the excitation frequency is fixed then sets of ODE's can result. An eigenvalue analysis can reveal the stability. Suppose $\Omega = \omega_N + \omega_M$ then we get the following set of ODE's:

$$\begin{cases} \dfrac{dG_M}{d\tau} = C_1(M,N) \cdot G_N + C_2(M,N) \cdot H_N, \\ \dfrac{dH_M}{d\tau} = C_2(M,N) \cdot G_N + C_3(M,N) \cdot H_N, \\ \dfrac{dG_N}{d\tau} = C_1(N,M) \cdot G_M + C_2(N,M) \cdot H_M, \\ \dfrac{dH_N}{d\tau} = C_2(N,M) \cdot G_M + C_3(N,M) \cdot H_M. \end{cases}$$

with
$$\begin{cases} C_1(i,j) = D_{ij}\cdot\frac{1}{4}\frac{\omega_j}{\omega_i}\left(1-\omega_j\frac{\pi}{L}c\right)\sin(\beta L)(-1)^{i+j+1}, \\ C_2(i,j) = D_{ij}\cdot\frac{1}{4}\frac{\omega_j}{\omega_i}\left(1+\omega_j\frac{\pi}{L}c\right)\left(1+\cos(\beta L)(-1)^{i+j+1}\right), \\ C_3(i,j) = D_{ij}\cdot\frac{1}{4}\frac{\omega_j}{\omega_i}\left(1+\omega_j\frac{\pi}{L}c\right)\sin(\beta L)(-1)^{i+j+1}, \\ D(i,j) = \left(\frac{2}{\pi}\right)\cdot\frac{-2ij\beta\frac{L}{\pi}}{\left(i-j+\beta\frac{L}{\pi}\right)\left(i-j-\beta\frac{L}{\pi}\right)\left(i+j+\beta\frac{L}{\pi}\right)\left(i+j-\beta\frac{L}{\pi}\right)}. \end{cases}$$

Suppose $\Omega = \omega_M - \omega_N$ with M>N then we get the following set of ODE's:

$$\begin{cases} \frac{dG_M}{d\tau} = C_1(M,N)\cdot G_N + C_5(M,N)\cdot H_N, \\ \frac{dH_M}{d\tau} = -C_5(M,N)\cdot G_N + C_3(M,N)\cdot H_N, \\ \frac{dG_N}{d\tau} = C_1(N,M)\cdot G_M - C_2(N,M)\cdot H_M, \\ \frac{dH_N}{d\tau} = C_2(N,M)\cdot G_M + C_3(N,M)\cdot H_M, \end{cases}$$

with $C_5 = D_{ij}\cdot\frac{1}{4}\frac{\omega_j}{\omega_i}\left(1-\omega_j\frac{\pi}{L}c\right)\left(1+\cos(\beta L)(-1)^{i+j+1}\right).$

Section C: Analytical model for RWIV

In this section additional explanation of the analytical model including lift and drag is given.

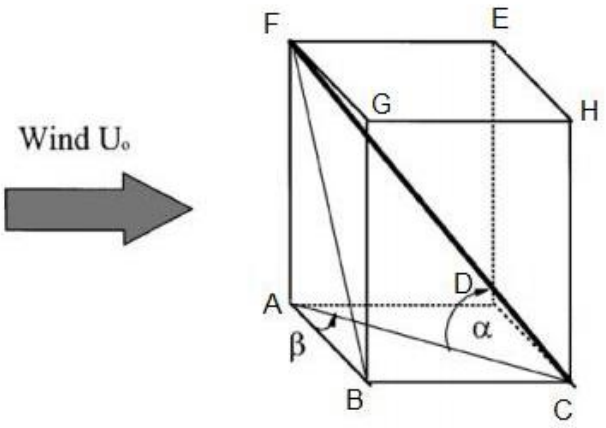

Figure D.1: A representation of an inclined cable of a cable-stayed bridge under influence of wind.

Consider a rigid and uniform cylinder to represent a cable segment with length L, inclined under angle α, spring supported at both ends and the yaw angle of the incident wind is β, as depicted in figure D.1. Since the cylinder isn't perpendicular to the direction of the mean wind U0, one needs to find the component of the mean wind perpendicular to the cylinder denoted by U.

Note that:

$$|BC| = L\cos(\alpha)\cos(\beta),$$
$$|FB| = \sqrt{L^2\cos^2(\alpha)\cos^2(\beta) + L^2\sin^2(\alpha)}.$$

Now look at plane FBC in figure D.2,

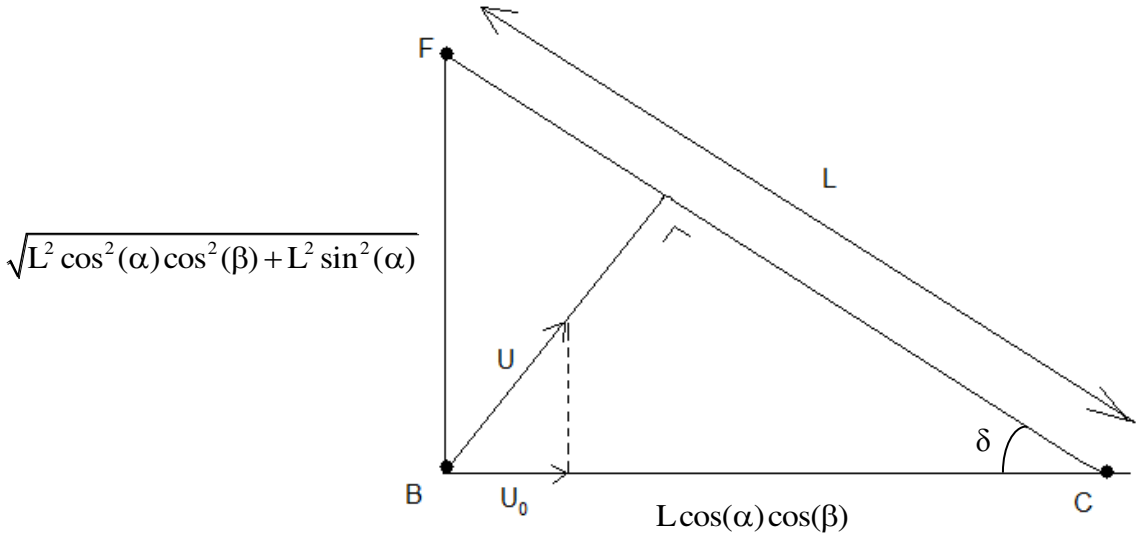

Figure D.2: Plane FBC with a schematic representation of the vector U and U_0.

Note that $\sin(\delta) = \sqrt{\cos^2(\alpha)\cos^2(\beta) + \sin^2(\alpha)}$ so that $U = U_0\sqrt{\cos^2(\alpha)\cos^2(\beta) + \sin^2(\alpha)}.$

Moreover:

$$\cos^2(\alpha)\cos^2(\beta) + \sin^2(\alpha) = \cos^2(\alpha)\cos^2(\beta) + 1 - \cos^2(\alpha) = 1 - \cos^2(\alpha)\sin^2(\beta)$$
$$= \cos^2(\beta) + \sin^2(\beta) - \cos^2(\alpha)\sin^2(\beta) = \cos^2(\beta) + \sin^2(\beta)\sin^2(\alpha).$$

So that: $U = U_0\sqrt{\cos^2(\alpha)\cos^2(\beta) + \sin^2(\alpha)} = U_0\sqrt{\sin^2(\alpha)\sin^2(\beta) + \cos^2(\beta)}.$

The angle of attack is defined as γ, now look a plane ABC in figure D.3:

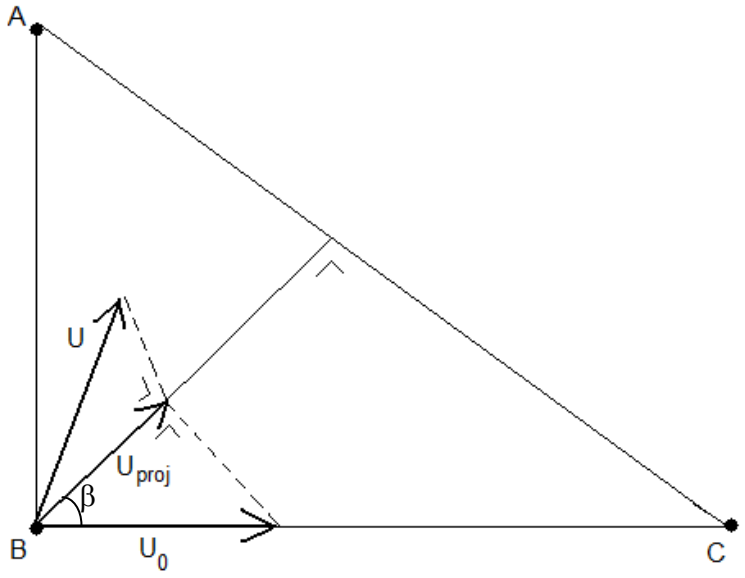

Figure D.3 plane ABC with vectors U, U projected on the plane ABC, and U_0

Note that $\angle ABC = \beta$, $U_{proj} = U_0\cos(\beta)$.

Now look at the small vector triangle below.

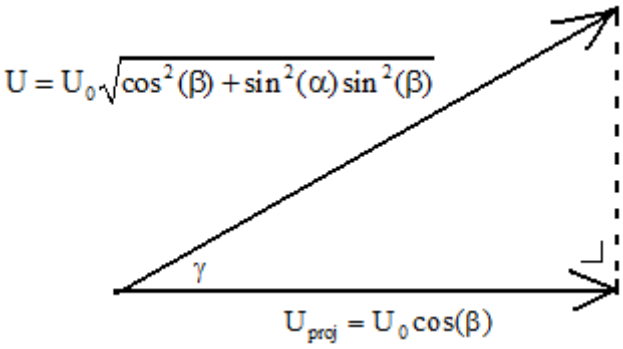

Figure D.4: The upper triangle perpendicular to triangle ABC.

Pythagoras gives the length of the dotted line in figure D.4 as: $U_0 \sin(\alpha)\sin(\beta)$, so that there can be concluded that:

$$\sin(\gamma) = \frac{\sin(\alpha)\sin(\beta)}{\sqrt{\cos^2(\beta) + \sin^2(\alpha)\sin^2(\beta)}}.$$

Section D: M-code to solve combination resonances

The M-code to solve the equation is given below.

```
clear all
clc
syms n m d f B
sol_vec = [];

%== part 1 ==% => rn - rm = r1 + r2 met n = m + 1
B = -sqrt(d*n^4+f*n^2 +1) + sqrt(d*m^4+f*m^2 +1) + sqrt(1^4*d+1^2*f+1)+
sqrt(d*2^4+f*2^2 +1);
B = subs(B,d,0.24);

for q=1:10
B=subs(B,n,q+1);
B=subs(B,m,q);
A=solve(B,'f');
sol_vec(q)=A(1);

% syms n m d f B
B = -sqrt(d*n^4+f*n^2 +1) + sqrt(d*m^4+f*m^2 +1) + sqrt(1^4*d+1^2*f+1)+
sqrt(d*2^4+f*2^2 +1);
B = subs(B,d,0.24);
end
sol_vec'




%== part 2 ==% => rn - rm = r1 + r2 met n = m + 2

B = -sqrt(d*n^4+f*n^2 +1) + sqrt(d*m^4+f*m^2 +1) + sqrt(1^4*d+1^2*f+1)+
sqrt(d*2^4+f*2^2 +1);
B = subs(B,d,0.24);

for q=1:10
B=subs(B,n,q+2);
B=subs(B,m,q);
A=solve(B,'f');
sol_vec2(q)=A(1);

% syms n m d f B
B = -sqrt(d*n^4+f*n^2 +1) + sqrt(d*m^4+f*m^2 +1) + sqrt(1^4*d+1^2*f+1)+
sqrt(d*2^4+f*2^2 +1);
B = subs(B,d,0.24);
end
vpa(sol_vec2')
```

```
%===part 3==% rn - rm = 2*r1
B = -sqrt(d*n^4+f*n^2 +1) + sqrt(d*m^4+f*m^2 +1) + 2*sqrt(1^4*d+1^2*f+1);
B = subs(B,d,0.24);

for q=1:10
B=subs(B,n,q+1);
B=subs(B,m,q);
A=solve(B,'f');
sol_vec3(q)=A(1);


% syms n m d f B
B = -sqrt(d*n^4+f*n^2 +1) + sqrt(d*m^4+f*m^2 +1) + 2*sqrt(1^4*d+1^2*f+1);
B = subs(B,d,0.24);
end
vpa(sol_vec3')
```

Section E: The asymptotic validity of formal approximations

In this paragraph the well-posedness of the problem 2.1-2.4, given below, is considered to verify that the earlier presented asymptotic approximation indeed are justifiable estimates of the exact solution. Because the proof is almost exactly the same as in section 2 of [11], the section has been altered here so as to fit the proof to problem 2.1-2.4.

The problem under consideration is:

$$(2.1)\quad w_{tt} + w_{xxxx} - q^2 w_{xx} + p^2 w = \varepsilon f(x,t,w,\varepsilon), \qquad 0 < x < \pi,\ t > 0,$$

$$(2.2)\quad w(0,t) = w(\pi,t) = 0, \qquad t \geq 0,$$

$$(2.3)\quad w_{xx}(0,t) = w_{xx}(\pi,t) = 0, \qquad t \geq 0,$$

$$(2.4)\quad w(x,0) = w_0(x,\varepsilon),\ w_t(x,0) = w_1(x,\varepsilon), \qquad 0 < x < \pi.$$

Where ε, p, q are constants $\varepsilon \in [-\varepsilon_0, \varepsilon_0]$ and $p, q \geq 0$ and where f,w_0(x), w_1(x) satisfy:

(2.5) f and all first- second- and third-order partial deratives of f with respect to x,w are

$$C([0,\pi]\times[0,\infty]\times\mathbb{R}\times[-\varepsilon_0,\varepsilon_0,\mathbb{R}],\quad f(0,t,0;\varepsilon) = f(\pi,t,0;\varepsilon) \equiv 0,\quad \text{for } t \geq 0.$$

(2.6) $$w_0, \frac{\partial w_0}{\partial x}, \frac{\partial^2 w_0}{\partial x^2}, \frac{\partial^3 w_0}{\partial x^3}, \frac{\partial^4 w_0}{\partial x^4}, w_1, \frac{\partial w_1}{\partial x}, \frac{\partial^2 w_1}{\partial x^2}, \frac{\partial^2 w_1}{\partial x^2} \in C([0,\pi]\times[-\varepsilon_0,\varepsilon_0],\mathbb{R})$$ with

$$w_0(0;\varepsilon) = w_0(\pi,\varepsilon) = \frac{\partial^2 w_0}{\partial x^2}(0;\varepsilon) = \frac{\partial^2 w_0}{\partial x^2}(\pi;\varepsilon) \equiv 0,$$

$$w_1(0;\varepsilon) = w_1(\pi,\varepsilon) = \frac{\partial^2 w_1}{\partial x^2}(0;\varepsilon) = \frac{\partial^2 w_1}{\partial x^2}(\pi;\varepsilon) \equiv 0.$$

(2.7) f and all first- second- and third-order partial deratives of f with respect to x,w are uniformly bounded for all t,x, ε .

A classical solution is defined as a function that is three times differentiable with respect to x on $[0,\pi]\times[0,\infty]$ and for which the fourth order partial derative with respect to x is continuous on $[0,\pi]\times[0,\infty]$ and that satisfies 2.1-2.4 and where f, u_0, u_1 satisfy 2.6-2.8.

An equivalent integral equation will be used in the proof of the well-posedness of the problem 2.1-2.4; this equation is obtained via Green's function G for the linear operator:

$L = \frac{\partial}{\partial t^2} + \frac{\partial}{\partial x^4} - q^2 \frac{\partial}{\partial x^2} + p^2$, with simply supported boundary conditions:

(2.8) $$w(x,t) = \varepsilon \int_0^t \int_0^\pi G(\xi,\tau,x,t) f(\xi,\tau,w;\varepsilon) d\xi d\tau + w_1(x,t;),$$

where $G(\xi,\tau,x,t) = \frac{2}{\pi}\sum_{n=1}^{\infty} \frac{1}{\sqrt{n^4 + q^2 n^2 + p^2}} \sin\left(\sqrt{n^4 + q^2 n^2 + p^2}\,(t-\tau)\right) H(t-\tau)\sin(n\xi)\sin(nx).$

for $\xi, x \in [0,\pi], \tau, t \geq 0$ where H(.) is the Heaviside function. If f=0 then the solution is:

$$w_1(x,t;\varepsilon) = \int_0^\pi \left\{ G(\xi,0,x,t)\, w_1(\xi;\varepsilon) - G_\tau(\xi,0,x,t)\, w_0(\xi;\varepsilon) \right\} d\xi.$$

From the next section it will become clear that there's a constant M_1 such that $|w_1(x,t;\varepsilon)| \leq M_1$. Note that G is uniformly bounded for the range of variables in question. This is because of

$$|G(\xi,\tau,x,t)| = \left| \frac{2}{\pi}\sum_{n=1}^{\infty} \frac{1}{\sqrt{n^4 + q^2 n^2 + p^2}} \sin\left(\sqrt{n^4 + q^2 n^2 + p^2}\,(t-\tau)\right) H(t-\tau)\sin(n\xi)\sin(nx) \right| \leq$$

$$\frac{2}{\pi}\sum_{n=1}^{\infty} \frac{1}{\sqrt{n^4 + q^2 n^2 + p^2}} \leq \frac{2}{\pi}\sum_{n=1}^{\infty} \frac{1}{n^2} = \frac{2}{\pi}\frac{\pi^2}{6} = \frac{\pi}{3},$$

thus there is a constant M_4 such that $|G(\xi,\tau,x,t)| \leq M_4$. Moreover since f and $\frac{\partial f}{\partial w}$ are assumed to be continuous and uniformly bounded for the range of variables in question there are constant M_2, M_3 such that

$$|f(x,t,v_1;\varepsilon)| \leq M_2,$$

(2.14) $$|f(x,t,v_1;\varepsilon) - f(x,t,v_1;\varepsilon)| \leq M_3 \|v_1 - v_2\|.$$

For the proof the solution used is defined in $\Omega_L = \left\{ (x,t) \,|\, 0 \leq x \leq \pi, 0 \leq t \leq L|\varepsilon|^{-1} \right\}$.

In this section we will show that a formal approximation of the solution of the initial-boundary value problem (2.1)–(2.4) is also an asymptotic approximation, i.e., the difference between the formal approximation and the exact solution $\to 0$ as $\epsilon \to 0$, on a timescale of $1/\epsilon$.

Suppose we construct a three times continuously differentiable function $v(x,t;\epsilon)$ on Ω_L with v_{xxxx} continuous and which satisfies

$$v_{tt} + v_{xxxx} - \gamma^2 v_{xx} + p^2 v = \epsilon f(x,t,v;\epsilon) + |\epsilon|^m \mathcal{R}_1(x,t;\epsilon), \qquad 0 < x < \pi,\ t > 0, \tag{3.1}$$

$$v(0,t;\epsilon) = v(\pi,t;\epsilon) = 0, \qquad t \geq 0, \tag{3.2}$$

$$v_{xx}(0,t;\epsilon) = v_{xx}(\pi,t;\epsilon) = 0, \qquad t \geq 0, \tag{3.3}$$

$$v(x,0;\epsilon) = w_0(x;\epsilon) + |\epsilon|^{m-1}\mathcal{R}_2(x;\epsilon) = v_0(x;\epsilon), \qquad 0 < x < \pi, \tag{3.4}$$

$$v_t(x,0;\epsilon) = w_1(x;\epsilon) + |\epsilon|^{m-1}\mathcal{R}_3(x;\epsilon) = v_1(x;\epsilon), \qquad 0 < x < \pi, \tag{3.5}$$

with $m > 1$, where $\epsilon, p, \gamma, f, w_0, w_1$ satisfy the same conditions as in section 2, equations (2.6)–(2.8) and where $\mathcal{R}_1, \mathcal{R}_2, \mathcal{R}_3$ satisfy

(3.6) $\mathcal{R}_1$ and all first-, second-, and third-order partial derivatives of $\mathcal{R}_1$ with respect to x,t are $\in C([0,\pi]\times[0,\infty]\times[-\epsilon_0,\epsilon_0],\mathbb{R})$ and $\mathcal{R}_1(0,t;\epsilon) = \mathcal{R}_1(\pi,t;\epsilon) \equiv 0$ for $t \geq 0$,

(3.7) $$\mathcal{R}_2, \frac{\partial \mathcal{R}_2}{\partial x}, \frac{\partial^2 \mathcal{R}_2}{\partial x^2}, \frac{\partial^3 \mathcal{R}_2}{\partial x^3}, \frac{\partial^4 \mathcal{R}_2}{\partial x^4}, \mathcal{R}_3, \frac{\partial \mathcal{R}_3}{\partial x}, \frac{\partial^2 \mathcal{R}_3}{\partial x^2} \in C([0,\pi]\times[-\epsilon_0,\epsilon_0],\mathbb{R})$$
with $\mathcal{R}_2(0;\epsilon) = \mathcal{R}_2(\pi;\epsilon) = \dfrac{\partial^2 \mathcal{R}_2}{\partial x^2}(0;\epsilon) = \dfrac{\partial^2 \mathcal{R}_2}{\partial x^2}(\pi;\epsilon) \equiv 0$, and
$\mathcal{R}_3(0;\epsilon) = \mathcal{R}_3(\pi;\epsilon) = \dfrac{\partial^2 \mathcal{R}_3}{\partial x^2}(0;\epsilon) = \dfrac{\partial^2 \mathcal{R}_3}{\partial x^2}(\pi;\epsilon) \equiv 0$,

(3.8) $\mathcal{R}_1$ and all first-, second-, and third-order partial derivatives of $\mathcal{R}_1$ with respect to x,t are uniformly bounded for all x,t,ϵ considered.

Figure E.1a: The first part of the (adapted) proof described in [11].

We now state the following theorem.

THEOREM 3.1. *Let v satisfy (3.1)–(3.5), where f, w_0, and w_1 satisfy (2.6)–(2.8) and $\mathcal{R}_1$, $\mathcal{R}_2$, and $\mathcal{R}_3$ satisfy (3.7)–(3.9). Then for $m > 1$ the formal approximation v is an asymptotic approximation (as $\epsilon \to 0$) of the solution w of the nonlinear initial-boundary value problem (2.1)–(2.4), for $(x,t) \in \Omega_L$. This means that, as $\epsilon \to 0$,*

$$|w(x,t) - v(x,t;\epsilon)| = \mathcal{O}(|\epsilon|^{m-1}) \text{ for } 0 \le x \le \pi \text{ and } 0 \le t \le L|\epsilon|^{-1},$$

in which L is a sufficiently small, positive constant independent of ϵ.

Proof. Let $\hat{f}(x,t,v;\epsilon) = f(x,t,v;\epsilon) + |\epsilon|^{m-1}\mathcal{R}_1(x,t;\epsilon)$, and let v_l be given by

$$v_l(x,t;\epsilon) = \int_0^\pi \{G(\xi,0;x,t)v_1(\xi;\epsilon) - G_\tau(\xi,0;x,t)v_0(\xi;\epsilon)\}\, d\xi.$$

Suppose v_l satisfies $\|v_l\| \le \frac{1}{2}M_1$ and $\hat{f}$ satisfies (2.13)–(2.14). It then follows from Theorem 2.1 that (3.1)–(3.5) has a unique, three times continuously differentiable solution $v(x,t;\epsilon)$ on Ω_L, with v_{xxxx} continuous; v is also a solution of the equivalent integral equation

$$(3.9)\quad v(x,t;\epsilon) = \epsilon \int_0^t \int_0^\pi G(\xi,\tau;x,t)\hat{f}(\xi,\tau,v;\epsilon)d\xi d\tau + v_l(x,t;\epsilon) \equiv (Tv)(x,t;\epsilon).$$

Since the functions $\mathcal{R}_1, \mathcal{R}_2, \mathcal{R}_3$ satisfy (3.7)–(3.9), it follows that there are constants M_5, M_6, M_7, M_8 such that

$$(3.10)\quad |\mathcal{R}_1(x,t;\epsilon)| \le M_5,\ |\mathcal{R}_2(x;\epsilon)| \le M_6,\ \left|\frac{\partial^2 \mathcal{R}_2(x;\epsilon)}{\partial x^2}\right| \le M_7,\ |\mathcal{R}_3(x;\epsilon)| \le M_8$$

for all $(x,t) \in \Omega_L$, $\epsilon \in [-\epsilon_0, \epsilon_0]$, and $w, v_1, v_2 \in C_{M_1}(\Omega_L)$. Subtracting the integral equation (3.9) from the integral equation (2.8), using (2.14), (2.15), (3.10), (B.1), the fact that $w, v \in C_{M_1}(\Omega_L)$, and the fact that $(x,t) \in \Omega_L$, it follows that

Figure E.1b: The second part of the (adapted) proof described in [11].

$$
\begin{aligned}
&|w(x,t)-v(x,t;\epsilon)| \\
&\le |\epsilon| \left| \int_0^t \int_0^\pi G(\xi,\tau;x,t) \left\{ f(\xi,\tau,w;\epsilon) - \hat{f}(\xi,\tau,v;\epsilon) \right\} d\xi d\tau \right| + |w_l(x,t;\epsilon) - v_l(x,t;\epsilon)| \\
&\le |\epsilon| \left| \int_0^t \int_0^\pi G(\xi,\tau;x,t) \left\{ f(\xi,\tau,w;\epsilon) - f(\xi,\tau,v;\epsilon) \right\} d\xi d\tau \right| \\
&\quad + |\epsilon|^m \left| \int_0^t \int_0^\pi G(\xi,\tau;x,t) \mathcal{R}_1(\xi,\tau;\epsilon) d\xi d\tau \right| \\
&\quad + \left| \int_0^\pi G(\xi,0;x,t) \left\{ w_1(\xi;\epsilon) - v_1(\xi;\epsilon) \right\} d\xi \right| \\
&\quad + \left| \int_0^\pi G_\tau(\xi,0;x,t) \left\{ w_0(\xi;\epsilon) - v_0(\xi;\epsilon) \right\} d\xi \right| \\
&\le |\epsilon| \left| \int_0^t \int_0^\pi |G(\xi,\tau;x,t)| \, |f(\xi,\tau,w;\epsilon) - f(\xi,\tau,v;\epsilon)| d\xi d\tau \right| \\
&\quad + |\epsilon|^m \left| \int_0^t \int_0^\pi |G(\xi,\tau;x,t)| \, |\mathcal{R}_1(\xi,\tau;\epsilon)| d\xi d\tau \right| \\
&\quad + |\epsilon|^{m-1} \left| \int_0^\pi |G(\xi,0;x,t)| \, |\mathcal{R}_3(\xi;\epsilon)| d\xi \right| + |\epsilon|^{m-1} \left| \int_0^\pi G_\tau(\xi,0;x,t) \, \mathcal{R}_2(\xi;\epsilon) d\xi \right| \\
&\le |\epsilon| \left| \int_0^t \int_0^\pi M_4 M_3 \|w-v\| d\xi d\tau \right| + |\epsilon|^m \left| \int_0^t \int_0^\pi M_4 M_5 d\xi d\tau \right| \\
&\quad + |\epsilon|^{m-1} \left| \int_0^\pi M_4 M_8 d\xi \right| + |\epsilon|^{m-1} \pi^2 \max_{0 \le x \le \pi} \left\{ p |\mathcal{R}_2(x;\epsilon)| + \left| \frac{\partial^2 \mathcal{R}_2(x;\epsilon)}{\partial x^2} \right| \right\} \\
&\le |\epsilon| t \pi M_3 M_4 \|w-v\| + |\epsilon|^m t \pi M_4 M_5 + |\epsilon|^{m-1} \pi \left(M_4 M_8 + \pi p M_6 + \pi M_7 \right) \\
&\le \pi L M_3 M_4 \|w-v\| + |\epsilon|^{m-1} \pi \left(L M_4 M_5 + M_4 M_8 + \pi p M_6 + \pi M_7 \right) \\
&\le k \|w-v\| + |\epsilon|^{m-1} \pi \left(L M_4 M_5 + M_4 M_8 + \pi p M_6 + \pi M_7 \right)
\end{aligned}
$$

for all $(x,t) \in \Omega_L$ and with $0 < k < 1$. If the maximum of $|w-v|$ on the left-hand side is taken for $(x,t) \in \Omega_L$, we obtain

$$
\|w-v\| \le |\epsilon|^{m-1} \frac{\pi}{1-k} \left(L M_4 M_5 + M_4 M_8 + \pi p M_6 + \pi M_7 \right).
$$

So, for $(x,t) \in \Omega_L$, $|w(x,t) - v(x,t;\epsilon)| = \mathcal{O}(|\epsilon|^{m-1})$ as $\epsilon \to 0$. Hence, for $m > 1$ the function v is an asymptotic approximation (as $\epsilon \to 0$) of the solution w of the initial-boundary value problem (2.1)–(2.4). This completes the proof. □

Figure E.1c: The third and final part of the (adapted) proof described in [11].

Energy and boundedness of the solution

The operator L is self-adjoint and we know that $L(G)=\delta, L(w)=\varepsilon f$ and with usage of the integral

$\int_t\int_D wL^*(G)-GL(w)\ dVdt=0,$ we can find the equivalent integral equation via integration by parts with use of the boundary conditions.

Now multiply the PDE $G_{\tau\tau}+G_{\xi\xi\xi\xi}-q^2G_{\xi\xi}+p^2G=\delta(x-\xi,t-\tau)$ with w and integrate ξ over $0\le\xi\le\pi$ and τ over $0\le\tau\le t$ combined with the initial and boundary conditions for w and G. Below each of the terms is derived:

$$\int_0^t G_{\tau\tau}w\ d\tau=\left[G_\tau w\right]_0^t-\int_0^t G_\tau w_t d\tau=\left(\cancel{G_\tau w|_{(\xi,t)}}-G_\tau w_0\right)-\left[Gw_\tau\right]_0^t+\int_0^t Gw_{\tau\tau}dt$$

$$=\cancel{-Gw_\tau|_{(\xi,t)}}+Gw_1-G_\tau w_0+\int_0^t Gw_{\tau\tau}dt.$$

Where the terms drop out because of the causality of the green function G. In the derivation of the other terms the boundary conditions will be invoked:

$$\int_0^\pi G_{\xi\xi\xi\xi\xi}wd\xi=\cancel{G_{\xi\xi\xi\xi}w|_0^\pi}-\int_0^\pi G_{\xi\xi\xi\xi}w_\xi d\xi=\cancel{-G_{\xi\xi\xi}w_\xi|_0^\pi}+\int_0^\pi G_{\xi\xi}w_{\xi\xi}d\xi.$$

$$\int_0^\pi G_{\xi\xi}w_{\xi\xi}d\xi=\cancel{G_\xi w_{\xi\xi}|_0^\pi}-\int_0^\pi G_\xi w_{\xi\xi\xi}d\xi=\cancel{-Gw_{\xi\xi\xi}|_0^\pi}+\int_0^\pi Gw_{\xi\xi\xi\xi}d\xi.$$

$$\int_0^\pi G_{\xi\xi}w\ d\xi=\cancel{G_\xi w|_0^\pi}-\int_0^\pi G_\xi w_\xi d\xi=-Gw_\xi|_0^\pi+\int_0^\pi Gw_{\xi\xi}d\xi.$$

$$\int_0^\pi\int_0^t \delta(x-\xi,t-\tau)wd\tau d\xi=w(x,t).$$

Now we get:

$$w(x,t)=\int_0^t\int_0^\pi G(\xi,\tau,x,t)\left(w_{tt}+w_{\xi\xi\xi\xi}-q^2w_{\xi\xi}+p^2w\right)d\xi d\tau+\int_0^\pi G(\xi,0,x,t)w_1-G_\tau(\xi,0,x,t)w_0\ d\xi\ \rightarrow$$

$$w(x,t)=\varepsilon\int_0^t\int_0^\pi G(\xi,\tau,x,t)f\left(\xi,\tau,w(\xi,\tau),\varepsilon\right)d\xi d\tau+\int_0^\pi G(\xi,0,x,t)w_1-G_\tau(\xi,0,x,t)w_0\ d\xi.$$

Note that Green function can be found explicitly by solving the following problem:

$$
\begin{aligned}
&G_{tt} + G_{xxxx} - q^2 G_{xx} + p^2 G = \delta(x-\xi, t-\tau), \quad x, \xi \in (0,\pi), t > 0, \tau > 0,\\
&G(\xi, \tau, 0, t) = G(\xi, \tau, \pi, t) \equiv 0, \qquad t > 0, \tau > 0,\\
&G_{xx}(\xi, \tau, 0, t) = G_{xx}(\xi, \tau, \pi, t) \equiv 0, \qquad t > 0, \tau > 0,\\
&G(\xi, \tau, x, t) \equiv 0, \qquad \tau \geq t.
\end{aligned}
$$

This inhomogeneous PDE must be solved using a Fourier series with undetermined coefficients. The boundary conditions suggest a sine series:

$$G(\xi, \tau, x, t) = \sum_{n=1}^{\infty} g_n(\xi, \tau, t) \sin(nx),$$

substitution in the PDE gives:

$$
\begin{aligned}
&\ddot{g}_n + (n^4 + q^2 n^2 + p^2) = \frac{2}{\pi} \int_0^{\pi} \delta(x-\xi)\delta(t-\tau)\sin(nx)dx,\\
&g_n(\xi, \tau; 0) = g_n(\xi, \tau; \tau) \equiv 0.
\end{aligned}
$$

The RHS becomes : $\frac{2}{\pi} \int_0^{\pi} \delta(x-\xi)\delta(t-\tau)\sin(nx)dx = \frac{2}{\pi}\delta(t-\tau)\sin(n\xi).$

The homogeneous solution becomes zero due to the boundary conditions. Using variation of parameters $g_n = c_1(t)\cos\left(\sqrt{n^4 + q^2 n^2 + p^2}\, t\right) + c_2(t)\sin\left(\sqrt{n^4 + q^2 n^2 + p^2}\, t\right)$ the particular solution gives:

$$g_n = \frac{2}{\pi} \frac{1}{\sqrt{n^4 + q^2 n^2 + p^2}} \sin\left(\sqrt{n^4 + q^2 n^2 + p^2}\,(t-\tau)\right) H(t-\tau)\sin(n\xi),$$

which leads to the final solution:

$$G(\xi, \tau, x, t) = \frac{2}{\pi} \sum_{n=1}^{\infty} \frac{1}{\sqrt{n^4 + q^2 n^2 + p^2}} \sin\left(\sqrt{n^4 + q^2 n^2 + p^2}\,(t-\tau)\right) H(t-\tau)\sin(n\xi)\sin(nx).$$

Now an upper bound of the solution of w(x,t) will be determined corresponding to the PDE below.

$$\begin{cases} w_{tt} + w_{xxxx} - q^2 w_{xx} + p^2 w = 0, & 0 < x < \pi,\ t > 0, \\ w(0,t) = w(\pi,t) = 0, & t \geq 0, \\ w_{xx}(0,t) = w_0(x;\varepsilon), \quad w_{xx}(\pi,t) = w_1(x;\varepsilon), & t \geq 0,\ 0 < x < \pi. \end{cases}$$

The upper bound can be found via the energy. Multiply the PDE with w_t and integrate x over $0 \leq x \leq \pi$ and t over $0 \leq t \leq t_0$ combined with the initial and boundary conditions gives the total energy. Below each of the terms is derived:

$$\int_0^{t_0} w_{tt} w_t dt = \frac{1}{2} w_t^2 \Big|_0^{t_0} = \frac{1}{2}\left[w_t^2(x,t_0) - g^2(x) \right].$$

$$\int_0^{\pi} w_{xxxx} w_t dx = \cancel{\left[w_{xxx} w_t \right]_0^{\pi}} - \int_0^{\pi} w_{xxx} w_t dx = \cancel{\left[-w_{xx} w_{xt} \right]_0^{\pi}} + \int_0^{\pi} w_{xx} w_{xxt} dx \rightarrow$$

$$\int_0^{t_0} w_{xx} w_{xxt} dt = \left[w_{xx}^2 \right]_0^{t_0} - \int_0^{t_0} w_{xxt} w_{xx} dt \rightarrow \int_0^{t_0} w_{xxt} w_{xx} dt = \left[\frac{w_{xx}^2}{2} \right]_0^{t_0} = \frac{1}{2}\left[w_{xx}^2(x,t_0) - \left(\frac{d^2 f}{dx^2} \right)^2 \right].$$

$$\int_0^{\pi} w_{xx} w_t dx = \cancel{\left[w_x w_t \right]_0^{\pi}} - \int_0^{\pi} w_x w_{xt} dx \rightarrow$$

$$\int_0^{t_0} w_x w_{xt} dt = \left[w_x^2 \right]_0^{t_0} - \int_0^{t_0} w_{xt} w_x dt = \int_0^{t_0} w_x w_{xt} dt = \left[\frac{w_x^2}{2} \right]_0^{t_0} = \frac{1}{2}\left[w^2(x,t_0) - \left(\frac{df}{dx} \right)^2 \right].$$

$$\int_0^{t} w w_t dt = \left[\frac{1}{2} w^2 \right]_0^{t_0} = \frac{1}{2}\left[w^2(x,t_0) - f^2(x) \right].$$

Thus the total energy is:

$$\int_0^{\pi} w_t^2(x,t_0) + w_{xx}^2(x,t_0) + (p^2 + q^2) w^2(x,t_0) dx =$$

$$\int_0^{\pi} g^2(x) + \left(\frac{d^2 f}{dx^2} \right)^2 + q^2 \left(\frac{df}{dx} \right)^2 + p^2 f^2(x) dx.$$

We know that w_x exists and is continuous so:

$$w(x,t) = \cancel{w(0,t)} + \int_0^x w_\xi(\xi,t)d\xi = \int_0^x w_\xi(\xi,t)d\xi.$$

Since w_{xx} exists and is continuous and since we have Dirichlet boundary conditions we know that there exists an $\eta \in (0,L)$ with $w_x(\eta,t) = 0,$ so

$$w_x(x,t) = \cancel{w_x(\eta,t)} + \int_\eta^x w_{\xi\xi}(\xi,t)d\xi = \int_\eta^x w_{\xi\xi}(\xi,t)d\xi.$$

Now first an upper bound for w_x will be determined (with use of Hölder's inequality):

$$|w_x(x,t)| = \left|\int_\eta^x w_{\xi\xi}(\xi,t)d\xi\right| \le \int_0^\pi |w_{\xi\xi}(\xi,t)|\,d\xi \le$$

$$\left(\int_0^\pi 1^2 dx\right)^{1/2}\left(\int_0^\pi w_{xx}^2 dx\right)^{1/2} \le \sqrt{\pi}\left(\int_0^\pi w_t^2 + w_{xx}^2 + \left(q^2+p^2\right)w^2 dx\right)^{1/2} =$$

$$\sqrt{\pi}\left(\int_0^\pi g^2(x) + \left(\frac{d^2f}{dx^2}\right)^2 + q^2\left(\frac{df}{dx}\right)^2 + p^2 f^2(x)\,dx\right)^{1/2} \le$$

$$\sqrt{\pi}\left(\int_0^\pi \|g^2\|_\infty + \left\|\left(\frac{d^2f}{dx^2}\right)^2\right\|_\infty + q^2\left\|\left(\frac{df}{dx}\right)^2\right\|_\infty + p^2\left\|f^2\right\|_\infty dx\right)^{1/2} \le$$

$$\pi\left(\|g\|_\infty + \left\|\left(\frac{d^2f}{dx^2}\right)\right\|_\infty + q\left\|\left(\frac{df}{dx}\right)\right\|_\infty + p\|f\|_\infty\right).$$

Now the maximum of w(x,t) can be found:

$$|w(x,t)| \le \int_0^x |w_\xi(\xi,t)|\,d\xi \le \int_0^\pi |w_x(x,t)|\,dx \le \int_0^\pi \pi\left(\|g\|_\infty + \left\|\left(\frac{d^2f}{dx^2}\right)\right\|_\infty + q\left\|\left(\frac{df}{dx}\right)\right\|_\infty + p\|f\|_\infty\right)dx \to$$

$$|w(x,t)| \le \pi^2\left(\|g\|_\infty + \left\|\left(\frac{d^2f}{dx^2}\right)\right\|_\infty + q\left\|\left(\frac{df}{dx}\right)\right\|_\infty + p\|f\|_\infty\right).$$

Now if g(x) = 0 then

$$\left| \int_0^{\pi} G_{\tau}(\xi, 0, x, t) f(\xi)\, d\xi \right| \le \pi^2 \left\| \left(\frac{d^2 f}{dx^2} \right) \right\|_{\infty} + q \left\| \left(\frac{df}{dx} \right) \right\|_{\infty} + p \| f \|_{\infty} .$$

and if f(x) = 0 then

$$\left| \int_0^{\pi} G(\xi, 0, x, t) g(\xi)\, d\xi \right| \le \| g \|_{\infty} .$$

Section F: The block signal

Below are the two integrals worked out.

$$I_1 = \int_0^{\pi}\left(\sum_{k=-\infty}^{\infty}\delta\left(\frac{L}{\pi}x-\Omega\left(\frac{L}{\pi c}t-c_k\right)\right)-\delta\left(\frac{L}{\pi}x-\Omega\left(\frac{L}{\pi c}t-d_k\right)\right)\right)\cdot\sin(nx)\sin(mx)dx =$$

$$\sum_k \sin\left(n\Omega\left(\frac{1}{c}t-\frac{\pi}{L}c_k\right)\right)\sin\left(m\Omega\left(\frac{1}{c}t-\frac{\pi}{L}c_k\right)\right)-\sin\left(n\Omega\left(\frac{1}{c}t-\frac{\pi}{L}d_k\right)\right)\sin\left(m\Omega\left(\frac{1}{c}t-\frac{\pi}{L}d_k\right)\right)=$$

$$\sum_k \frac{1}{2}\cos\left((n-m)\Omega\left(\frac{1}{c}t-\frac{\pi}{L}c_k\right)\right)+\frac{1}{2}\cos\left((n+m)\Omega\left(\frac{1}{c}t-\frac{\pi}{L}c_k\right)\right)$$

$$-\frac{1}{2}\cos\left((n-m)\Omega\left(\frac{1}{c}t-\frac{\pi}{L}d_k\right)\right)-\frac{1}{2}\cos\left((n+m)\Omega\left(\frac{1}{c}t-\frac{\pi}{L}d_k\right)\right),$$

note that for a given t the series in k reduces to a finite summation.

Moreover each cosine can be written in such a way that the phase is no longer present:

$$\cos\left((n-m)\Omega\left(\frac{1}{c}t-\frac{\pi}{L}c_k\right)\right)-\cos\left((n-m)\Omega\left(\frac{1}{c}t-\frac{\pi}{L}d_k\right)\right)=$$

$$\cos(at)\left(\cos(bc_k)-\cos(bd_k)\right)+\sin(at)\left(\sin(bc_k)-\sin(bd_k)\right),$$

with $a=(n-m)\Omega\frac{1}{c},\ \ b=(n-m)\Omega\frac{\pi}{L},$

$$\cos\left((n+m)\Omega\left(\frac{1}{c}t-\frac{\pi}{L}c_k\right)\right)-\cos\left((n+m)\Omega\left(\frac{1}{c}t-\frac{\pi}{L}d_k\right)\right)=$$

$$\cos(et)\left(\cos(fc_k)-\cos(fd_k)\right)+\sin(et)\left(\sin(fc_k)-\sin(fd_k)\right),$$

with $e=(n+m)\Omega\frac{1}{c},\ \ f=(n+m)\Omega\frac{\pi}{L}.$

So the result is:

$$\sum_{n=1}^{\infty}\sum_{k}-\frac{\omega_n}{4}\left(\cos(bc_k)-\cos(bd_k)\right)G_n\left\{\sin\left((\omega_n+a)t\right)+\sin\left((\omega_n-a)t\right)\right\}$$

$$+\frac{\omega_n}{4}\left(\cos(bc_k)-\cos(bd_k)\right)H_n\left\{\cos\left((\omega_n+a)t\right)+\cos\left((a-\omega_n)t\right)\right\}$$

$$-\frac{\omega_n}{4}\left(\sin(bc_k)-\sin(bd_k)\right)G_n\left\{\cos\left((a-\omega_n)t\right)-\cos\left((\omega_n+a)t\right)\right\}$$

$$+\frac{\omega_n}{4}\left(\sin(bc_k)-\sin(bd_k)\right)H_n\left\{\sin\left((\omega_n+a)t\right)+\sin\left((a-\omega_n)t\right)\right\}$$

$$-\frac{\omega_n}{4}\left(\cos(fc_k)-\cos(fd_k)\right)G_n\left\{\sin\left((\omega_n+e)t\right)+\sin\left((\omega_n-e)t\right)\right\}$$

$$+\frac{\omega_n}{4}\left(\cos(fc_k)-\cos(fd_k)\right)H_n\left\{\cos\left((\omega_n+e)t\right)+\cos\left((e-\omega_n)t\right)\right\}$$

$$-\frac{\omega_n}{4}\left(\sin(fc_k)-\sin(fd_k)\right)G_n\left\{\cos\left((e-\omega_n)t\right)-\cos\left((\omega_n+e)t\right)\right\}$$

$$+\frac{\omega_n}{4}\left(\sin(fc_k)-\sin(fd_k)\right)H_n\left\{\sin\left((\omega_n+e)t\right)+\sin\left((e-\omega_n)t\right)\right\}.$$

$$I_2=\int_0^{\pi}\left(\sum_{k=-\infty}^{\infty}Q\left(\frac{L}{\pi}x-\Omega\left(\frac{L}{\pi c}t-c_k\right)\right)-Q\left(\frac{L}{\pi}x-\Omega\left(\frac{L}{\pi c}t-d_k\right)\right)\right)\cdot\sin(nx)\sin(mx)dx=$$

$$\sum_k\int_{\Omega\left(\frac{1}{c}t-\frac{\pi}{L}c_k\right)}^{\Omega\left(\frac{1}{c}t-\frac{\pi}{L}d_k\right)}\sin(nx)\sin(mx)\,dx=\sum_k\frac{1}{2}\int_{\Omega\left(\frac{1}{c}t-\frac{\pi}{L}c_k\right)}^{\Omega\left(\frac{1}{c}t-\frac{\pi}{L}d_k\right)}\cos\big((n-m)x\big)-\cos\big((n+m)x\big)\,dx=$$

$$\sum_k\frac{1}{2}\left[\frac{1}{n-m}\sin\big((n-m)x\big)-\frac{1}{n+m}\sin\big((n+m)x\big)\right]_{\Omega\left(\frac{1}{c}t-\frac{\pi}{L}c_k\right)}^{\Omega\left(\frac{1}{c}t-\frac{\pi}{L}d_k\right)}=$$

$$\sum_k\frac{1}{2(n-m)}\sin\left((n-m)\Omega\left(\frac{1}{c}t-\frac{\pi}{L}d_k\right)\right)-\frac{1}{2(n+m)}\sin\left((n+m)\Omega\left(\frac{1}{c}t-\frac{\pi}{L}d_k\right)\right)-$$

$$\frac{1}{2(n-m)}\sin\left((n-m)\Omega\left(\frac{1}{c}t-\frac{\pi}{L}c_k\right)\right)+\frac{1}{2(n+m)}\sin\left((n+m)\Omega\left(\frac{1}{c}t-\frac{\pi}{L}c_k\right)\right)=$$

$$\sum_k\frac{1}{2(n-m)}\left\{\sin\big(at-bd_k\big)-\sin(at-bc_k)\right\}+\frac{1}{2(n+m)}\left\{\sin(et-fc_k)-\sin(et-fd_k)\right\}=$$

$$\sum_k\frac{1}{2(n-m)}\sin(at)\left\{\cos(bd_k)-\cos(bc_k)\right\}-\frac{1}{2(n-m)}\cos(at)\left\{\sin(bd_k)-\sin(bc_k)\right\}+$$

$$\frac{1}{2(n+m)}\sin(et)\left\{\cos(fd_k)-\cos(fc_k)\right\}-\frac{1}{2(n+m)}\cos(et)\left\{\sin(fd_k)-\sin(fc_k)\right\}.$$

The total result is:

$$\sum_{n=1}^{\infty}\sum_{k}\frac{-\omega_n^2}{4(n-m)}\left\{\cos(bd_k)-\cos(bc_k)\right\}G_n\left\{\sin\left((a+\omega_n)t\right)+\sin\left((a-\omega_n)t\right)\right\}+$$

$$\frac{-\omega_n^2}{4(n-m)}\left\{\cos(bd_k)-\cos(bc_k)\right\}H_n\left\{\cos\left((a-\omega_n)t\right)-\cos\left((a+\omega_n)t\right)\right\}+$$

$$\frac{\omega_n^2}{4(n-m)}\left\{\sin(bd_k)-\sin(bc_k)\right\}G_n\left\{\cos\left((a+\omega_n)t\right)+\cos\left((a-\omega_n)t\right)\right\}+$$

$$\frac{\omega_n^2}{4(n-m)}\left\{\sin(bd_k)-\sin(bc_k)\right\}H_n\left\{\sin\left((a+\omega_n)t\right)+\sin\left((\omega_n-a)t\right)\right\}+$$

$$\frac{-\omega_n^2}{4(n+m)}\left\{\cos(fd_k)-\cos(fc_k)\right\}G_n\left\{\sin\left((e+\omega_n)t\right)+\sin\left((e-\omega_n)t\right)\right\}+$$

$$\frac{-\omega_n^2}{4(n+m)}\left\{\cos(fd_k)-\cos(fc_k)\right\}H_n\left\{\cos\left((e-\omega_n)t\right)-\cos\left((e+\omega_n)t\right)\right\}+$$

$$\frac{\omega_n^2}{4(n+m)}\left\{\sin(fd_k)-\sin(fc_k)\right\}G_n\left\{\cos\left((e+\omega_n)t\right)+\cos\left((e-\omega_n)t\right)\right\}+$$

$$\frac{\omega_n^2}{4(n+m)}\left\{\sin(fd_k)-\sin(fc_k)\right\}H_n\left\{\sin\left((e+\omega_n)t\right)+\sin\left((\omega_n-e)t\right)\right\}.$$

Below are the cases 3 and 4:

Case 3 $e = \omega_N - \omega_M$ with N > M

$$\begin{cases} 2\omega_M \dfrac{dG_M}{d\tau} = \displaystyle\sum_k \left(\frac{\omega_N^2}{4(N+M)} - \frac{\omega_N}{4} \right) \left(\cos(fc_k) - \cos(fd_k)\right) G_N - \left(\frac{\omega_N^2}{4(N+M)} + \frac{\omega_N}{4} \right) \left(\sin(fc_k) - \sin(fd_k)\right) H_N, \\ 2\omega_M \dfrac{dH_M}{d\tau} = \displaystyle\sum_k -\left(\frac{\omega_N}{4} + \frac{\omega_N^2}{4(N+M)} \right) \left(\cos(fc_k) - \cos(fd_k)\right) H_N + \left(\frac{\omega_N}{4} + \frac{\omega_N^2}{4(N+M)} \right) \left(\sin(fc_k) - \sin(fd_k)\right) G_N, \\ 2\omega_N \dfrac{dG_N}{d\tau} = \displaystyle\sum_k \left(\frac{\omega_M^2}{4(M+N)} + -\frac{\omega_M}{4} \right) \left(\cos(fc_k) - \cos(fd_k)\right) G_M + \left(\frac{\omega_M}{4} - \frac{\omega_M^2}{4(M+N)} \right) \left(\sin(fc_k) - \sin(fd_k)\right) H_M, \\ 2\omega_N \dfrac{dH_N}{d\tau} = \displaystyle\sum_k \left(-\frac{\omega_M}{4} + \frac{\omega_M^2}{4(M+N)} \right) \left(\cos(fc_k) - \cos(fd_k)\right) H_M + \left(-\frac{\omega_M}{4} + \frac{\omega_M^2}{4(M+N)} \right) \left(\sin(fc_k) - \sin(fd_k)\right) G_M. \end{cases}$$

Case 4 $e = \omega_N + \omega_M$

$$\begin{cases} 2\omega_M \dfrac{dG_M}{d\tau} = \displaystyle\sum_k \left(\frac{\omega_N}{4} + \frac{\omega_N^2}{4(N+M)} \right) \left(\cos(fc_k) - \cos(fd_k)\right) G_N + \left(\frac{\omega_N}{4} + \frac{\omega_N^2}{4(N+M)} \right) \left(\sin(fc_k) - \sin(fd_k)\right) H_N, \\ 2\omega_M \dfrac{dH_M}{d\tau} = \displaystyle\sum_k \left(-\frac{\omega_N^2}{4(N+M)} + \frac{\omega_N}{4} \right) \left(\cos(fc_k) - \cos(fd_k)\right) H_N + \left(\frac{\omega_N}{4} + \frac{\omega_N^2}{4(N+M)} \right) \left(\sin(fc_k) - \sin(fd_k)\right) G_N, \\ 2\omega_N \dfrac{dG_N}{d\tau} = \displaystyle\sum_k \left(\frac{\omega_M}{4} + \frac{\omega_M^2}{4(M+N)} \right) \left(\cos(fc_k) - \cos(fd_k)\right) G_M + \left(\frac{\omega_M}{4} + \frac{\omega_M^2}{4(M+N)} \right) \left(\sin(fc_k) - \sin(fd_k)\right) H_M, \\ 2\omega_N \dfrac{dH_N}{d\tau} = \displaystyle\sum_k \left(-\frac{\omega_M^2}{4(M+N)} + \frac{\omega_M}{4} \right) \left(\cos(fc_k) - \cos(fd_k)\right) H_M + \left(\frac{\omega_M}{4} + \frac{\omega_M^2}{4(M+N)} \right) \left(\sin(fc_k) - \sin(fd_k)\right) G_M. \end{cases}$$

Section G: The quadratic term

An analysis of resonance cases
Several cases for resonance must be analyzed:

$$\mathrm{I}:\ \begin{cases} m = k + l + d, \\ \pm\sqrt{m^4 + m^2\mu^2} = \pm\sqrt{k^4 + k^2\mu^2} \pm \sqrt{l^4 + l^2\mu^2}, \end{cases}$$

$$\mathrm{II}:\ \begin{cases} m = k + l - d, \\ \pm\sqrt{m^4 + m^2\mu^2} = \pm\sqrt{k^4 + k^2\mu^2} \pm \sqrt{l^4 + l^2\mu^2}, \end{cases}$$

$$\mathrm{III}:\ \begin{cases} m = k - l + d, \\ \pm\sqrt{m^4 + m^2\mu^2} = \pm\sqrt{k^4 + k^2\mu^2} \pm \sqrt{l^4 + l^2\mu^2}, \end{cases}$$

$$\mathrm{IV}:\ \begin{cases} m = k - l - d, \\ \pm\sqrt{m^4 + m^2\mu^2} = \pm\sqrt{k^4 + k^2\mu^2} \pm \sqrt{l^4 + l^2\mu^2}, \end{cases}$$

$$\mathrm{V}:\ \begin{cases} m = -k - l + d, \\ \pm\sqrt{m^4 + m^2\mu^2} = \pm\sqrt{k^4 + k^2\mu^2} \pm \sqrt{l^4 + l^2\mu^2}, \end{cases}$$

where d is odd and $k, l, m \geq 1.$

It's clear that if $\sqrt{m^4 + m^2\mu^2} = -\sqrt{k^4 + k^2\mu^2} - \sqrt{l^4 + l^2\mu^2}$ then there are no solutions. The following cases remain.

Case I(i)

$$\begin{cases} m = k + l + d, \\ \sqrt{m^4 + m^2\mu^2} = \sqrt{k^4 + k^2\mu^2} + \sqrt{l^4 + l^2\mu^2}, \quad (*) \end{cases}$$

with $k, l, m \geq 1, \quad d = 2j + 1, \ j = 0, 1, 2, \ldots$

This set of equations has **no solutions**! Two proofs are given below.

Proof 1
Squaring both sides of (*) and reordering gives (introduce $x = \mu^2$):

$$m^4 + m^2 x = k^4 + k^2 x + l^4 + l^2 x + 2lk\sqrt{\left(k^2 + x\right)\left(l^2 + x\right)} \leftrightarrow$$

$$\underbrace{\left(m^4 - k^4 - l^4\right)}_{a} + x\underbrace{\left(m^2 - k^2 - l^2\right)}_{b} = 2lk\sqrt{\left(k^2 + x\right)\left(l^2 + x\right)} \leftrightarrow$$

$$\left(a + bx\right)^2 = 4l^2k^2\left(k^2 + x\right)\left(l^2 + x\right) \leftrightarrow$$

$$x^2\left(4k^2l^2 - b^2\right) + x\left(4k^2l^2(k^2 + l^2) - 2ab\right) + \left(4k^2l^2 - a^2\right) = 0.$$

Notice a quadratic equation in x: $Ax^2+Bx+C=0$; from Routh-Hurwitz it can be deduced that if $\frac{B}{A}>0,\ \frac{C}{A}>0$ then all zeros are in the left half plane. In this case it means that $\mu_{1,2}^2<0$ so no solutions are found. The signs of A,B and C must be investigated to draw this conclusion.

$$A: 4k^2l^2-\left(d^2+2(lk+md+kd)\right)^2<0.$$
$$B: 4k^4l^2+4k^2l^4-2(m^4-k^4-l^4)(m^2-k^2-l^2).$$

Note that $m^4-k^4-l^4>4k^3l+4l^3k$ and that $m^2-k^2-l^2>2kl$ so

$$2\left(m^4-k^4-l^4\right)\left(m^2-k^2-l^2\right)>2kl(4k^3l+4kl^3)=16k^4l^2+16k^2l^4,$$

so we find B < 0.

$$C: 4k^4l^4-a^2=\left(2k^2l^2-a\right)\left(2k^2l^2+a\right),$$

note that $2k^2l^2+a>0$ and $a=m^4-k^4-l^4>6k^2l^2$ so $\left(2k^2l^2-a\right)<0$ so we find C < 0.

The conclusion is that: $\frac{B}{A}>0$ and $\frac{C}{A}>0$.

Proof 2
The RHS of (*) is always smaller then the LHS:

$$\sqrt{k^4+k^2\mu^2}+\sqrt{l^4+l^2\mu^2}<k\sqrt{m^2+\mu^2}+l\sqrt{m^2+\mu^2}<(k+l+d)\sqrt{m^2+\mu^2}=\sqrt{m^4+m^2\mu^2}.$$

Case I(ii)

$$\begin{cases} m=k+l+d, \\ \sqrt{m^4+m^2\mu^2}=\sqrt{k^4+k^2\mu^2}-\sqrt{l^4+l^2\mu^2}, \end{cases}$$

Note that $m^4>k^4+l^4$ and $m^2>k^2+l^2$ due to the first equation now squaring of the second equation and reordering gives:

$$2\sqrt{\left(k^4+k^2\mu^2\right)\left(l^4+l^2\mu^2\right)}=k^4+l^4-m^4+\mu^2\left(k^2+l^2-m^2\right)<0.$$

So **no solutions** exist for case I(ii). A second proof is constructed analogously to proof 2 of Case I(i).

Case I(iii)

$$\begin{cases} m=k+l+d, \\ \sqrt{m^4+m^2\mu^2}=-\sqrt{k^4+k^2\mu^2}+\sqrt{l^4+l^2\mu^2}, \end{cases}$$

This is the same as case I(i) with the role of k and l switched.

Case II(i)

$$\begin{cases} m = k + l - d, & (6.3) \\ \sqrt{m^4 + m^2\mu^2} = \sqrt{k^4 + k^2\mu^2} + \sqrt{l^4 + l^2\mu^2}. & (6.4) \end{cases}$$

The same arguments can be applied as in [11] with the inequality adapted leading to the same (and more) modes that gives resonance. Define $g(u) = \sqrt{u^2 + u\mu^2}$ now using Taylor's theorem around u = A^2:

$g(u) = g(A) + (u - A)g'(\xi)$ with $\xi \in (a, u)$ with the assumption that $u \geq a$.

$$g'(\xi) = \frac{2u + \mu^2}{2\sqrt{u^2 + \mu^2 u}} \leq \frac{2\left(u + \mu^2\right)}{2\sqrt{u^2 + \mu^2 u}} \leq \frac{\left(u + \mu^2\right)}{\sqrt{u^2 + \mu^2 u}} \leq \frac{\left(u + u\mu^2\right)}{\sqrt{u^2 + \mu^2 u}} = \frac{1}{\sqrt{u^2 + \mu^2 u}} \leq 1 \text{ for } u, \mu^2 \geq 1.$$

Now the inequality becomes:

$$g(u) \leq g(A) + (u - A) = \sqrt{A^2 + A\mu^2} + u - A.$$

Substitute x^2=u and A = a^2 results in $x^2 < \sqrt{x^4 + x^2\mu^2} \leq \sqrt{a^4 + a^2\mu^2} + x^2 - a^2$ for $x \geq a,\ x, \mu \geq 1.$

Note that $m^2 \leq \sqrt{m^4 + m^2\mu^2} \leq k^2 + l^2 - 2 + 2\sqrt{1 + \mu^2}$ since $l,\ k,\ d \geq 1$ and by definition $m^2 = k^2 + l^2 + d^2 + 2(kl - (l + k)d) = k^2 + l^2 + \nu$ with $\nu = d^2 + 2(kl - (l + k)d)$, comparing the two equations leads to:

$$\nu < 2\left(\sqrt{1 + \mu^2} - 1\right).$$

From the definition of ν we see that ν is odd. Case II(i) hasn't got solutions for $\nu \leq 0$. To see this introduce $M = m^2,\ K = k^2,\ L = l^2$:

$$\begin{cases} M = K + L + \nu, \\ \sqrt{M^2 + M\mu^2} = \sqrt{K^2 + K\mu^2} + \sqrt{L^2 + L\mu^2}. \end{cases}$$

Assume that $\nu \leq 0$ then

$$N - K - M \leq 0 \quad \rightarrow N \leq K + M \quad \rightarrow \quad N^2 \leq (K + M)^2 = K^2 + 2KM + M^2,$$

but also : $N\mu^2 \leq K\mu^2 + M\mu^2$.

Addition of the two equations leads to:

$$N^2 + N\mu^2 \le K^2 + 2KM + M^2 + K\mu^2 + M\mu^2 \leftrightarrow$$
$$\left(\sqrt{N^2 + N\mu^2}\right)^2 \le K^2 + 2KM + M^2 + K\mu^2 + M\mu^2 \leftrightarrow$$
$$\left(\sqrt{K^2 + K\mu^2} + \sqrt{M^2 + M\mu^2}\right)^2 \le K^2 + K\mu^2 + 2KM + M^2 + M\mu^2 \leftrightarrow$$
$$K^2 + K\mu^2 + 2\sqrt{K^2 + K\mu^2}\sqrt{M^2 + M\mu^2} + M^2 + M\mu^2 \le K^2 + K\mu^2 + 2KM + M^2 + M\mu^2 \leftrightarrow$$
$$2\sqrt{K^2 + K\mu^2}\sqrt{M^2 + M\mu^2} \le 2KM \leftrightarrow$$
$$\sqrt{K^2 + K\mu^2}\sqrt{M^2 + M\mu^2} \le KM \leftrightarrow$$
$$(K^2 + K\mu^2)(M^2 + M\mu^2) \le K^2M^2 \leftrightarrow$$
$$K^2M^2 + KM^2\mu^2 + K^2M\mu^2 + KM\mu^4 \le K^2M^2 \leftrightarrow$$
$$KM^2\mu^2 + K^2M\mu^2 + KM\mu^4 \le 0.$$

Which leads to a contradiction since K and M are natural numbers and $\mu > 0$.

So case II(i) only has solutions for $\nu > 0$. We see that for $\mu^2 \le 45$ we have $\nu < 11.56$ and we know ν is odd, this means that $\nu = 1,3,..,11,13$ have to be investigated. Suppose d = 1 then from the definition of ν we can derive $l_* = 1 + \frac{1+\nu}{2(k-1)}$ where the star is added to distinguish the letter l from the number 1. For $\nu = 1,\ l_* = 1 + \frac{1}{k-1}$ then the only possible solution is $k = l_* = 2$ which leads to n = 3 according to equation 6.3 and equation 6.4 then satisfies for $\mu^2 = \frac{17}{7}$.

For $\nu = 3,\ l_* = 1 + \frac{2}{k-1}$ the two possible solutions are $k = 2,\ l_* = 3$ or $k = 3,\ l_* = 2$. Due to symmetry in k and l_* it suffices to look at $k = 2,\ l_* = 3$ then m=4 according to equation 6.3 and equation 6.4 is satisfied for $\mu^2 = 9,27$ .For $\nu = 5,\ l_* = 1 + \frac{3}{k-1}$ then the two possible solutions are $k = 2,\ l_* = 4$ or $k = 4,\ l_* = 2$. Due to symmetry in k and l_* it suffices to examine $k = 2,\ l_* = 4$ then m = 5 according to equation 6.3 and equation 6.4 is satisfied for $\mu^2 = 18.48$.

For $\nu = 7,\ l_* = 1 + \frac{4}{k-1}$ three possible solutions are $k = 2,\ l_* = 5$ or $k = 5,\ l_* = 2$ or $k = l_* = 3$. Due to symmetry in k and l_* it suffices to examine the cases $k = 2,\ l_* = 5$ and $k = l_* = 3$. If $k = 2,\ l_* = 5$ the m = 6 according to equation 6.3 and equation 6.4 is satisfied for $\mu^2 = 30,01$. If $k = l_* = 3$ then m = 5 according to equation 6.3 and equation 6.4 is satisfied for $\mu^2 = \frac{301}{11} \approx 27.36$. This analysis can be continued for $\nu = 9,11,13,....$ For $\nu > 9$ no solutions exist where $\mu^2 \le 45.$

Suppose d = 3 from the definition of ν we can derive $l = 3 + \frac{9+\nu}{2(k-3)}$. For $\nu = l,\ l_* = 3 + \frac{5}{k-3}$ two possible solutions are $k = 4,\ l_* = 8$ and $k = 8,\ l_* = 4$. Due to symmetry in k and l_* it suffices to examine the cases $k = 4,\ l_* = 8$. Then it follows from equation 6.3 that m = 9, and equation 6.4 is satisfied for $\mu^2 = 2.066$. This analysis can be continued for $\nu = 3,5,7,\ldots$, the values for the resonance modes up to $\mu^2 \leq 45$ have been omitted but the calculation is similar to the one above.

m,l,k,d	μ^2
3,2,2,1	17/7
4,2,3,1	9,27
5,2,4,1	18,48
6,3,3,1	27,36
6,2,5,1	30,01
7,2,6	43,86
19,6,18	2,028
...	...

Table G.1: Only for special cases of μ^2 resonance can occur.

Due to symmetry in l and k the values of l and k can be switched. This table only gives a part of all values where resonance occurs for $\mu^2 \leq 45.$

Case II(ii)

$$\begin{cases} m = k + l - d, \\ \sqrt{m^4 + m^2\mu^2} = \sqrt{l^4 + l^2\mu^2} - \sqrt{k^4 + k^2\mu^2}. \end{cases}$$

This is equivalent to case I(i) with m and l switched and d replaced by d+2k and to case II(i) with m and l switched and d replaced by -d+2k.

Case II(iii)

$$\begin{cases} m = k + l - d, \\ \sqrt{m^4 + m^2\mu^2} = -\sqrt{l^4 + l^2\mu^2} + \sqrt{k^4 + k^2\mu^2}. \end{cases}$$

This is equivalent to case II(ii) with l and k switched.

Case III(i)

$$\begin{cases} m = l - k + d, \\ \sqrt{m^4 + m^2\mu^2} = \sqrt{l^4 + l^2\mu^2} + \sqrt{k^4 + k^2\mu^2}. \end{cases}$$

This is equivalent to case I(i) where d is replaced by d+2k and to case II(i) where d is replaced by -d+2k.

Case III(ii)

$$\begin{cases} m = l - k + d, \\ \sqrt{m^4 + m^2\mu^2} = -\sqrt{l^4 + l^2\mu^2} + \sqrt{k^4 + k^2\mu^2}. \end{cases}$$

This is equivalent to Case III(ii) with l and k switched.

Case IV(i)

$$\begin{cases} m = l - k - d, \\ \sqrt{m^4 + m^2\mu^2} = \sqrt{l^4 + l^2\mu^2} + \sqrt{k^4 + k^2\mu^2}. \end{cases}$$

This is equivalent to case I(ii) with m and l switched.

Case IV(ii)

$$\begin{cases} m = l - k - d, \\ \sqrt{m^4 + m^2\mu^2} = \sqrt{l^4 + l^2\mu^2} - \sqrt{k^4 + k^2\mu^2}. \end{cases}$$

This is equivalent to case I(i) with m and l switched.

Case IV(iii)

$$\begin{cases} m = l - k - d, \\ \sqrt{m^4 + m^2\mu^2} = -\sqrt{l^4 + l^2\mu^2} + \sqrt{k^4 + k^2\mu^2}. \end{cases}$$

This is equivalent to case IV(ii) with l and k switched.

Case V(i)

$$\begin{cases} m = -l - k + d, \\ \sqrt{m^4 + m^2\mu^2} = \sqrt{l^4 + l^2\mu^2} + \sqrt{k^4 + k^2\mu^2}. \end{cases}$$

This is equivalent to case I(i) where d is replaced by d + 2k + 2l and to case II(i) where d is replaced by -d+2k+2l.

Case V(ii)

$$\begin{cases} m = -l - k + d, \\ \sqrt{m^4 + m^2\mu^2} = \sqrt{l^4 + l^2\mu^2} + \sqrt{k^4 + k^2\mu^2}. \end{cases}$$

This is equivalent to case V(i) with m and l switched.

Case V(iii)

$$\begin{cases} m = -l - k + d, \\ \sqrt{m^4 + m^2\mu^2} = -\sqrt{l^4 + l^2\mu^2} + \sqrt{k^4 + k^2\mu^2}. \end{cases}$$

This is equivalent to case V(ii) where l and k are switched.

Section H: The cubic term

In this section we show how the cases where resonance occurs can be derived. The Φ can be expanded using goniometric formulas:

$$
\begin{aligned}
\Phi = \frac{1}{4}\omega_m\omega_k\omega_j[& \\
&\left(-C_1G_j + C_2H_j\right)\cos\left((\omega_m + \omega_k + \omega_j)t\right) + \\
&\left(-C_2G_j - C_1H_j\right)\sin\left((\omega_m + \omega_k + \omega_j)t\right) + \\
&\left(C_1G_j + C_2H_j\right)\cos\left((\omega_m + \omega_k - \omega_j)t\right) + \\
&\left(C_2G_j - C_1H_j\right)\sin\left((\omega_m + \omega_k - \omega_j)t\right) + \\
&\left(C_3G_j + C_4H_j\right)\cos\left((\omega_m - \omega_k + \omega_j)t\right) + \\
&\left(-C_4G_j + C_3H_j\right)\sin\left((\omega_m - \omega_k + \omega_j)t\right) + \\
&\left(-C_3G_j + C_4H_j\right)\cos\left((\omega_m - \omega_k - \omega_j)t\right) + \\
&\left(C_4G_j + C_3H_j\right)\sin\left((\omega_m - \omega_k - \omega_j)t\right)],
\end{aligned}
$$

with

$$
\begin{aligned}
C_1 &= G_mH_k + H_mG_k, \quad & C_2 &= -G_mG_k + H_mH_k, \\
C_3 &= -G_mH_k + H_mG_k, \quad & C_4 &= G_mG_k + H_mH_k.
\end{aligned}
$$

The terms of Φ can cause secular terms if

$$
\pm\sqrt{n^4 + n^2\mu^2} = \pm\sqrt{m^4 + m^2\mu^2} \pm \sqrt{k^4 + k^2\mu^2} \pm \sqrt{j^4 + j^2\mu^2}\ .
$$

To determine the contribution of the sums derived in §7.2 the following resonance cases must be investigated:

$$
\begin{aligned}
\mathrm{I}&: \begin{cases} n = m + k + j, \\ \pm\sqrt{n^4 + n^2\mu^2} = \pm\sqrt{m^4 + m^2\mu^2} \pm \sqrt{k^4 + k^2\mu^2} \pm \sqrt{j^4 + j^2\mu^2}, \end{cases} \\
\mathrm{II}&: \begin{cases} n = -m - k + j, \\ \pm\sqrt{n^4 + n^2\mu^2} = \pm\sqrt{m^4 + m^2\mu^2} \pm \sqrt{k^4 + k^2\mu^2} \pm \sqrt{j^4 + j^2\mu^2}, \end{cases} \\
\mathrm{III}&: \begin{cases} n = m + k - j, \\ \pm\sqrt{n^4 + n^2\mu^2} = \pm\sqrt{m^4 + m^2\mu^2} \pm \sqrt{k^4 + k^2\mu^2} \pm \sqrt{j^4 + j^2\mu^2}. \end{cases}
\end{aligned}
$$

It's clear that the cases do not have solutions where:

$$
\sqrt{n^4 + n^2\mu^2} = -\sqrt{m^4 + m^2\mu^2} - \sqrt{k^4 + k^2\mu^2} - \sqrt{j^4 + j^2\mu^2}.
$$

Case I(i)

$$\begin{cases} n = m + k + j, \\ \sqrt{n^4 + n^2\mu^2} = \sqrt{m^4 + m^2\mu^2} + \sqrt{k^4 + k^2\mu^2} + \sqrt{j^4 + j^2\mu^2}. \quad (*) \end{cases}$$

This set of equations has no solutions. The proof is outlined below.

The RHS of (*) is always smaller then the LHS:

$$\sqrt{k^4 + k^2\mu^2} + \sqrt{m^4 + m^2\mu^2} + \sqrt{j^4 + j^2\mu^2} < k\sqrt{n^2 + \mu^2} + m\sqrt{n^2 + \mu^2} + j\sqrt{n^2 + \mu^2}$$

$$< (k + m + j)\sqrt{n^2 + \mu^2} = \sqrt{n^4 + n^2\mu^2}.$$

Case I(ii)

$$\begin{cases} n = m + k + j, \\ \sqrt{n^4 + n^2\mu^2} = \sqrt{m^4 + m^2\mu^2} + \sqrt{k^4 + k^2\mu^2} - \sqrt{j^4 + j^2\mu^2}. \end{cases}$$

A proof that this set of equations has no solutions can be constructed along the same lines as the proof of case I(i).

Case I(iii)

$$\begin{cases} n = m + k + j, \\ \sqrt{n^4 + n^2\mu^2} = \sqrt{m^4 + m^2\mu^2} - \sqrt{k^4 + k^2\mu^2} - \sqrt{j^4 + j^2\mu^2}. \end{cases}$$

A proof that this set of equations has no solutions can be constructed along the same lines as the proof of case I(i).

Case II

$n = -m - k + j$ is the same as I with n and j switched.

Case III(i)

$$\begin{cases} n = m + k - j, \\ \sqrt{n^4 + n^2\mu^2} = \sqrt{m^4 + m^2\mu^2} + \sqrt{k^4 + k^2\mu^2} + \sqrt{j^4 + j^2\mu^2}. \end{cases}$$

We know $n^2 = m^2 + k^2 + j^2 + 2(mk - mj - kj)$. We introduce $\lambda = 2(mk - mj - kj)$ and $N = n^2, K = k^2, J = j^2$. Look at the following set of equations:

$$\begin{cases} N = M + K + J + \lambda, \\ \sqrt{N^2 + N\mu^2} = \sqrt{M^2 + M\mu^2} + \sqrt{K^2 + K\mu^2} + \sqrt{J^2 + J\mu^2}. \end{cases}$$

Assume that $\lambda \le 0$ then

$N - M - K - J \le 0 \;\rightarrow\; N < M + K + J \;\rightarrow\; N < (M+K+J)^2 = M^2 + K^2 + J^2 + 2(MK + KJ + MJ)$

but also $N\mu^2 \le K\mu^2 + M\mu^2 + J\mu^2$. Addition of the two equations leads to:

$$M^2 + M\mu^2 + K^2 + K\mu^2 + J^2 + J\mu^2 + 2\sqrt{\left(M^2 + M\mu^2\right)\left(K^2 + K\mu^2\right)}$$
$$+2\sqrt{\left(M^2 + M\mu^2\right)\left(J^2 + J\mu^2\right)} + 2\sqrt{\left(K^2 + K\mu^2\right)\left(J^2 + J\mu^2\right)} \le$$
$$M\mu^2 + K\mu^2 + J\mu^2 + M^2 + K^2 + J^2 + 2MK + 2KJ + 2MJ.$$

or

$$\sqrt{\left(M^2 + M\mu^2\right)\left(K^2 + K\mu^2\right)} + \sqrt{\left(M^2 + M\mu^2\right)\left(J^2 + J\mu^2\right)} + \sqrt{\left(K^2 + K\mu^2\right)\left(J^2 + J\mu^2\right)} \le MK + KJ + MJ.$$

But this can never be true because of an terms-wise failing of the inequality:

$$\sqrt{\left(M^2 + M\mu^2\right)\left(K^2 + K\mu^2\right)} \ge MK,$$
$$\sqrt{\left(M^2 + M\mu^2\right)\left(J^2 + J\mu^2\right)} \ge MJ,$$
$$\sqrt{\left(K^2 + K\mu^2\right)\left(J^2 + J\mu^2\right)} \ge MJ.$$

The conclusion is that $\lambda > 0$.

In some cases there can be resonance depending on the value of μ^2. We again use the inequality derived in the previous section of the appendix: $x^2 < \sqrt{x^4 + x^2\mu^2} \le \sqrt{a^4 + a^2\mu^2} + x^2 - a^2$ for $x \ge a,\ x, \mu \ge 1.$

Using this inequality we can derive that:

$n^2 < \sqrt{n^4 + \mu^2} \le m^2 + k^2 + j^2 - 3 + 3\sqrt{1 + \mu^2}$ since $n, m, k, j \ge 1.$

We also know that $n^2 = m^2 + k^2 + j^2 + 2(mk - mj - kj) = m^2 + k^2 + j^2 + \lambda$ this gives us:

$\lambda < 3\left(\sqrt{1 + \mu^2} - 1\right)$. With $\mu^2 < 10$ the possible values of λ are 2, 4, 6 and 8. Take $\lambda = 2$ and due to symmetry in m and k, assume that $m \ge k$. For $m = k$ we get $\lambda = 2m(m - 2j)$ which means that there are no solutions for $\lambda < 10$ which implies that there are also no solutions for $0 < \mu^2 < 10$, so we take $m > k$. From the definition of λ we have $m(k - j) = \frac{\lambda}{2} + kj > 0$ so $k - j > 0$, $k > j$ which implies that $m > k > j \ge 1 \;\rightarrow\; j \ge 1, k \ge 2, m \ge 3$ and $n \ge 4$.

Note that this means that If $\lambda = 2$ then $mk - mj - kj = 1$, if $j = 1$ then $m = 1 + \frac{2}{k-1}$. The only possible solutions is $m = 3,\ k = 2$ with $n = 4$ leading to $\mu^2 = 2, 60$, due to symmetry in k and m, they can be switched. Continuing in this way for $j \geq 2$ all of the modes can be found linked to a specific μ^2 which can cause resonance.

Case III(ii)(a)

$$\begin{cases} n = m + k - j, \\ \sqrt{n^4 + n^2\mu^2} = \sqrt{m^4 + m^2\mu^2} + \sqrt{k^4 + k^2\mu^2} - \sqrt{j^4 + j^2\mu^2}. \end{cases}$$

This set of equations has the obvious solutions k = n and j = m. Due to symmetry in m, k they can be switched.

Case III(ii)(b)

$$\begin{cases} n = m + k - j, \\ \sqrt{n^4 + n^2\mu^2} = \sqrt{m^4 + m^2\mu^2} - \sqrt{k^4 + k^2\mu^2} + \sqrt{j^4 + j^2\mu^2}. \end{cases}$$

This set of equations has the obvious solutions m = n and j = k.

Case III(ii) (c)

$$\begin{cases} n = m + k - j, \\ \sqrt{n^4 + n^2\mu^2} = -\sqrt{m^4 + m^2\mu^2} + \sqrt{k^4 + k^2\mu^2} + \sqrt{j^4 + j^2\mu^2}. \end{cases}$$

This set of equations is the same as III(ii)(b) with m and k switched. Using a similar analysis as in Case III(i) it can be shown that the solutions given in III(ii)(a)-(c) are the only solutions.

Case III(a)

$$\begin{cases} n = m + k - j, \\ \sqrt{n^4 + n^2\mu^2} = -\sqrt{m^4 + m^2\mu^2} - \sqrt{k^4 + k^2\mu^2} + \sqrt{j^4 + j^2\mu^2}. \end{cases}$$

This case is the same as I(i) with n and j switched.

Case III(b)

$$\begin{cases} n = m + k - j, \\ \sqrt{n^4 + n^2\mu^2} = \sqrt{m^4 + m^2\mu^2} - \sqrt{k^4 + k^2\mu^2} - \sqrt{j^4 + j^2\mu^2}. \end{cases}$$

This case is the same as III(i) with n and m, k and j switched.

Case III(c)

$$\begin{cases} n = m + k - j, \\ \sqrt{n^4 + n^2\mu^2} = -\sqrt{m^4 + m^2\mu^2} + \sqrt{k^4 + k^2\mu^2} - \sqrt{j^4 + j^2\mu^2}. \end{cases}$$

This case is the same as III(iii)(b) with m and k switched.

References

[1] Y.Hikami and N.Shiraishi, 'Rain-wind induced vibrations of cables in cable stayed bridges', Journal of wind engineering and industrial aerodynamics, vol. 29, 1988.
[2] H.Yamamuchi, 'Analytical study on growth mechanism of rain vibration of cables', Journal of wind engineering and industrial aerodynamics, vol. 33, 1990.
[3] S.V. Alekseenko, D.M.Markovich et. al. 'Rivulet flow of liquid on the outer surface of an inclined cylinder', Journal of applied mechanics and technical physics, vol. 37, no.4, 1997
[4] D.Q. Cao, R.W. Tucker, C. Wang, 'A stochastic approach to cable dynamics with moving rivulets, Journal of sound and vibration', p291-304, 2003.
[5] Y.L. Xu and L.Y. Wang, 'Analytical study of wind-rain-induced cable vibration: SDOF model', Journal of wind engineering and industrial aerodynamics, vol. 91, p27-40, 2003.
[6] R. S. Phelan, P.Sarkar et. al., 'Full-scale measurements to investigate rain-wind induced cable-stay vibration and its mitigation', Journal of bridge engineering, 2006.
[7] C.Lemaitre, M.Alam et. al., 'Rainwater rivulets on a cable subject to wind', C.R. Mecanique 334, 2006.
[8] U.Peil and O.Dreyer, 'Rain-wind induced vibrations in laminar and turbulent flow', wind and structures, vol. 10 no.1, p83-97, 2007.
[9] M. Gu, X.Q Du, S.Y. Li, 'Experimental and theoretical simulations on wind-rain-induced vibration of 3-D rigid stay cables', journal of sound and vibration 320, 2009.
[10] H.J. Zou and Y.L. XU, 'Wind-rain-induced vibration and control of stay cables in a cable-stayed bridge', Structural control and health monitoring, vol. 14, p1013-1033, 2007.
[11] W.T. van Horssen, J. Boertjens, 'Weakly nonlinear beam equations: an asymptotic analysis', Phd thesis Delft University of technology, 2000.
[12] J. Reusink, 'Zware dempers houden tuien definitief in bedwang', Bouwen met staal 137, juli/augustus 1997.
[13] M. amabili, 'Nonlinear vibrations and stability of shell and plates', Cambridge university press, p145, 2008.
[14] V. Birman, 'Non-linear beam-type vibrations of a long cylindrical shells', Nonlinear mechanics vol. 2, p327-334,1987.
[15] G. Suweken, 'A mathematical analysis of a belt system with a low and time-varying velocity', Phd thesis Technische Universiteit Delft, 2003.
[16] S. Graham Kelly, 'Fundamentals of mechanical vibrations', Mcgrawhill, 2000.
[17] J. Hijmissen, 'On aspects of boundary damping for cables and vertical beams', Phd Thesis, TU Delft, 2008.
[18] W.T. Horssen, 'An asymptotic analysis of a class of nonlinear hyperbolic equations', Phd thesis, TU Delft, 1988.
[19] S. Zhan, 'Experimental study of wind-rain-induced cable vibrations using a new model setup scheme', Journal of wind engineering and industrial aerodynamics, vol. 96, p2438-2451, 2008.
[20] Source of picture I.1: http://ta.twi.tudelft.nl/users/vuik/information/erasmus.html.
[21] Y. Hartono, 'Mathematical models for rain-wind induced vibrations of simple structures', Phd thesis, Delft university of technology, printed by optima, 2004.
[22] H.J. Zou, Y.L. Xu, 'Wind–rain-induced vibration and control of stay cables in a cable-stayed bridge', Structural control and health monitoring, vol. 14, p1013–1033, 2007.

Acknowledgements

This thesis is the reflection of more than 3/4 year of work in collaboration with the Department of Applied Mathematical Analysis of the University of Technology in Delft, The Netherlands. This thesis would not have been possible without the help and support of many people. Some of the support is explicitly cited in this thesis, others are more implicit but as important.

First I have to mention Dr. Ir. P.C.J. Hoogenboom and prof. dr. A.V. Metrikine from the faculty of civil engineering of TU Delft for their help in setting up the model. Secondly Dr. Ir. P.T.L.M. van Woerkom from the faculty 3ME of TU Delft for his course in nonlinear differential equations in mechanics which was helpful in gaining a better understanding in these phenomena. In addition, Prof. dr. ir. A. W. Heemink has helped me via his course advanced modeling. Finally I'd like to thank Dr. P. Wilders for his help in solving differential equations.

The most important person to whom I owe a lot is my supervisor, Dr. Ir. W. T. van Horssen, from whom I have learnt a lot about Differential Equations, and Perturbation Methods which are the core of this thesis. I'm very grateful to him. He is not only an expert in Differential Equations and its related subjects but also a patient and caring person. I consider myself to be very lucky for having him as my supervisor.

June 2010, Delft
Dhiretjh Sewdoelaré